

Ministry of Energy, Mines & Petroleum Resources
Mining & Minerals Division
BC Geological Survey

**Assessment Report
Title Page and Summary**

TYPE OF REPORT [type of survey(s)]: PROSPECTING, ANALYSIS OF HISTORICAL GEOCHEMISTRY TOTAL COST: \$27,761.40

AUTHOR(S): Venessa Bennett **SIGNATURE(S):** _____

NOTICE OF WORK PERMIT NUMBER(S)/DATE(S): _____ **YEAR OF WORK:** 2019

STATEMENT OF WORK - CASH PAYMENTS EVENT NUMBER(S)/DATE(S): _____

PROPERTY NAME: Bronson Property

CLAIM NAME(S) (on which the work was done): BRONSON NE, BRONSON NORTH, BRONSON, BRONSON EAST

COMMODITIES SOUGHT: Cu, Co, Ag

MINERAL INVENTORY MINFILE NUMBER(S), IF KNOWN: 094K015, 094K019, 094K027 094K030, 094K041, 094K042, 094K052, 094K055

MINING DIVISION: Liard **NTS/BCGS:** 094K/03

LATITUDE: 58 ° 11 ' 37.57 " **LONGITUDE:** 125 ° 16 ' 44.80 " (at centre of work)

OWNER(S):
1) A.R. Raven 2) _____



MAILING ADDRESS:
P.O. Box 722
Smithers, B.C. V0J 2N0

OPERATOR(S) [who paid for the work]:
1) Fabled Copper Corp 2) _____

MAILING ADDRESS:
Suite 2300-1066 West Hastings Street
Vancouver, British Columbia, V6E 3X2

PROPERTY GEOLOGY KEYWORDS (lithology, age, stratigraphy, structure, alteration, mineralization, size and attitude):
Copper mineralization in diabase and quartz carbonate dyke(s) cutting Gataga and Aida Formation calcareous mudstone, dolomitic slate, silty mudstone

REFERENCES TO PREVIOUS ASSESSMENT WORK AND ASSESSMENT REPORT NUMBERS: 10960A, 05777, 28281

TYPE OF WORK IN THIS REPORT	EXTENT OF WORK (IN METRIC UNITS)	ON WHICH CLAIMS	PROJECT COSTS APPORTIONED (incl. support)
GEOLOGICAL (scale, area)			
Ground, mapping			
Photo interpretation	1: 5000 Scale Interpretation	BRONSON NE, BRONSON NORTH, 	4500
GEOPHYSICAL (line-kilometres)			
Ground			
Magnetic			
Electromagnetic			
Induced Polarization			
Radiometric			
Seismic			
Other			
Airborne			
GEOCHEMICAL (number of samples analysed for...)			
Soil			
Silt			
Rock	3 samples - Multielement assay data	BRONSON NE- includes all field costs	\$13,361.40
Other			
DRILLING (total metres; number of holes, size)			
Core			
Non-core			
RELATED TECHNICAL			
Sampling/assaying	Geochemical analysis of Bronson Ge	BRONSON NE, BRONSON NORTH, 	5400
Petrographic			
Mineralographic			
Metallurgic			
PROSPECTING (scale, area)			
PREPARATORY / PHYSICAL			
Line/grid (kilometres)			
Topographic/Photogrammetric (scale, area)			
Legal surveys (scale, area)			
Road, local access (kilometres)/trail			
Trench (metres)			
Underground dev. (metres)			
Other	Report preparation		4500.00
		TOTAL COST:	27,761.40

ASSESSMENT REPORT

describing

**HISTORICAL GEOCHEMICAL REVIEW AND IMAGE ANALYSIS INVESTIGATIONS OF THE
BRONSON PROPERTY
EVENT # 5777657**

NTS 94K
Latitude 58°11N; Longitude 125°16W

Liard Mining Division
British Columbia

prepared by

Venessa Bennett, Ph. D, P. Geo, Adv. Dip RS/GIS
Geomantia Consulting
33 Roundel Rd
Whitehorse, YT
Y1A 3H4
(867) 335 5245
geomantia@hotmail.com

for

A.R RAVEN (OWNER)
P.O. Box 722
SMITHERS, B.C. V0J 2N0
hirange@telus.net

&

FABLED COPPER CORP. (OPERATOR)

Table of Contents

1.0 : Introduction.....	1
1.1 Property, Location and Access.....	4
1.2 Physiography and Vegetation.....	4
1.3 Previous Work.....	5
2.0 Regional Geology and Geophysics.....	8
3.0 Mineralization and Deposit Models.....	16
4.0 Neoproterozoic Diabase Distribution.....	18
5.0 Bronson Property Geology and 2019 Prospecting Results.....	30
6.0 Historical Geochemical Analysis.....	40
6.1 Rock Analysis.....	49
6.2 Sample Catchment Basin Analysis – Bronson.....	63
6.3 Bronson Property Soil Data Analysis.....	80
7.0 Summary and Recommendations.....	117
8.0 References.....	119
APPENDIX 1: STATEMENT OF QUALIFICATIONS.....	122
APPENDIX 2: STATEMENT OF COSTS.....	124
APPENDIX 3: ANALYSIS CERTIFICATES.....	126

LIST OF FIGURES

Figure 1: Location of the Bronson Property, NW BC.....	2
Figure 2: Mineral Tenure for the Bronson Property.....	3
Figure 3: Regional Mineral occurrence Map.....	7
Figure 4: Regional Geological Setting.....	9
Figure 5: Stratigraphic column from Carne (2006).....	10
Figure 6: Total Residual Magnetic Field Data.....	13
Figure 7: Gravity – Bouguer Anomaly data.....	14
Figure 8: Overlapping residual gravity/magnetic anomalies, IOCG deposits.....	15
Figure 9: 1: 5000 scale search grid used to map diabase units.....	19
Figure 10: Location of Diabase dykes within search area.....	20
Figure 11: Diabase domain map.....	22
Figure 12: Diabase dyke intensity map.....	23
Figure 13: Diabase dyke intensity map & mineral occurrences distribution.....	24
Figure 14: Property scale residual aeromagnetic data & Diabase location.....	25
Figure 15: Deformation of diabase dykes.....	27
Figure 16: Two main generations of diabase dyking.....	28
Figure 17: Structural controls on diabase emplacement.....	29
Figure 18: Bronson Property Geology.....	31
Figure 19: Bronson property total magnetic field data.	32
Figure 20: (a) Diabase dyke suite 1. (b) Diabase dyke suite 2.....	34
Figure 21: Structural interpretation of the Bronson Property.....	35
Figure 20: Examples of mineralization from Bronson veining.....	36
Figure 22: Location and Cu percent grades of prospecting, Bronson property.....	38
Figure 23: Photographs of Bronson diabase assay samples.....	39
Figure 24: Location of 2005 rock prospecting samples.....	41

Figure 25: Location of 2005 regional silt samples.....	42
Figure 26: Location of 2005 Bronson and Book soil grids.....	43
Figure 27: Proportion of non-detects for 2005 rock samples.....	46
Figure 28: Proportion of non-detects for 2005 silt samples.....	47
Figure 29: Proportion of non-detects for 2005 Bronson and Book soil grids.....	48
Figure 30: X-Y Scatter plot of Cu versus S, As, Ag, Co and Ni.....	51
Figure 31: X-Y Scatter plot of Cu versus Mg and Mn.....	52
Figure 32: X-Y Scatter plot of Cu versus Fe and Elevation versus Cu and Co.....	53
Figure 33: Clustering dendrogram for 2005 rock prospecting samples.....	56
Figure 34: Eigenvalue vs principal component plot for 2005	58
Figure 35: Graphical representation of PCA loadings 2005 rock samples.....	62
Figure 36: Sample catchment basins for project area & for the Bronson Property.....	65
Figure 37: Bronson sample catchment basin results - Cu.....	69
Figure 38: Bronson sample catchment basin results – Cu with rock samples and diabase dykes superimposed.....	70
Figure 39: Bronson sample catchment basin results - S.....	71
Figure 40: Bronson sample catchment basin results - As.....	72
Figure 41: Bronson sample catchment basin results - Ni.....	73
Figure 42: Bronson sample catchment basin results - Co.....	74
Figure 43: Bronson sample catchment basin results - Principal Component 1.....	78
Figure 44: Bronson sample catchment basin results - Principal Component 1 with rock samples and diabase dykes superimposed.....	79
Figure 45: Scatterplots for Book 1 soil grid.....	87
Figure 46: Dot plots & IDW interpolation raster for Cu, Book 1 soil grid.....	89
Figure 47: Dot plots & IDW interpolation raster for Co, Book 1 soil grid.....	90
Figure 48: Dot plots & IDW interpolation raster for As, Book 1 soil grid.....	91

Figure 49: Dot plots & IDW interpolation raster for Ca, Book 1 soil grid.....	92
Figure 50: Dot plots & IDW interpolation raster for S, Book 1 soil grid.....	93
Figure 51: Dot plots & IDW interpolation raster for Ni, Book 1 soil grid.....	94
Figure 52: Dot plots & IDW interpolation raster for Pb, Book 1 soil grid.....	95
Figure 53: Scatterplots for Book2 soil.....	97
Figure 54: Dot plots & IDW interpolation raster for Cu, Book 2 soil grid.....	98
Figure 55: Dot plots & IDW interpolation raster for Co, Book 2 soil grid.....	99
Figure 56: Dot plots & IDW interpolation raster for Ca, Book 2 soil grid.....	100
Figure 57: Dot plots & IDW interpolation raster for Ni, Book 2 soil grid.....	101
Figure 58: Dot plots & IDW interpolation raster for Cr, Book 2 soil grid.....	102
Figure 59: Dot plots & IDW interpolation raster for Mn, Book 2 soil grid.....	103
Figure 60: Dot plots & IDW interpolation raster for K, Book 2 soil grid.....	104
Figure 61: Scatterplots for Bronson soil grid.....	106
Figure 62: Dot plots & IDW interpolation raster for Cu, Bronson soil grid.....	107
Figure 63: Dot plots & IDW interpolation raster for Co, Bronson soil grid.....	108
Figure 64: Dot plots & IDW interpolation raster for Ni, Bronson soil grid.....	109
Figure 65: Dot plots & IDW interpolation raster for S, Bronson soil grid.....	110
Figure 66: Dot plots & IDW interpolation raster for Mn, Bronson soil grid.....	111
Figure 67: Dot plots & IDW interpolation raster for Zn, Bronson soil grid.....	112
Figure 68: Dot plots & IDW interpolation raster for Ca, Bronson soil grid.....	113
Figure 69: Cluster analysis results for the Book 1, Book 2 and Bronson soil grids.....	116

LIST OF TABLES

Table 1: Bronson Property Claim Data Summary.....	4
Table 2: Bronson 2019 rock prospecting results.....	37
Table 3: Spearman Rank correlation matrix for 2005 rock prospects samples.....	54
Table 4: Eigenvalues from PCA 2005 rock prospect samples.....	60
Table 5: Loadings for statistically meaningful principal components (PC 1 – PC3).....	61
Table 6: Spearman Rank correlation matrix for 2005 Bronson contour soil samples.....	76
Table 7: Summary statistics for Cu-Co and pathfinders, Bronson contour soil dataset.....	77
Table 8: Book 1 Soil Grid summary statistics for Cu and pathfinders.....	81
Table 9: Spearman Rank correlation matrix results - Book 1 Soil Grid.....	82
Table 10: Book 2 Soil Grid summary statistics for Cu and pathfinders.....	83
Table 11: Spearman Rank correlation matrix results - Book 2 Soil Grid.....	84
Table 12: Bronson Soil Grid summary statistics for Cu and pathfinders.....	85
Table 13: Spearman Rank correlation matrix results - Bronson Soil Grids.....	86

1.0 INTRODUCTION

The following report presents results from detailed data compilation and analysis work carried out on high resolution multiband satellite imagery, regional aeromagnetic and gravity data and historical rock, silt and soil geochemical datasets in the vicinity of the Bronson property located in north western British Columbia (**Fig. 1**). The claims are currently owned by Mr. Alan R. Raven of Smithers, B.C and operated by Fabled Copper Corp. The Bronson property comprises 4 mineral tenures covering approximately 2,524.6 ha (**Fig. 2**). A half day was spent on the property in September 2019.

The Bronson property is located within the Muskwa Anticlinorium, a Proterozoic assemblage of sedimentary rocks considered to be temporally related to parts of the Wernecke Supergroup in Yukon, which host significant iron-oxide copper-gold (IOCG) mineralization (Carne, 2006). Several historic copper mines exist within the district, the most significant of which is the Magnum deposit which was discovered in the late 1960s and saw intermittent mining until 1974. Approximately 598 000 tonnes of copper ore was processed grading ~ 3.0 % (Coetzee, 2007).

The key objectives of this work were to:

- i) Compile and undertake detailed analysis of all available imagery and historical exploration datasets to assist in regional and local-scale targeting and providing a better understanding of Cu-Co mineralization within the district.
- ii) Centralize all available data in a compiled GIS workspace for future use by Fabled Copper Corp. staff.

All work was conducted by Geomantia Consulting who has been contracted by Fabled Copper Corp. to assist with data analysis and report writing. A Statement of Qualifications appears in Appendix I and the Statements of Costs appear in Appendix II.

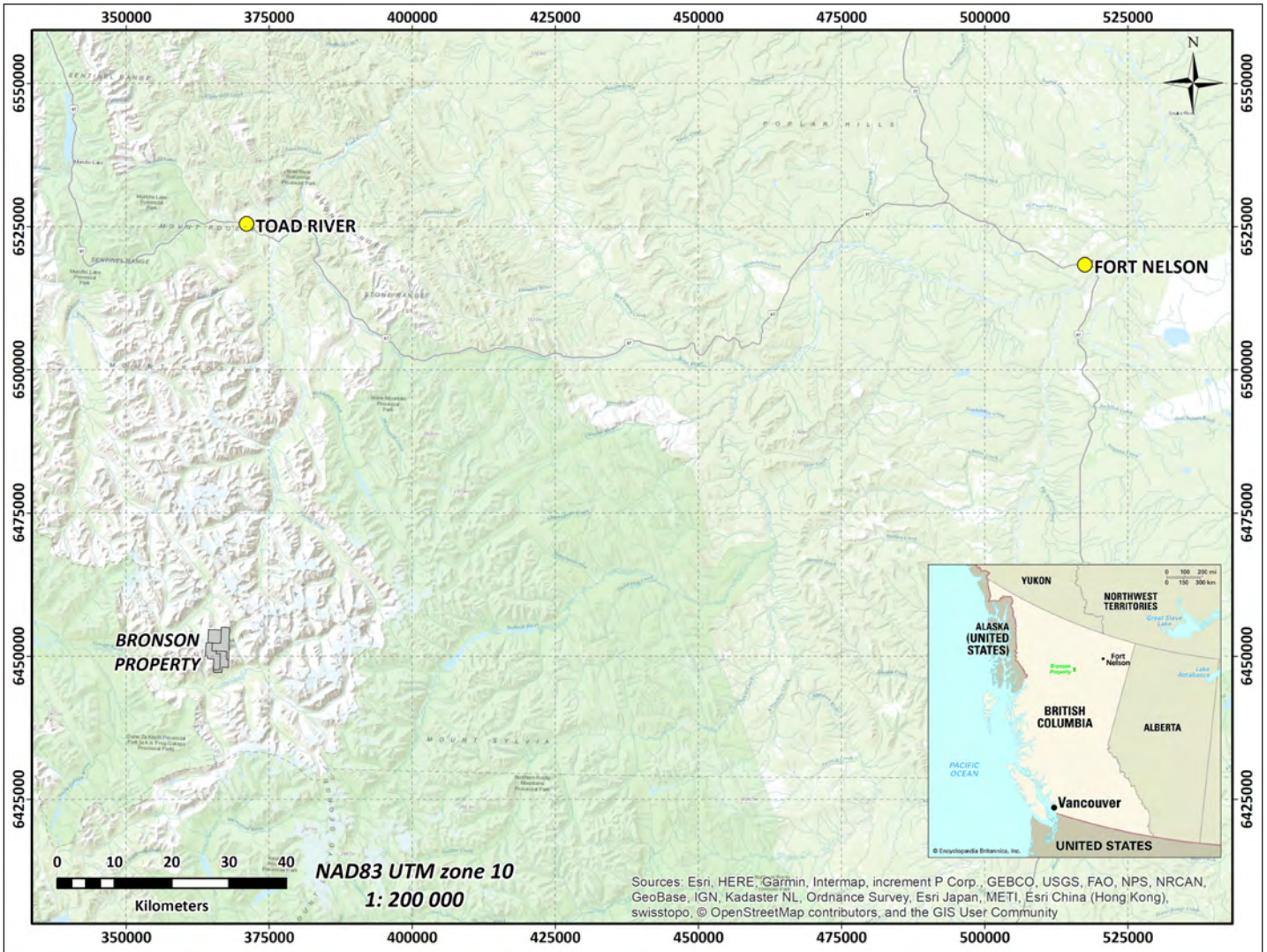


Figure 1: Location of the Bronson Property, NW BC

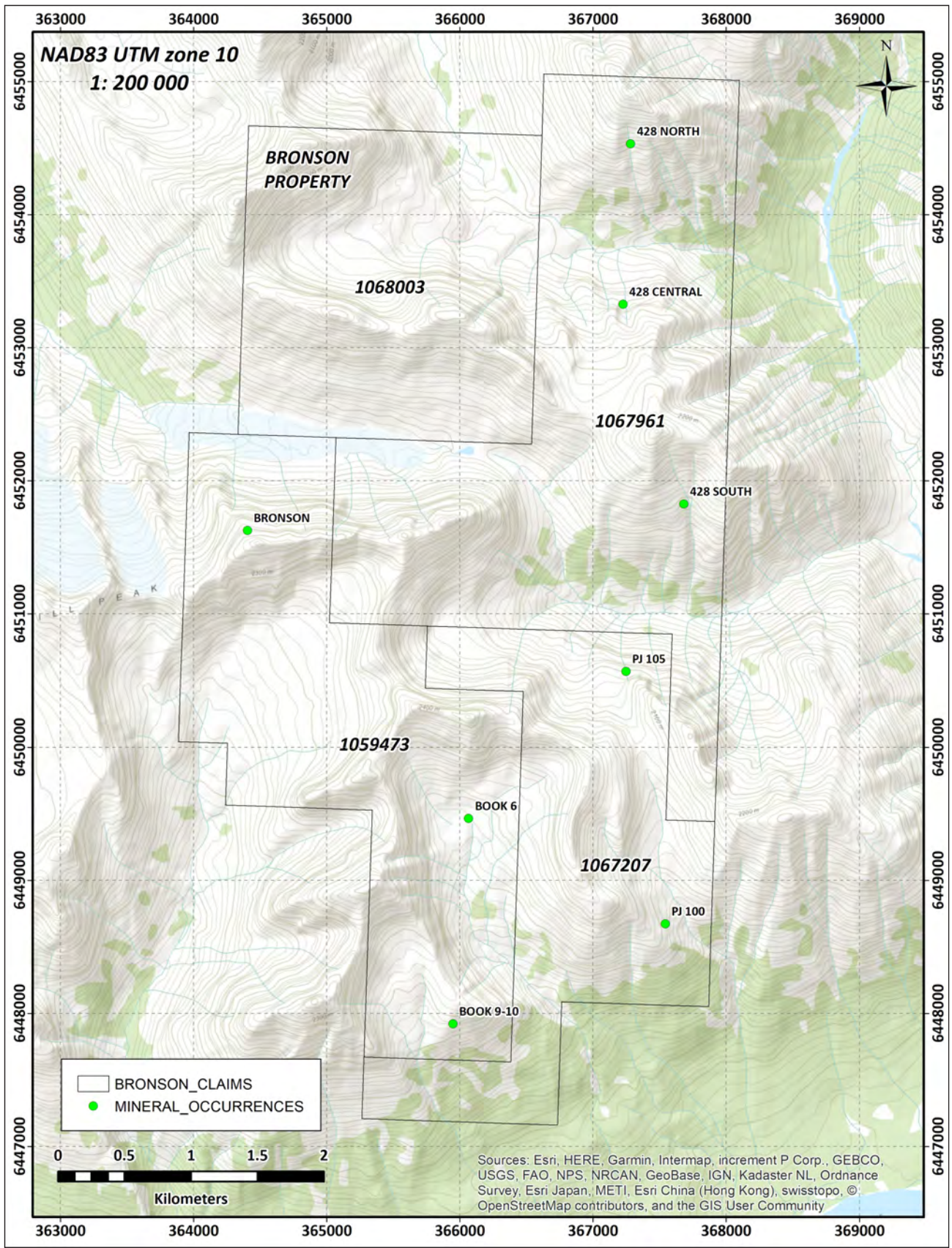


Figure 2: Mineral Tenure for the Bronson Property

1.1 PROPERTY, LOCATION AND ACCESS

The Bronson property is located approximately 530 km NNW of Prince George, 155 km WSW of Fort Nelson, B.C. and 74 km S of Toad River (**Fig. 1**). The claim area is centered at latitude 58°11'11.67" N, and longitude 125°11'32.51" W within the Northern Canadian Rocky Mountain Ecoregion², specifically in the eastern Muskwa Ecosection. The area is flanked by the Northern Rocky Mountain Park to the east, Muncho Lake Park to the north, Dune Za Keyih Park to the west and Kwadacha Wilderness Park to the south (Carne 2006). The four mineral tenures of the Bronson property are located in the Liard Mining Division on NTS map sheet 94K. Claim data are listed in **Table 1** while the locations of the individual tenures are shown on **Figure 2**.

Elevation ranges from 1400 m to 2480 m above mean sea level. Access is by helicopter from the Toad River airstrip. During field 2019 field activities attention was paid to outfitter's schedules and helicopter flight paths respected existing legislation pertaining to shared land use.

Tenure_No.	Claim_Name	Owner	Issue_Date	Good-To_Date	Area(Ha)
1067961	BRONSON NE	RAVEN, ALAN ROBERT	17-Apr-19	17-Apr-20	869.715
1068003	BRONSON NORTH	RAVEN, ALAN ROBERT	18-Apr-19	18-DApr-20	511.48
1059473	BRONSON	RAVEN, ALAN ROBERT	21-Mar-18	21-Mar-20	665.491
1067207	BRONSON EAST	RAVEN, ALAN ROBERT	13-Mar-19	13-Mar-20	477.882

Table 1: Bronson Property Claim Data Summary

1.2 PHYSIOGRAPHY & VEGETATION

The following is summarized from Carne (2005) and Campbell (2016). The Bronson property is centred on Churchill Peak and is characterized by significant topographic relief with pronounced peaks, jagged ridges and wide U-shaped valleys occupied by braided rivers. Lower

slopes are covered by open scree grading into moderate to dense growths of spruce trees on valley bottoms. Both the Alpine Tundra and the Spruce-Willow-Birch climatic zones are represented on the Muskwa property. Tree line is at approximately 1400 m. Local glaciation has produced numerous moraines and has deposited variable thicknesses of till up to an elevation of about 1500 m. A number of small glaciers still exist at high elevations particularly in north facing cirques. Creeks draining the property flow into the Gataga River and the North Gataga River.

This area is protected from moist Pacific air moving over the mountains to the west, however low-pressure storms in Alberta pushing moisture eastward over the Alberta Plateaus to the east can result in extreme rain events. In the winter and early spring, dense, cold Arctic air can invade this area by coming down the Interior Plains to the north.

1.3 PREVIOUS WORK

The following summary of work history in the project area is taken from Carne (2006). The discovery of copper mineralization in the Muskwa Anticlinorium in the early 1960s was followed by intense regional exploration focussed on the high grade copper bearing quartz-carbonate vein deposits. The work resulted in recognition of numerous copper occurrences, the most significant of which is the Magnum Deposit (**Fig. 3**). The Eagle vein at the Davis-Keays copper prospect underwent surface and underground development at the same time as the Magnum Deposit, with semi-proven reserves in 1971 of 1,119,089 tonnes grading 3.43 per cent copper (BC Minfile 094K 012). In the southern portion of the project area, the Bronson, Book 6, Book 9/10 and Toro prospects also received advanced exploration. The Bronson Prospect was explored in the early 1970s by Windermere Exploration Ltd. with drilling, prospecting and detailed mapping. This work investigated a discordant quartz-carbonate vein system containing areas of high grade copper mineralization. Mountaineers employed by Windermere conducted geological mapping and sampling of the showing, using ropes to access the sheer cliffs of Bronson Mountain. Reported grades range from 6 to 17 % copper and up to 4.8 g/t silver. Assays from a set of nearby subparallel veins were combined to produce a weighted average of

2.7% copper over a total width of 33.5 m (Assessment Report 2487). Subsequent to cessation of mining in 1974, major exploration activities ceased in the region until the early 2000's when Archer Cathro and Associates Ltd., carried out an regional exploration program to assess the district for Iron-Oxide-Copper-Gold (IOCG) mineral potential.

Exploration carried out by Archer Cathro and Associates Ltd. both on and in the vicinity of the Bronson property consisted of regional and detailed prospecting, regional silt and pan sampling, mapping and prospect scale-soil sampling. Geochemical sampling consisted of 30 rock samples, 761 soil samples and 17 silt samples. These data are re-evaluated and discussed below. A property-wide geophysical survey was flown by Sanders Geophysics Ltd. of Ottawa, Ontario. Approximately 9,002 line kilometres of airborne magnetic data were acquired. The traverse lines were flown at 400 m spacing and oriented at 58° with control lines at 2 km spacings and oriented at 148°. The survey was flown at a height of 150 m above the minimum drape surface. Raw magnetic data was processed by Aurora Geosciences Ltd. to remove the underlying regional magnetic gradient. No significant exploration work has occurred on the Bronson property since 2005.

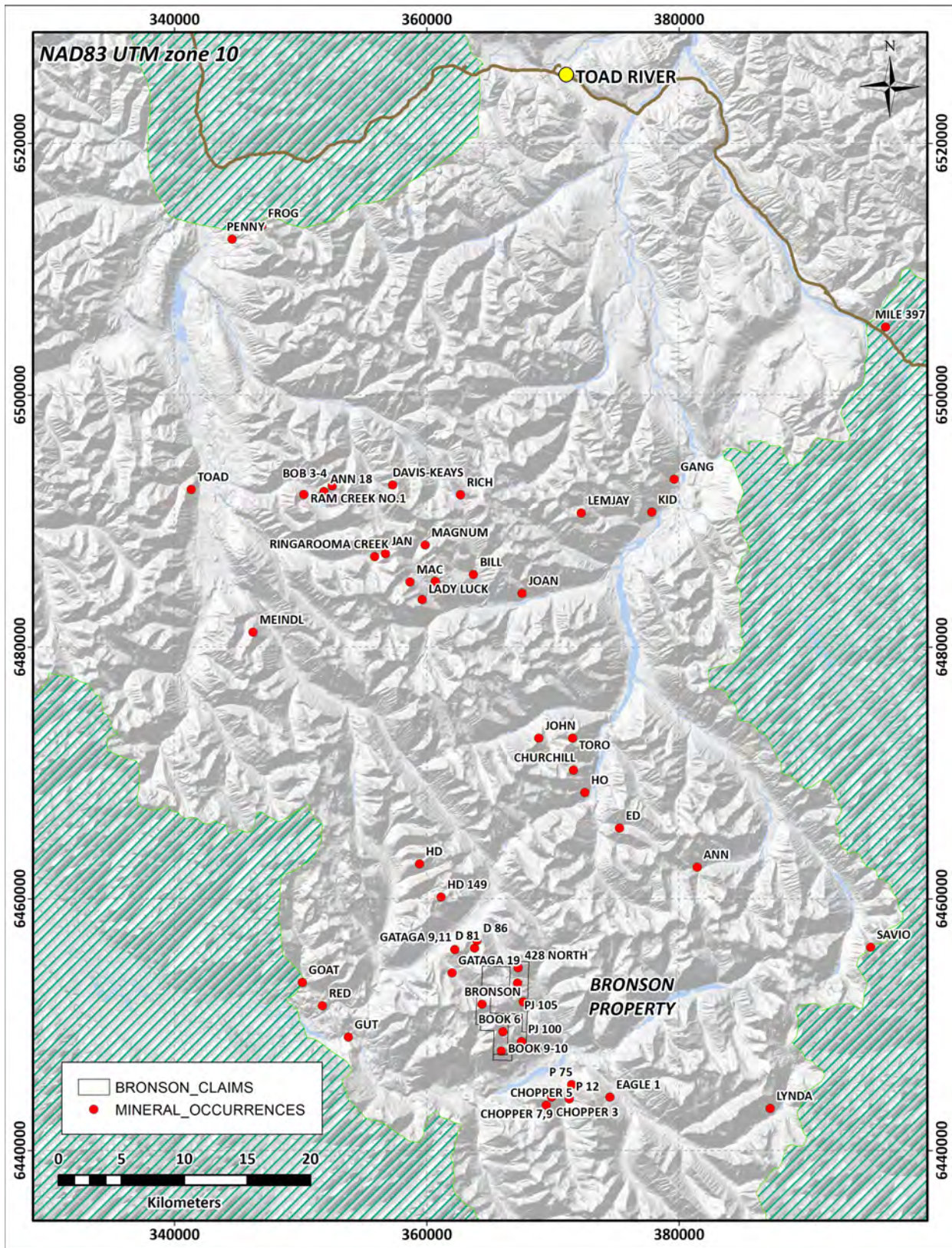


Figure 3: Regional Mineral occurrence Map

2.0 REGIONAL GEOLOGY and GEOPHYSICS

The following description of regional geology is summarized from Carne (2006). The Bronson property and surrounding Cu-Co vein occurrences are located in the Cordilleran Foreland Belt in the northern Rocky Mountains. The district is characterized by broad belt of sedimentary rocks that have undergone polyphase deformation, the youngest of which has resulted in open to tight and upright to inclined folding and a stack of northeast verging thrust or reactivated reverse faults (**Fig. 4**). The structural trend throughout the Rocky Mountains is predominantly northwest. The main structural feature in the Cu-Co vein district is the Muskwa Anticlinorium, a major north-northwest trending window that exposes rocks as old as Middle Proterozoic (Helikian).

The Pre-Paleozoic package is collectively referred to as the Muskwa Assemblage and consists of a 6400 m thick succession of argillaceous to fine grained siliciclastic strata and carbonates. Seven formations of Proterozoic age are represented in the anticlinorium (**Fig. 5**). From oldest to youngest, with approximately true thickness, they are the Chischa Fm (940 m), Tetsa Fm (320 m), George Fm (360-530 m), Henry Creek Fm (460 m), Tuchodi Fm (1500 m), Aida Fm and Gataga Fm (3000 m together). Paleozoic units unconformably overlie the Proterozoic rocks along a Lower Cambrian erosional surface.

The Tuchodi Fm is the oldest outcropping unit occurring with the Cu-Co district. It comprises medium to thin bedded quartzite and quartz flooded dolomitic siltstone and argillite. This formation is relatively resistant to weathering and often forms an obvious bench on hill slopes where overlain by the more recessive weathering Aida Fm and Gataga Fm.

The Aida Fm conformably overlies the Tuchodi Fm and is composed of buff weathered calcareous and dolomitic siltstone and mudstone with minor amounts of sandstone. Two generations of penetrative slaty cleavage are well developed in the rocks of this formation.

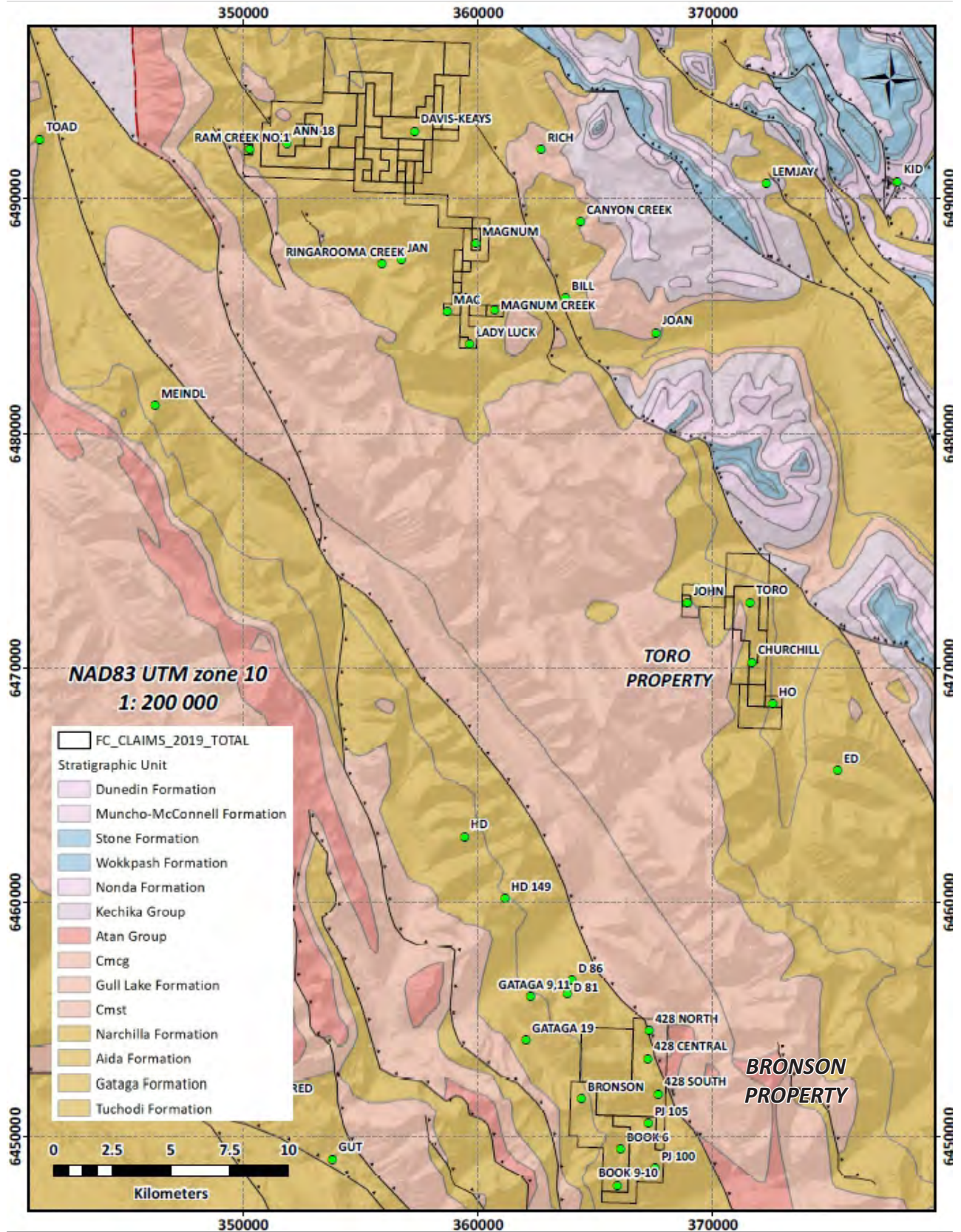


Figure 4: Regional Geological Setting

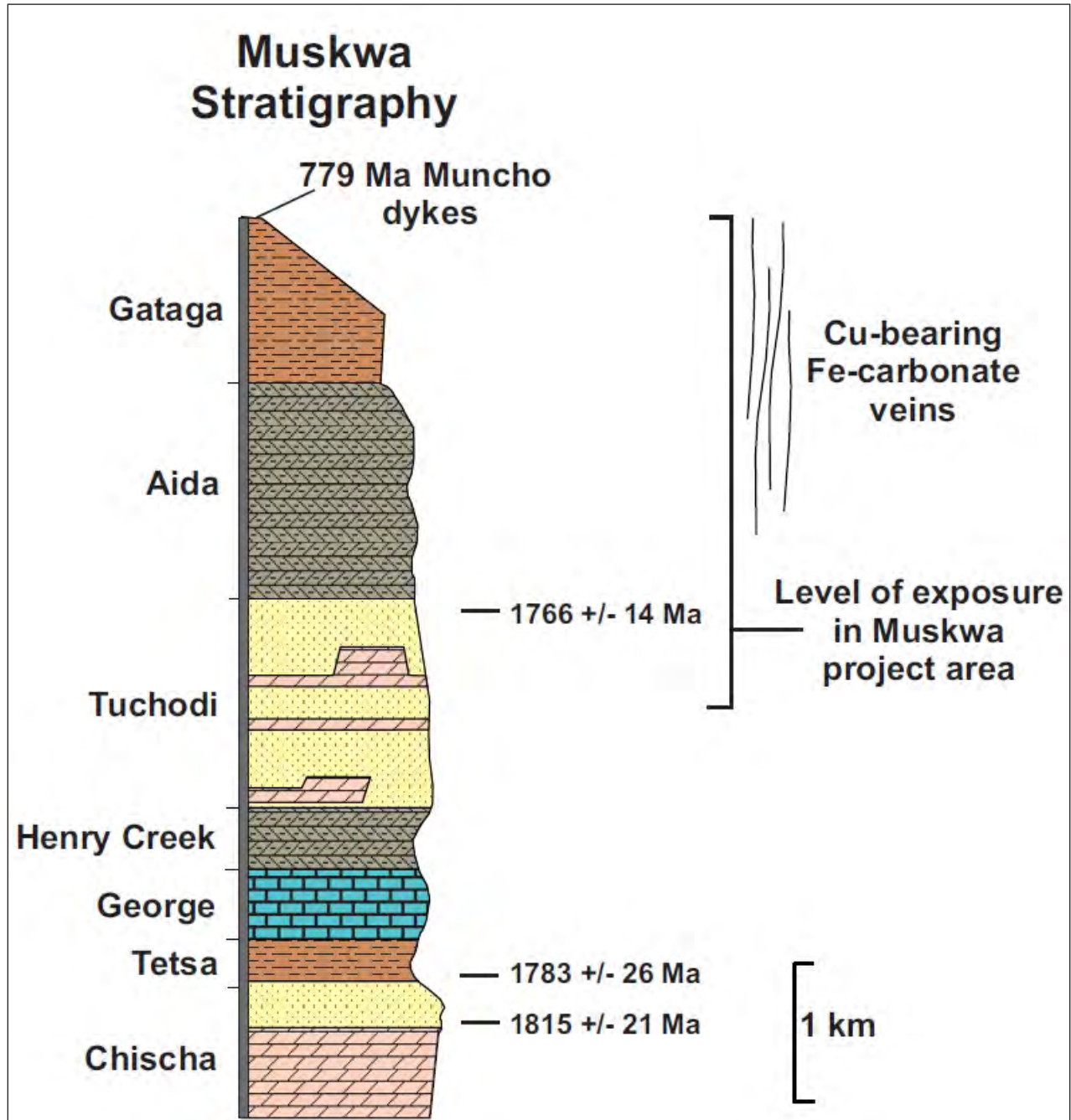


Figure 5: Stratigraphic column from Carne 2006

The Gataga Fm conformably overlies the Aida Fm and is characterized by black carbonaceous shales. Its rocks are well cleaved and dark weathered. Their lithologies and the presence of turbidite structures and soft sediment deformation indicate that the Aida Fm and Gataga Fm were deposited in a deep water setting (Ross et al., 2001).

Paleozoic stratigraphy in the region is Cambrian to Devonian in age. These strata unconformably overly the Proterozoic formations and are mainly composed of carbonaceous and siliceous units, including limestone, dolomite, quartzite and quartz pebble conglomerate.

The Proterozoic formations are crosscut by a series of apparently Hadrynian aged gabbro and diabase dykes. The dykes range between 5 to 35m in width and follow the main north-northwest structural orientation of the area. The majority of the dykes are moderately to strongly magnetic. They form prominent linear features that resist weathering.

Low grade metamorphism, mainly subgreenschist, is evident throughout the Proterozoic sedimentary package. Contact metamorphism along the periphery of the dykes is rare but, where present, consists of sericite and chlorite alteration.

Thrust faults, reverse faults and moderate folding characterize the structural history of the area. Late Helikian or early Hadrynian structures are represented by high angle fault zones that have been intruded by dyke swarms. These structural zones are considered to be deep-seated and have been observed to be up to 180 m wide, hinting at an extensional tectonic environment. Their inferred strike lengths are in the order of tens of kilometres. Copper bearing quartz carbonate veins were emplaced along these same structures and are mainly found along side the diabase units. Shearing is common along the dyke contacts with the wallrocks and veins.

Low angle, westerly dipping thrust faults have in some areas stacked Proterozoic basement rocks above the Paleozoic cover rocks. These faults are north-south trending and

extend over hundreds of kilometres. Faults and folds in the Muskwa area developed during Jurassic to Tertiary times.

Regional airborne magnetic and gravity surveys are available for the project area from Natural Resources Canada (NRCAN; **Figs. 6 & 7**). These were downloaded and assembled into the compilation GIS workspace for the project. The aeromagnetic data consists of residual total field and first vertical derivative data. Seven airborne gravity datasets are available including:

- i) Bouguer anomaly data
- ii) First vertical derivative
- iii) Free air gravity data
- iv) Horizontal gravity gradient data
- v) Isostatic residual gravity data
- vi) Total observed gravity data
- vii) Gravity anomaly data

Integrated gravity and magnetic data are critical targeting tools for IOCG mineralization. In many known deposits, mineralization occurs at the edge of a magnetic high and in the center of the residual positive gravity anomaly (Austin and Foss 2012; **Fig. 8**).

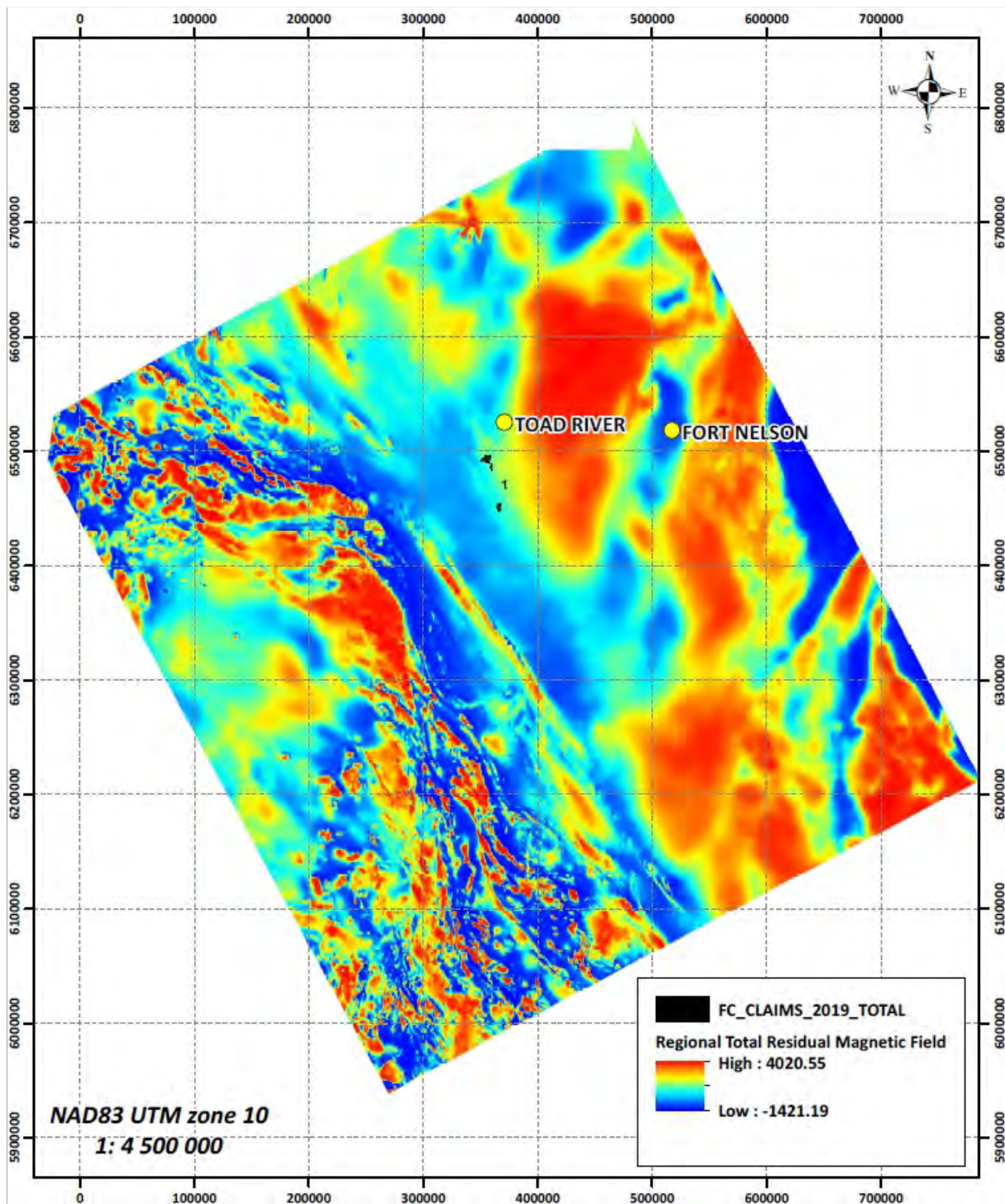


Figure 6: Total Residual Magnetic Field Data

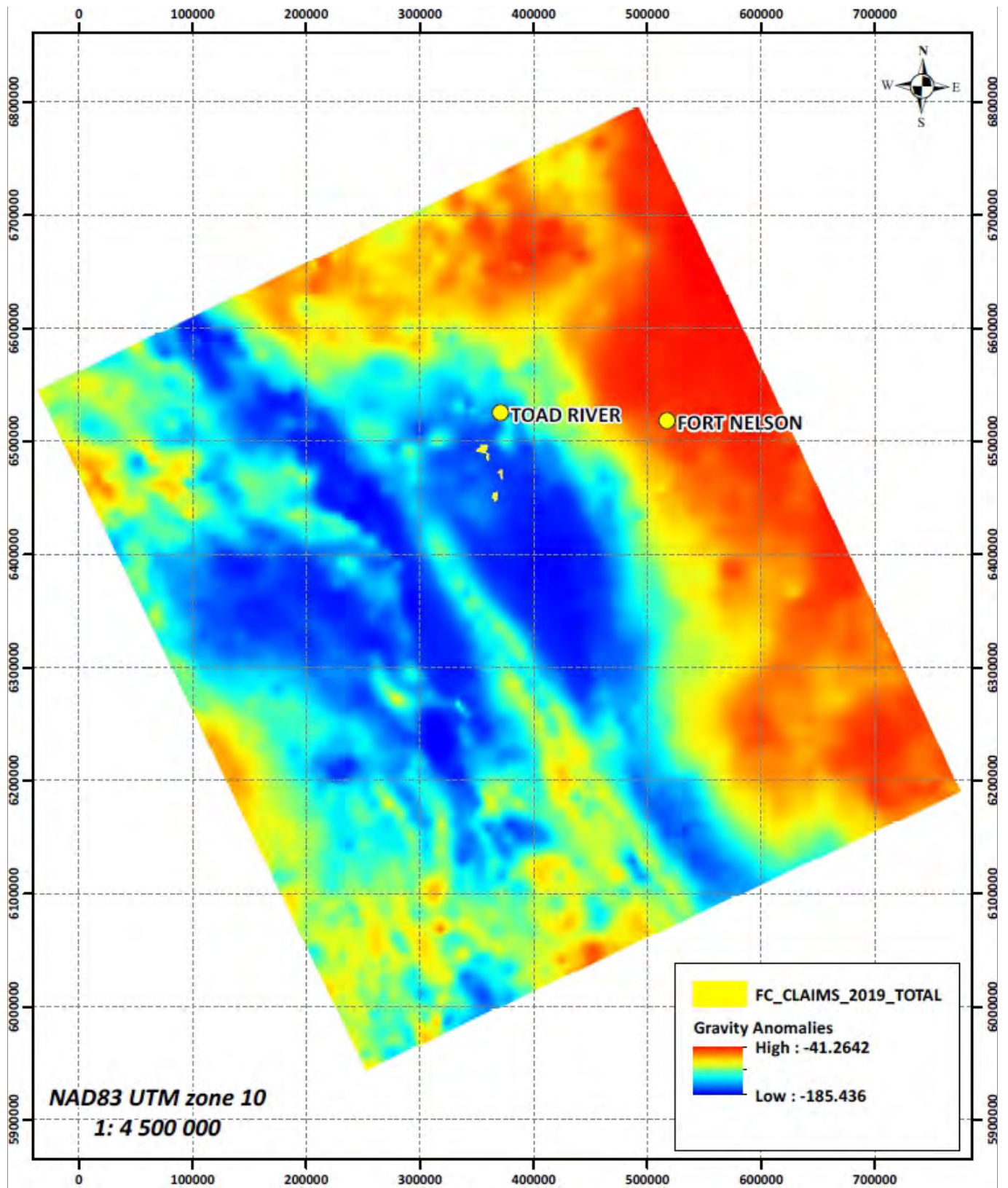


Figure 7: Gravity – Bouguer Anomaly data

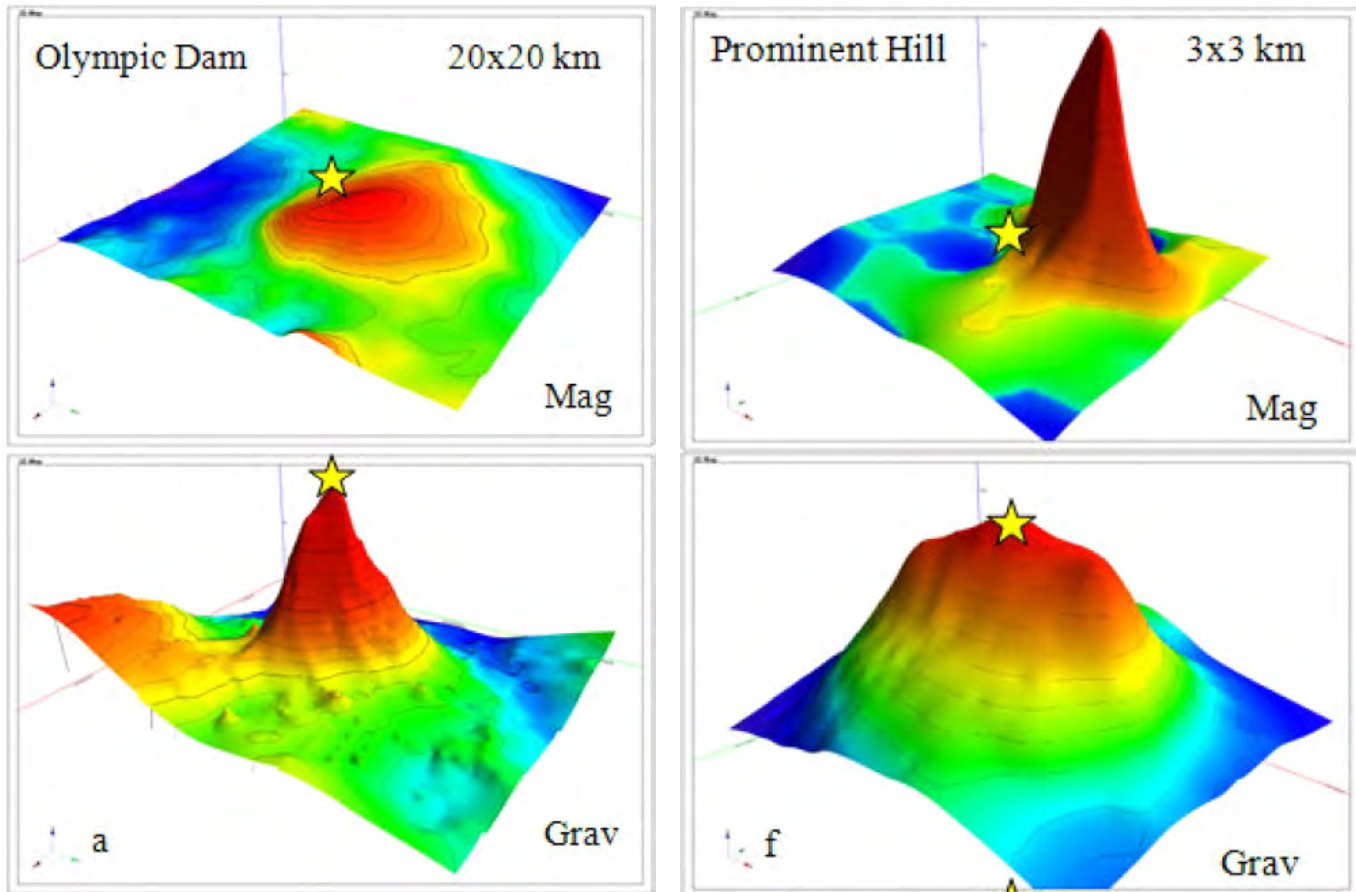


Figure 8: Examples of overlapping residual gravity and magnetic anomalies over known ICG deposits

3.0 MINERALIZATION AND DEPOSIT MODELS

Copper mineralization throughout the property is associated primarily with copper bearing quartz iron carbonate veins emplaced along NNW, N and NNE near vertical structures. The veins often have strike lengths over 1 km and range from stringer zones to widths of 4 m. Chalcopyrite and malachite are the dominant copper minerals with minor bornite and chalcocite. Mineralization consists of lenses, stringers and/or blebs of copper minerals in the host veins. The majority of the occurrences host patchy and sporadic mineralization throughout the structures. Copper mineralization is often better developed at the contact zones between the quartz-iron carbonate vein systems and adjacent diabase dykes, likely due to local elevated Fe contents.

In addition to the copper-bearing quartz iron-carbonate veins, several iron oxide breccia zones have been discovered in the region. The Dieppe and Matnik occurrences have both reported the presence of hematite breccias.

The IOCG deposit model was first suggested by Archer Cathro and Associates Ltd in 2005 for the Cu-Co mineralization present in the region. Iron-Oxide-Copper-Gold deposits are considered to be (i) magmatic-hydrothermal deposits containing economic quantities of Cu and Au, (ii) are structurally controlled containing significant breccia volumes and are (iii) often associated with pre-ore sodic or sodic-calcic alteration (Groves et al. 2010). Additionally, these deposits have abundant low-Ti iron oxides and/or iron silicates associated with, but generally paragenetically older than the Cu-Fe sulphides (Groves et al. 2010). Pyrite is generally low in overall abundance and widespread quartz veining or silicification is absent (Groves et al. 2010). Finally, IOCG deposits have clear temporal relationship to major magmatic intrusions. These systems are theorized to transition into the epithermal mineralizing environment if erosion is minimal and permits preservation.

Iron oxide-copper-gold (IOCG) mineralization is associated with the pathfinder elements **Ag, As, Au, Ba, Bi, Ca, Cd, Ce, Co, Cr, Cs, Cu, F, Fe, K, La, Mn, Mo, Ni, S, Sb, Se, Sn, Te, U and W** (Mark et al. Wang et al. 2013; Hill et al. 2014;) and are often preserved within hydrothermal alteration halos that can be linked to mineralization. As an example, an alteration signature may progress from regional Na-enriched, K-depleted alteration to camp-scale Mn, K, and Ba enrichment and Na-depleted alteration to deposit scale alteration enrichment in Ag, Au, Bi, Cu, Fe, K, Mo, Sb and U (Porter 2010).

An important objective of the analysis work presented in this report is to test whether the Cu-Co mineralization present in the project area shares any of the key features that characterize IOCG mineralizing systems.

4.0 NEOPROTEROZOIC DIABASE DYKE DISTRIBUTION

Neoproterozoic diabase units within the district have a spatial coincidence with Cu vein mineralization. The diabase units vary in orientation from NNW to N to NE. A district-scale understanding of the geometric distribution and dyking intensity of diabase units will:

- i) Better constrain the distribution of Cu prospective areas.
- ii) Provide constraints on structural controls associated with mineralization and diabase emplacement, and
- iii) Define structural blocks associated with Jurassic-Cretaceous compressional deformation.

Publicly available high resolution satellite imagery was used to map out and analyse the spatial distribution of Neoproterozoic diabase units within an area considered to be prospective for Cu-Co mineralization. Regional geology, aeromagnetic and gravity datasets were used to define the prospective area. The coincidence of Proterozoic stratigraphy and a regional Bouguer gravity anomaly low, east of the crustal scale Tintina fault, was selected as the area in which to map out the diabase units (**Fig. 9**).

A 1:5000 scale search grid was generated and each 5 k grid square was subsequently reviewed for the:

- i) Presence of diabase units which if present were digitized, and
- ii) Presence of significant iron oxide colour anomalies which were flagged for follow-up.

Diabase distribution

Neoproterozoic diabase was only observed in the central eastern portion of the search grid area (**Fig. 10**). Diabase orientations vary throughout the area of interest (AOI) from NNW

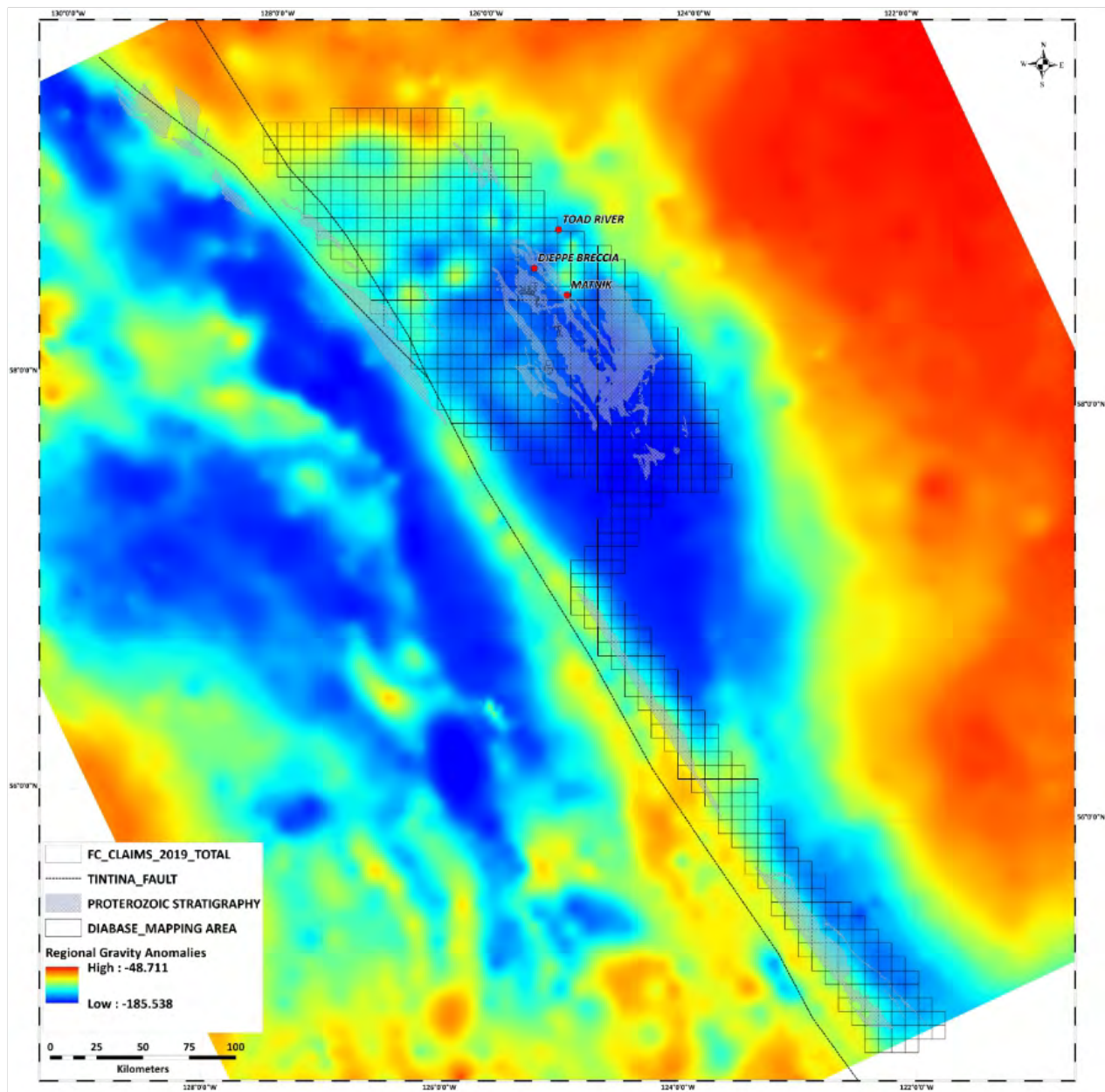


Figure 9: Regional aeromagnetic, gravity, regional geology and 1: 5000 scale search grid used to map diabase units.

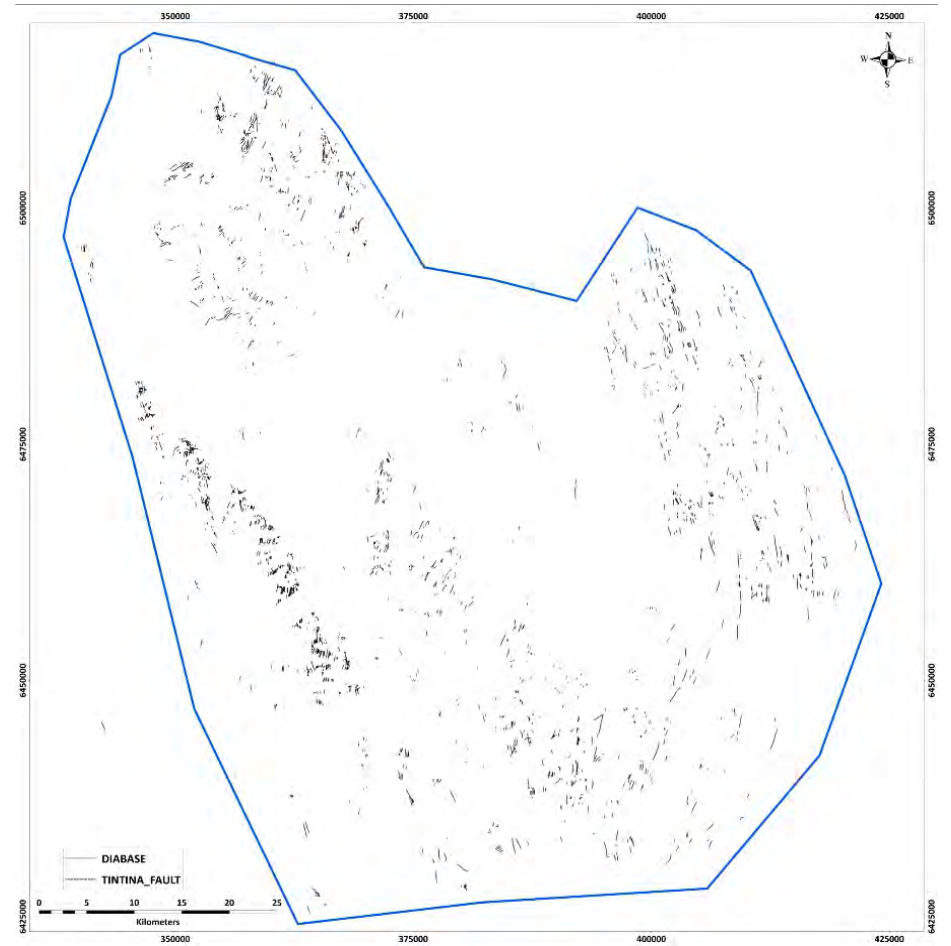
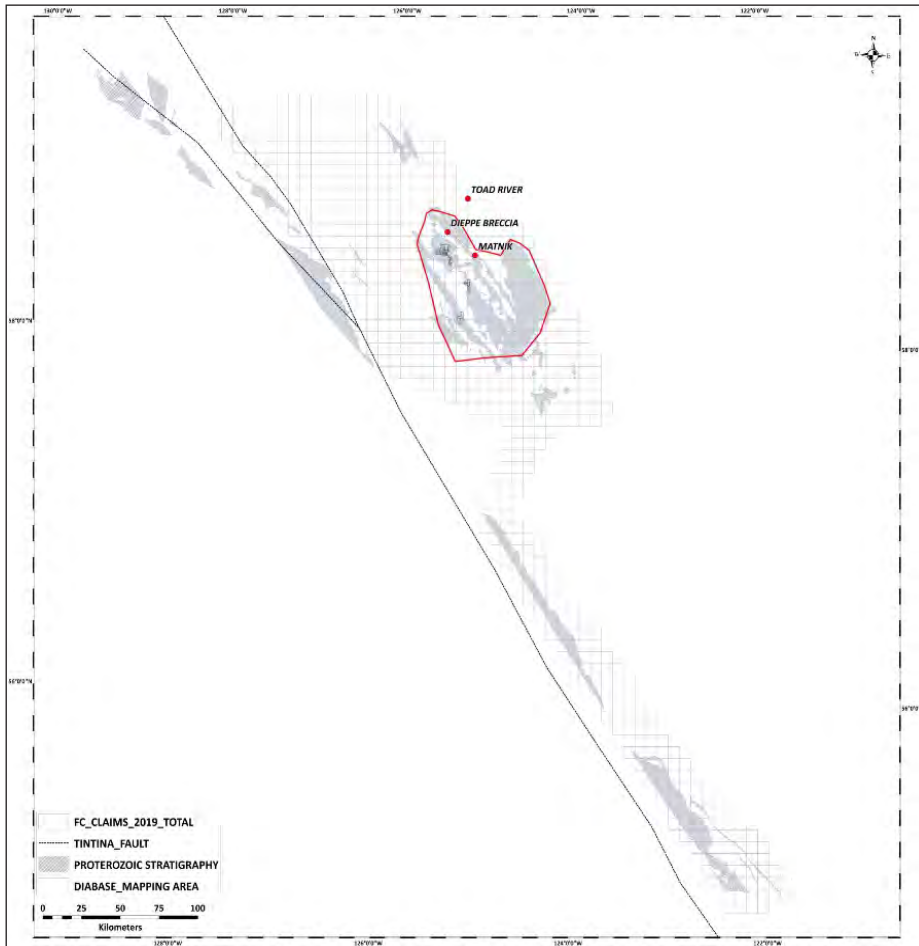


Figure 10: Location of Diabase dykes mapped restricted to central portion of search area.

through to N and NE. The Eagle, Magnum and Davis-Keays occurrences are associated with predominantly NNE to NE oriented diabase. The Toro occurrence is associated with NNE-NNW oriented diabase dykes and the Bronson occurrence is associated with predominantly NNE-striking diabase units.

Domains of similar diabase orientation can be subdivided into 12 main structural blocks which are considered to be the result of Jurassic-Cretaceous compressional deformation (**Fig. 11**). Rotation of these blocks during compression has resulted in changes in the orientation of the diabase currently observed within the AOI.

Diabase Dyke Intensity

Diabase dyking intensity (i.e. proportion of individual diabase dykes over a given area) also varies with the AOI. An analysis of diabase concentrations is presented in **Figure 12** and indicates that the most intense continuous dyking occurs on the western and north-eastern boundary of the AOI. The Book – Bronson – Mendl mineral occurrences are associated with the western zone of intense dyking which is thought to represent a Neoproterozoic major crustal tensional. It is important to note that no known mineral occurrences are present for a large portion of this trend SE of the Mendl occurrence (**Fig. 13**).

Property-scale aeromagnetic data show reasonable correlation between the occurrence of diabase and magnetic anomalies (**Fig. 14**), however, many NE-trending magnetic anomalies are not associated with diabase exposed at surface. Regional residual gravity data suggest the presence of positive gravity anomalies associated with the Mendl-Bronson-Book trend and also with the Matnik occurrence. The significance of these regional positive residual gravity anomalies should be evaluated.

Diabase Timing, Structural Setting and Generations

The diabase mapping exercise revealed several important features related emplacement and subsequent deformation. Key observations include:

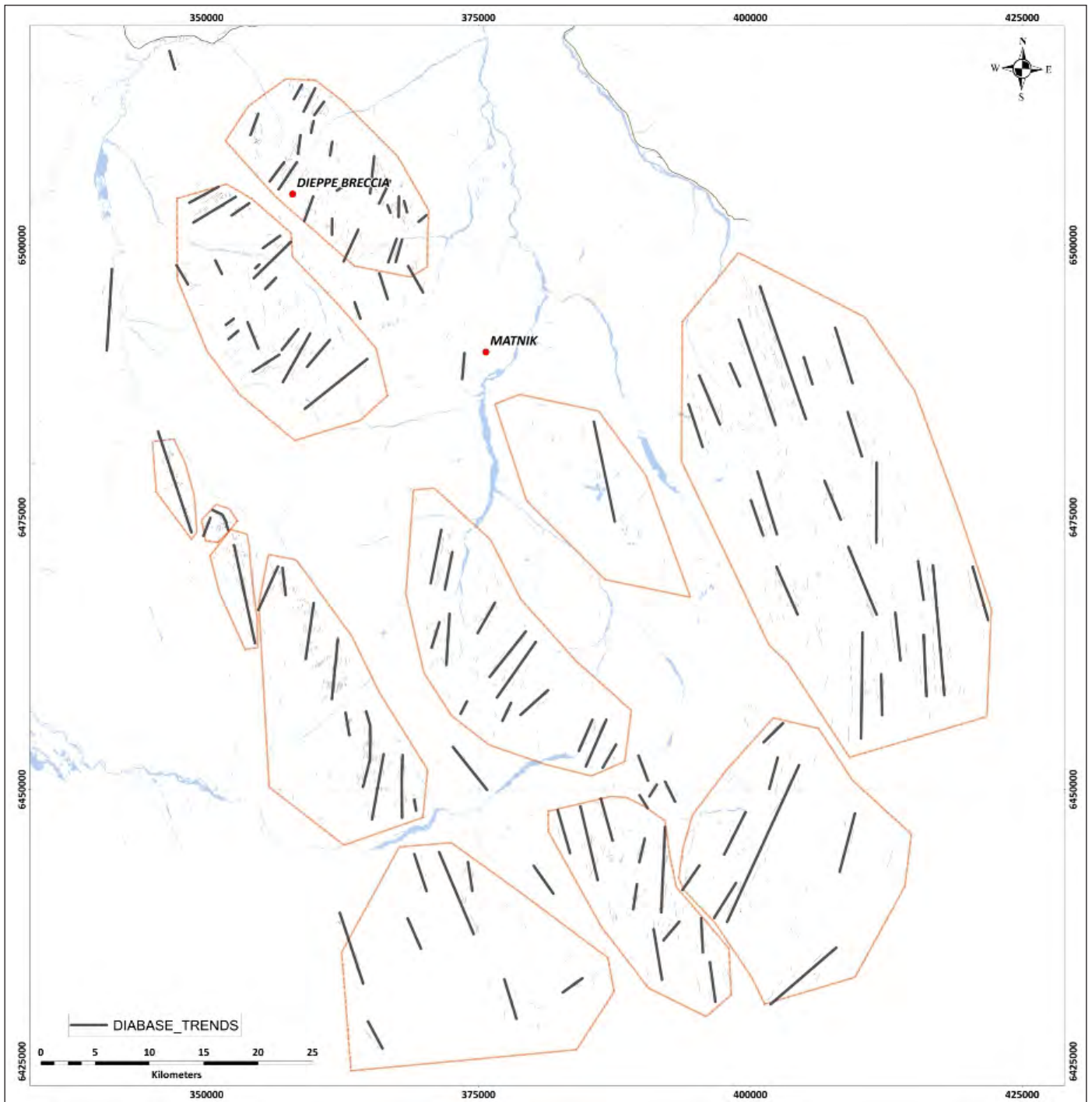


Figure 11: Diabase domain map. Each domain consists of diabase with a similar mean orientation.

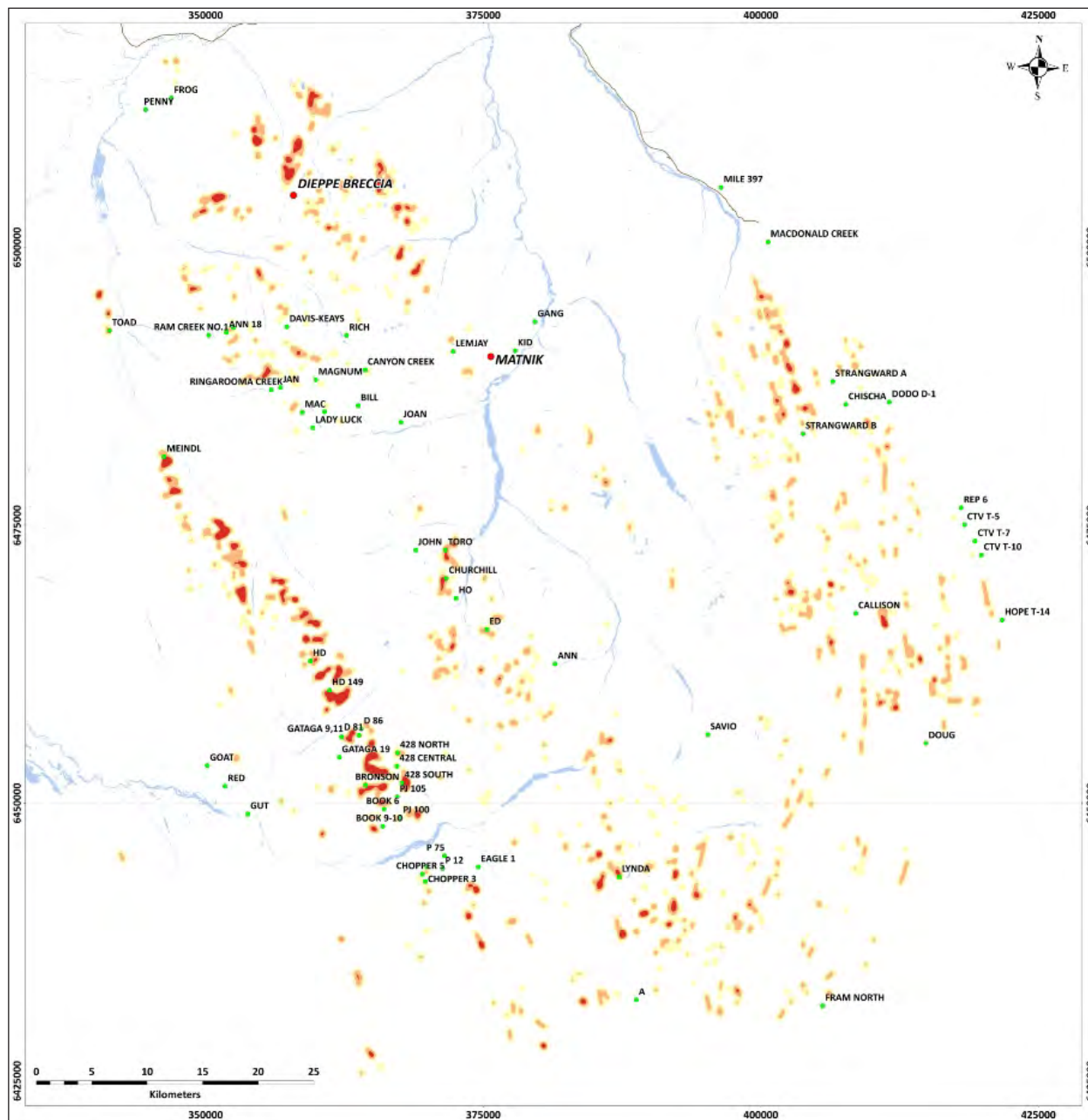


Figure 12: Diabase dyke intensity map illustrating locations where dyking is concentrated.

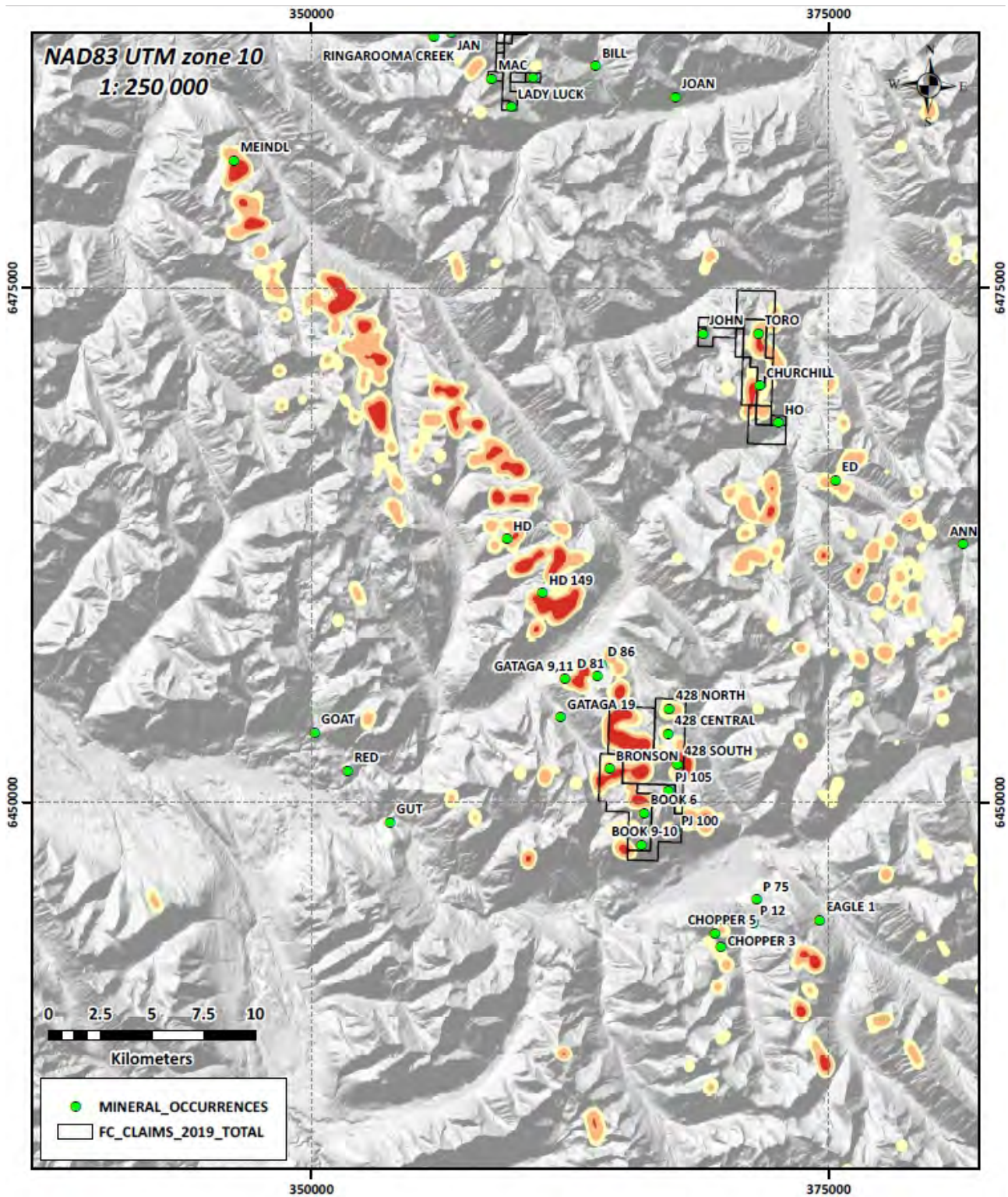


Figure 13: Diabase dyke intensity map showing lack of mineral occurrences SE of the Mendl occurrence.

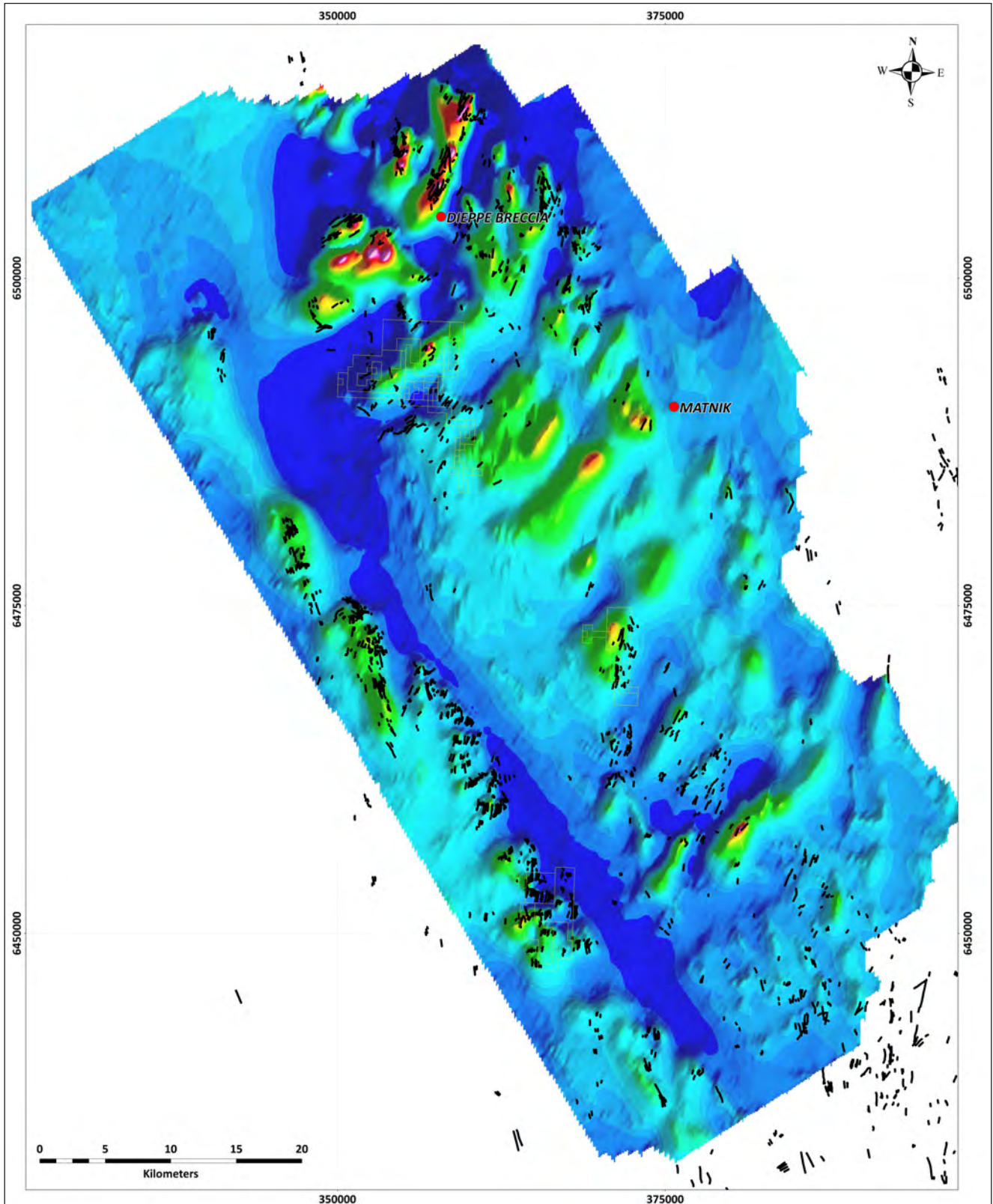


Figure 14: Correlation of property scale residual aeromagnetic data to location of concentrations of diabase units.

1. Folding of diabase is related to Jurassic-Cretaceous compressional deformation. Significant post-emplacment deformation has effected the diabase units in places of younger intense high strain (**Fig. 15**). The Paleozoic unconformity is also folded by this younger deformation event.
2. Two main diabase generations are observed including an early phase associated with two related by differently oriented dyking events and second order fault structures related to strike slip deformation and a younger second phase associated which appears to overprint the earlier emplacement event (**Fig. 16**).
3. The main diabase emplacement event is associated with strike – slip or transtensional faulting. First order bounding faults host diabase oriented N to NNW and second-order internal faults (connecting structures) host diabase emplaced along NNE to ENE structures (**Fig. 17**). A very similar structural setting is present at the historic Magnum mine.



Figure 15: Deformation of diabase dykes associated with Jurassic-Cretaceous compression.

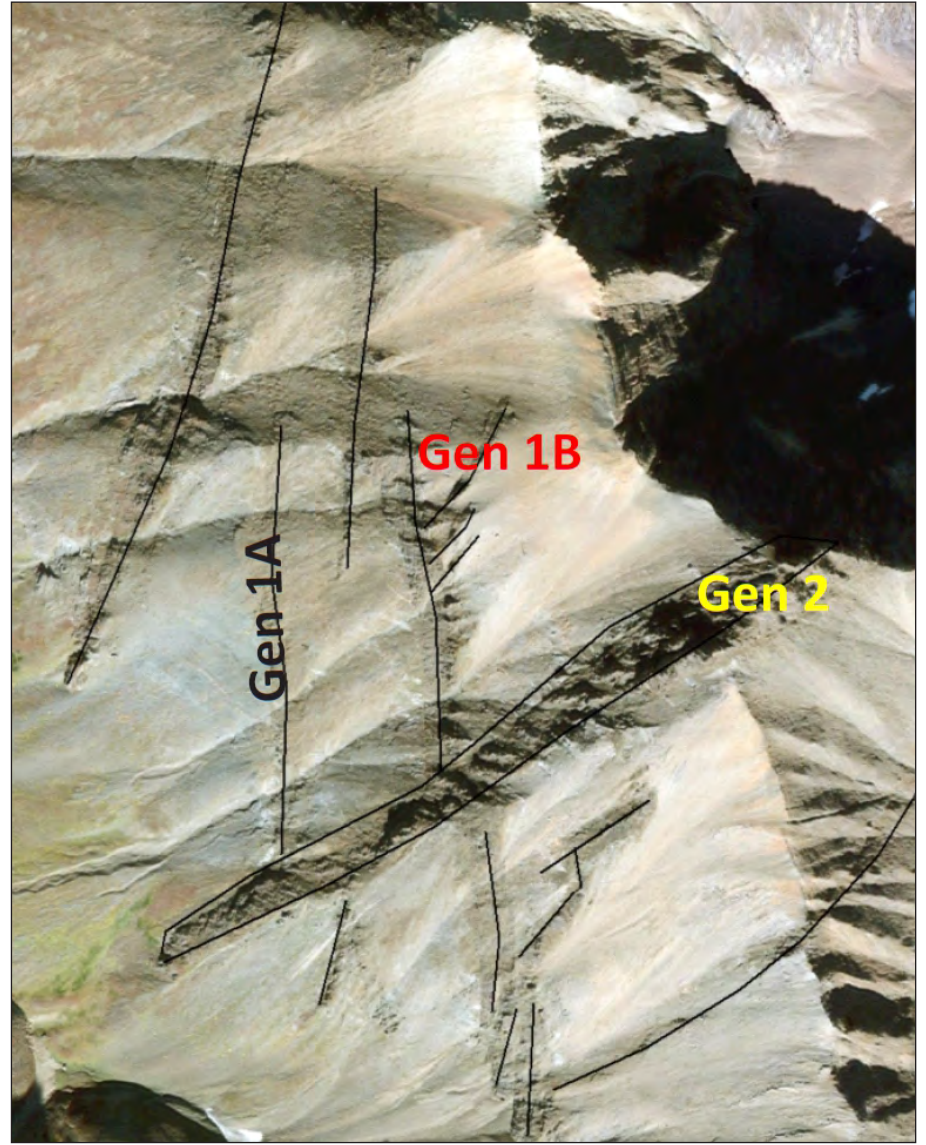


Figure 16: Two main generations of diabase dyking

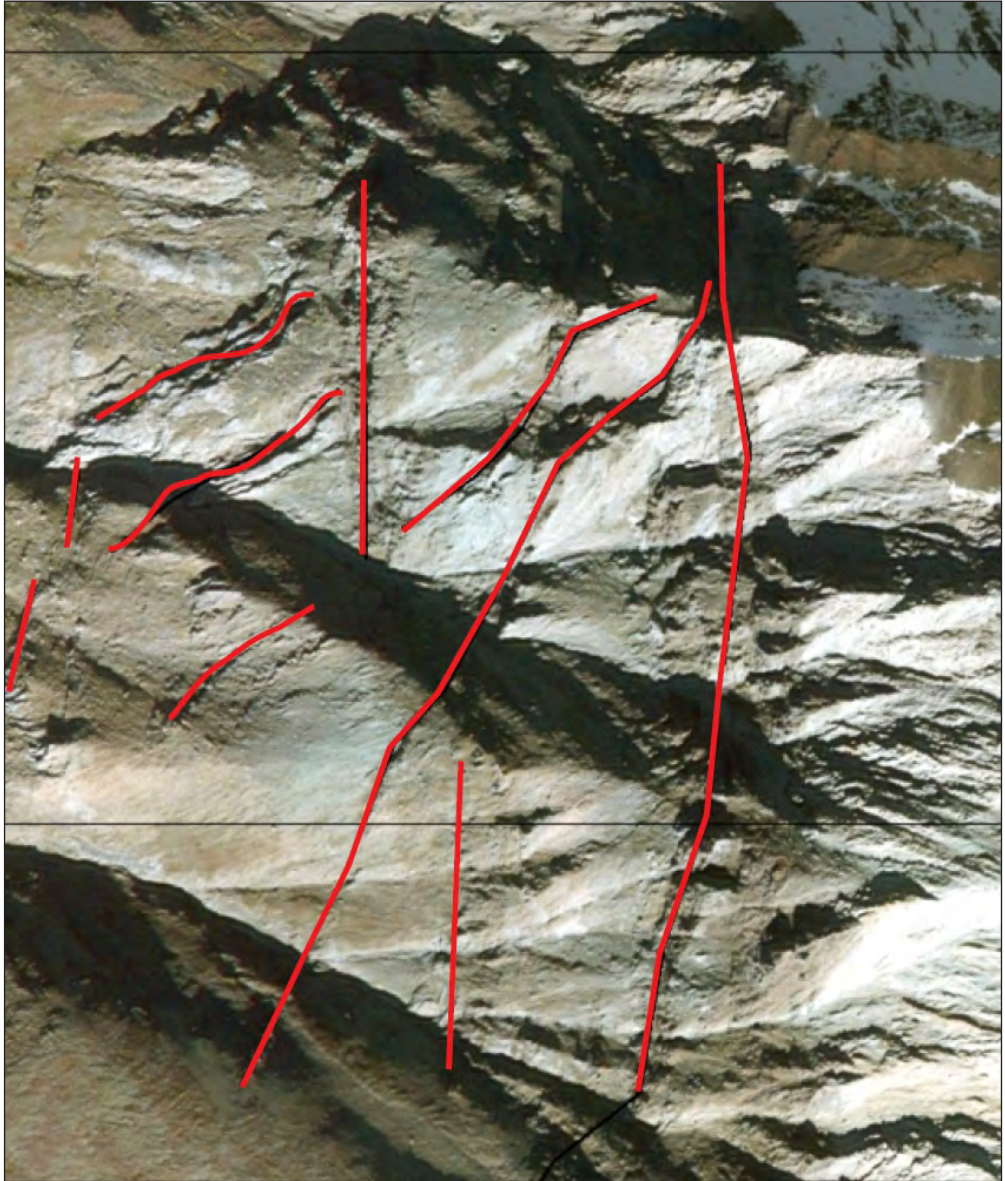


Figure 17: Structural controls on diabase emplacement.

5.0 BRONSON PROPERTY GEOLOGY

The geological map presented in **Figure 18** represents integration of (i) historic field mapping completed between 1970 -1980 (digitized hard copy maps), (ii) new interpretations from high resolution colour satellite imagery and (iii) property-scale aeromagnetic data.

Three main stratigraphic units underlie the Bronson property including the Paleoproterozoic Aida and Gataga Formations and the Ordovician Kechika Group. Diabase units intrude both the Aida and Gataga Formations but were not observed in the Kechika Group (**Fig. 18**). The Aida Formation consists of interbedded dolostone, limestone, shale, and sandstone. The Gataga Formation consists of dark grey to olive grey pyritic, non-calcareous shales with subordinate sandstone and siltstone. The Kechika Group occurs which occurs as a small window in the northeastern corner of the claim block, consists of massive limestone and calcareous quartz sandstone.

The stratigraphy is NNW trending and moderately to gently dipping SW throughout the property. No macroscale folding is observed from satellite imagery or in historical geological map interpretations. Younger limited transport thrust faulting of the Aida formation over the Gataga Formation occurs in the SE portion of the property. Additionally, the Gataga thrust is interpreted to occur between the Aida Formation and the Kechika Group in the northeastern corner of the Bronson property. Three main orientations of lineaments and later brittle faults are also observed across the property including first-order N-NNW lineaments and second-order ubiquitous NE and less well developed NW lineaments. These likely represent kinematically related fault sets associated with Cu-Co mineralization present across the Bronson Property.

The Bronson property is unique in the area due to the high proportion of diabase emplacement. Importantly, diabase dyke intensity appears to coincide with magnetic anomaly highs in property-scale aeromagnetic survey data (**Fig. 19**). Two main diabase events appear to be present within the Bronson property including (**Fig. 20**):

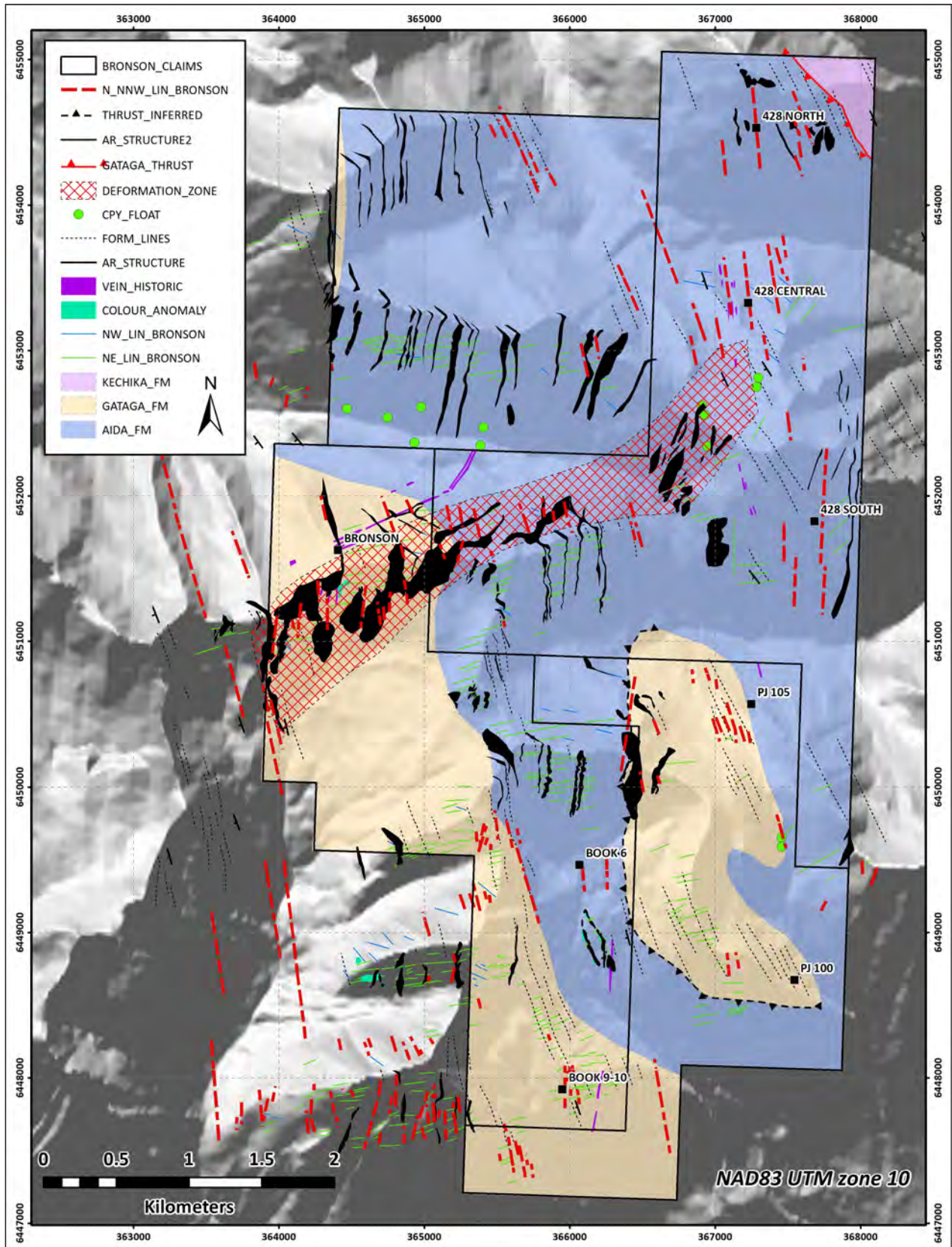


Figure 18: Bronson property geology drafted from high resolution satellite data and historic assessment report (AR - 10960A).

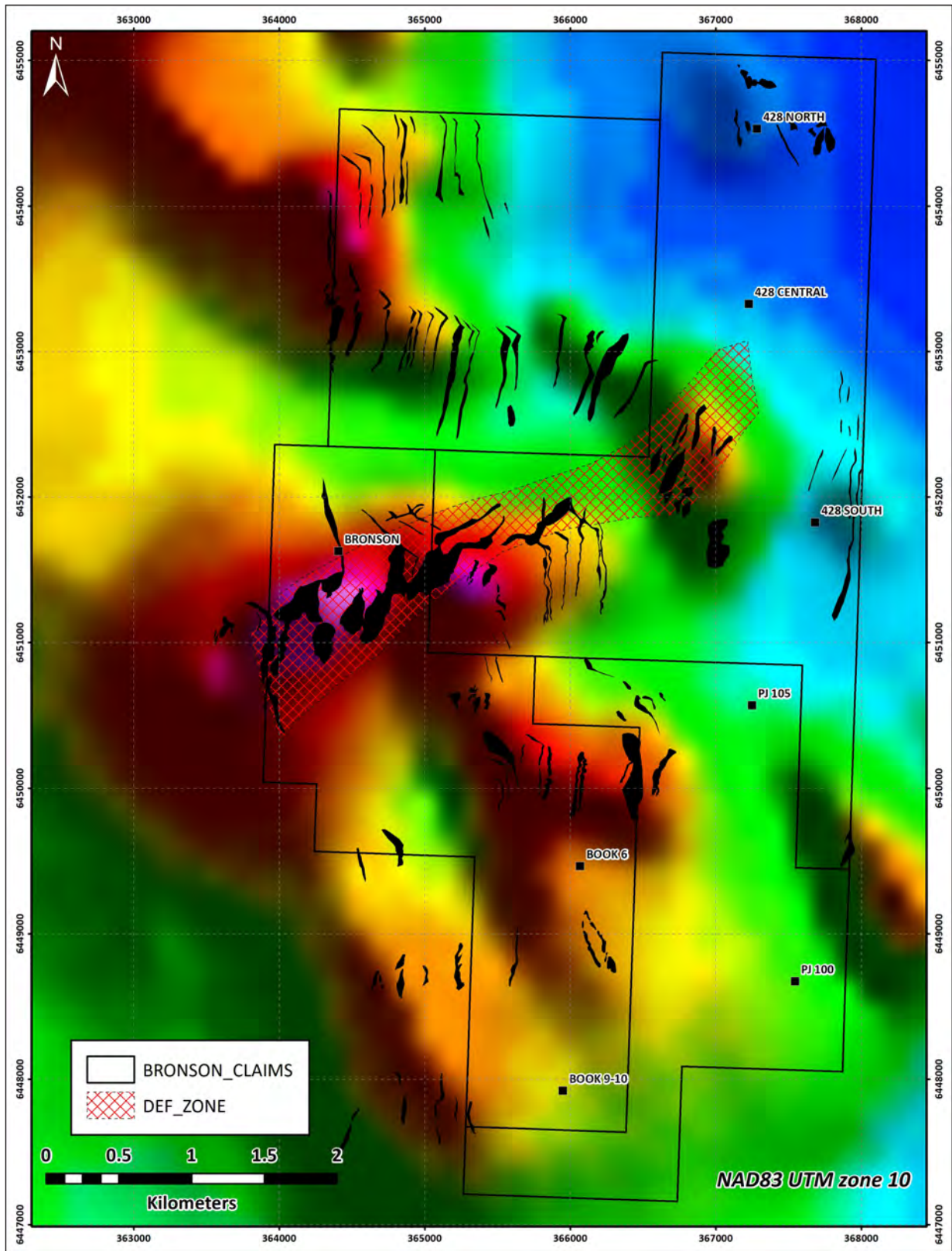


Figure 19: Bronson property total magnetic field data. Distribution of diabase dykes superimposed.

- (i) An older, more widespread, predominantly N-NNW suite characterized by generally narrower, and more continuous (with respect to strike-length) diabase units. Suite 1 diabase units show significant deformation and offsetting caused by overprinting NE-ENE trending faults (**Fig. 20a**)
- (ii) An overprinting, NE - ENE trending suite that is spatially restricted to the central portion of the Bronson property and characterized by large, strongly deformed bodies of diabase (**Fig. 20b**). This suite of diabase is restricted to a well-developed, ductile/brittle NE-ENE trending deformation corridor, approximately 3.5 km in length and up to 700 m in width. This generation of diabase does not occur outside this deformation zone.

Two suites of diabase were also observed during regional evaluations of diabase density and geometry. Importantly, the orientation of the ENE-trending suite 2 diabase units in the central portion of the Bronson claim blocks is parallel to the economically mineralized veins hosting the Magnum deposit.

Copper mineralization occurs as quartz-carbonate + chalcopyrite veins in close proximity to both suite 1 and 2 diabase units. Vein orientations are also characterized by both NNW and NE trending geometries suggesting a structural connection to diabase emplacement kinematics (**Fig. 18**). Integration of geophysical and geological data indicates that a larger scale trans-tensional fault system controls the disposition of both diabase and mineralization. North-trending (first-order) bounding structures are located on the east and west sides of the property and likely formed early in the transtensional structural setting. Diabase suite 1 were emplaced during this stage of deformation. As extension progressed, second-order and internal northeast trending brittle/ductile and brittle structures formed and facilitated the emplacement of larger bodies of diabase suite 2 (**Fig. 21**). The NE-ENE trending zones of transtensional deformation may represent fertile zones of Cu-Co mineralization and should be mapped and sampled in detail to better understand the three dimensional geometry.

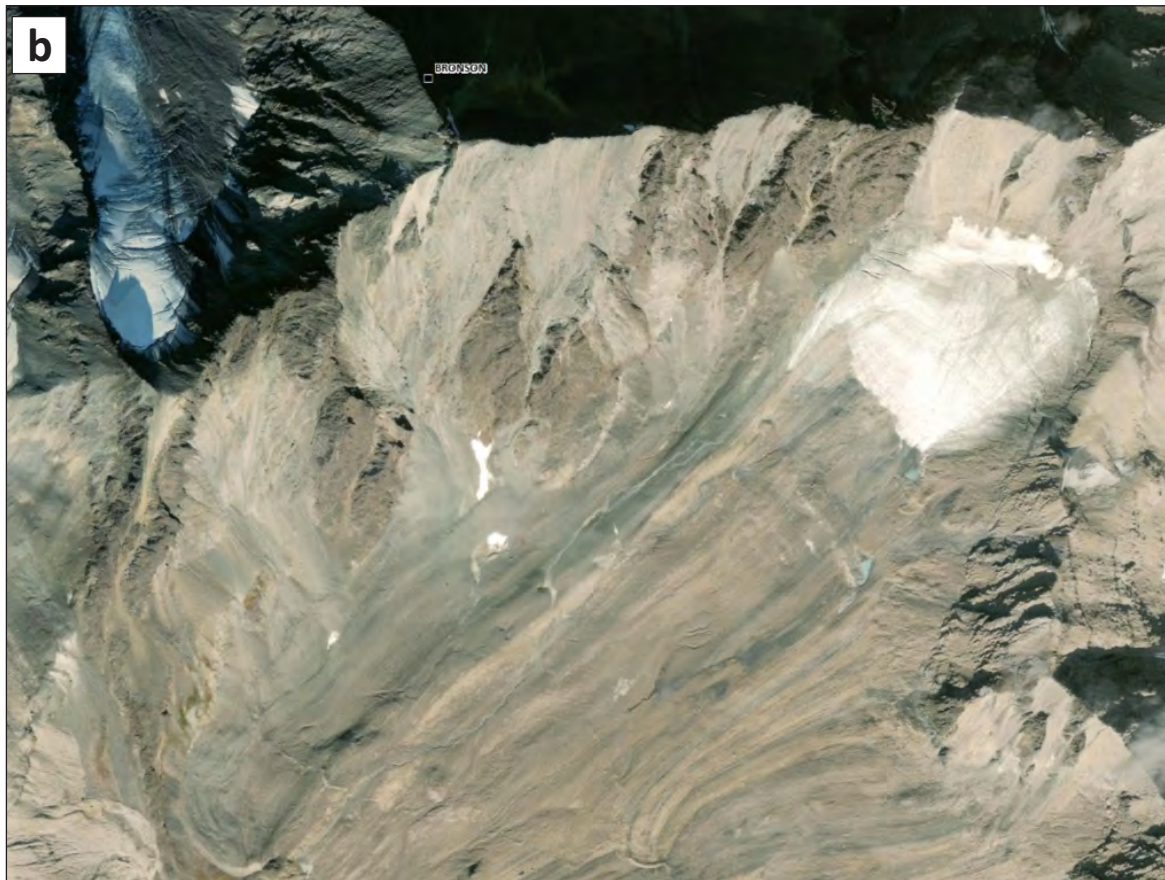


Figure 20: (a) Diabase dyke suite 1. (b) Diabase dyke suite 2.

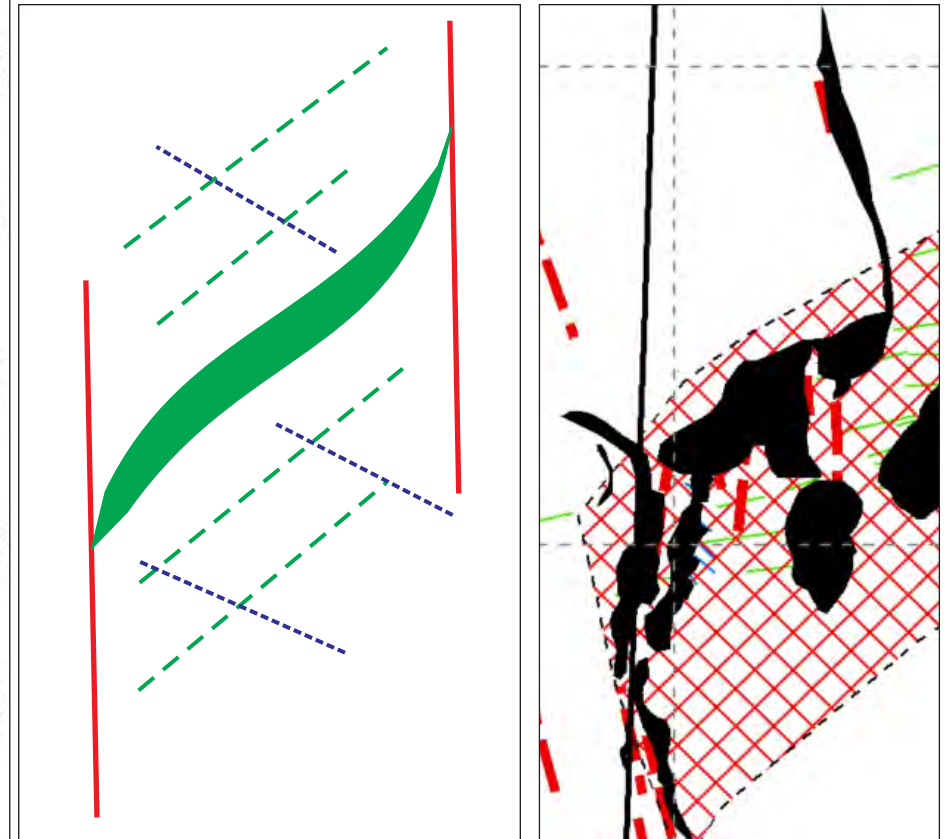
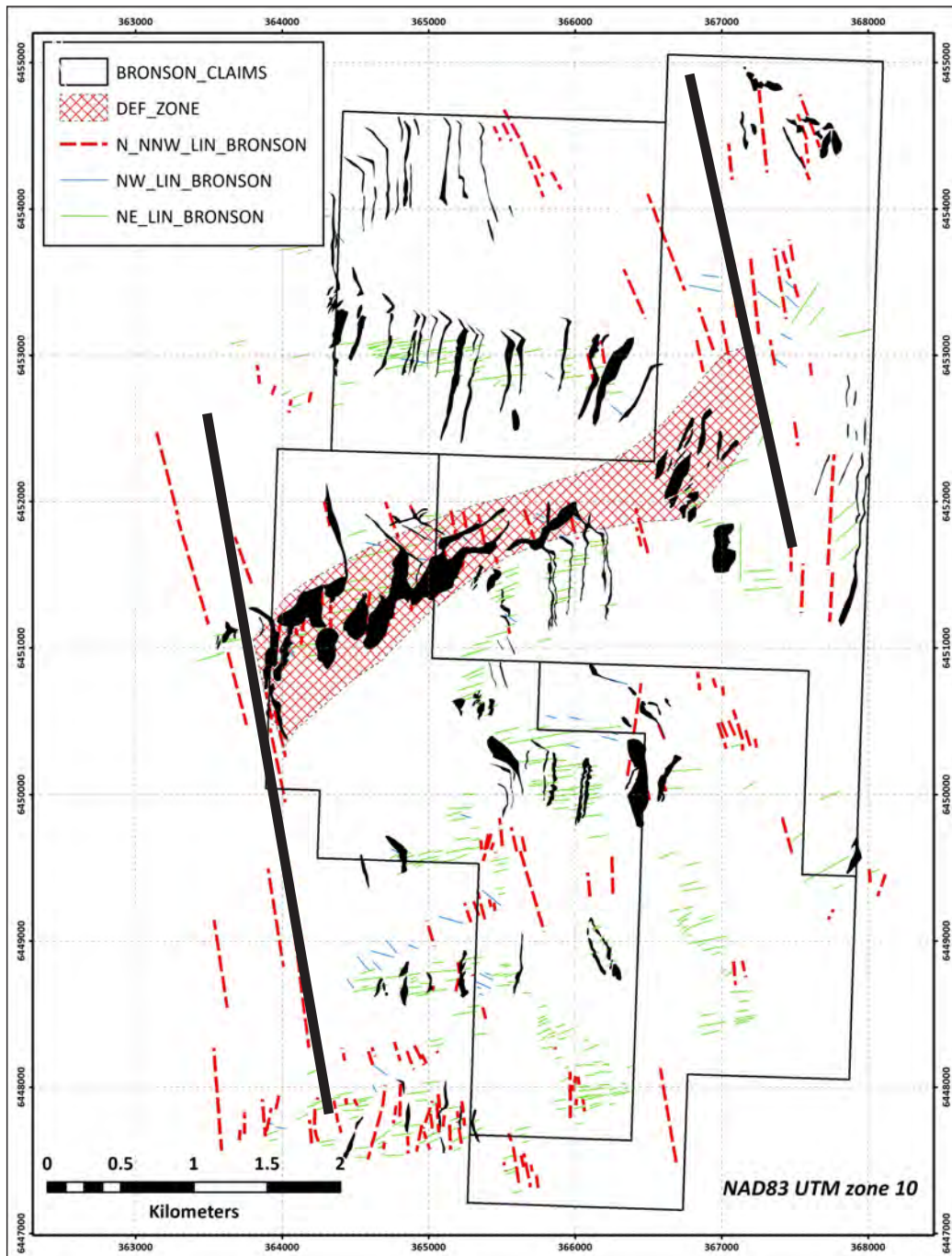


Figure 21: Structural interpretation of the Bronson Property. Mineralization appears controlled by a NNW trending sinistral trans-tensional shear zone with interior ENE trending structures potentially acting as zones of dilatancy and Cu precipitation,

One half day was spent on the Bronson property on the 22 September, 2019. This included 50 min transit time to the Bronson claims from Toad River via the Racing River, connecting to Churchill Creek and then circling west to connect to the Gataga River. Poor weather and marginal visibility restricted field activities to traverses on a single ridge line on the Bronson claims. In addition to a ground review of the mafic dykes, associated alteration and assessment of faulting on their margins from the ground, lower elevation helicopter flights were conducted to assess the mafic dyke swarms and their continuity across the valleys (~ 20 min).

A previous attempt was made to visit the property on September 21, departing Toad River via the Racing River, continuing into Churchill Creek and again circling west to access the Gataga River. Several attempts were made to access the claims by proceeding north up tributaries from the Gataga River. Snow, low ceiling and limited visibility meant landing on the claims was not possible. Approximately 1.5 hours of helicopter time (one way) on September 21 were used attempting to access the Bronson claims. A significant portion of this time was used flying several tributaries up to the Bronson claims and attempting to land.

Three rock samples of diabase were collected close to the central NE-trending deformation zone (**Fig. 22 and 23; Table 2**) on September 22. No appreciable Cu grades were observed. Minor elevation of K (percent) was observed in one sample (Y646071) suggestive of possible potassic alteration.

SAMPLEID	NAD83E_Z10	NAD83N_Z10	Elevation	DATE	Wt_Kg	Cu	Co	Fe	Ni	Ag	Mn	As	S	Ca	P	Mg	Al	K	Description
						pct	ppm	pct	ppm	ppm	ppm	pct	pct	pct	pct	pct	pct	pct	
Y646069	365523.566	6451228.289	2242.266	9/22/2019	1.02	0.024	0.002	4.55	0.004	0.99	0.04	0.0049	0.0249	2.17	0.11	0.91	2.11	0.04	Epidote_Hematite altered diabase
Y646070	365524.641	6451242.627	2243.246	9/22/2019	1.26	0.007	0.003	9.93	0.003	0.99	0.12	0.0049	0.7	1.93	0.201	3.96	3.79	0.22	Fine grained potassically altered diabase
Y646071	365529.243	6451244.699	2245.437	9/22/2019	1.19	0.005	0.002	6.88	0.002	0.99	0.16	0.0049	0.0249	11.11	0.084	2.82	3.15	0.02	Chlorite-carbonate altered diabase

Table 2: Bronson 2019 rock prospecting results

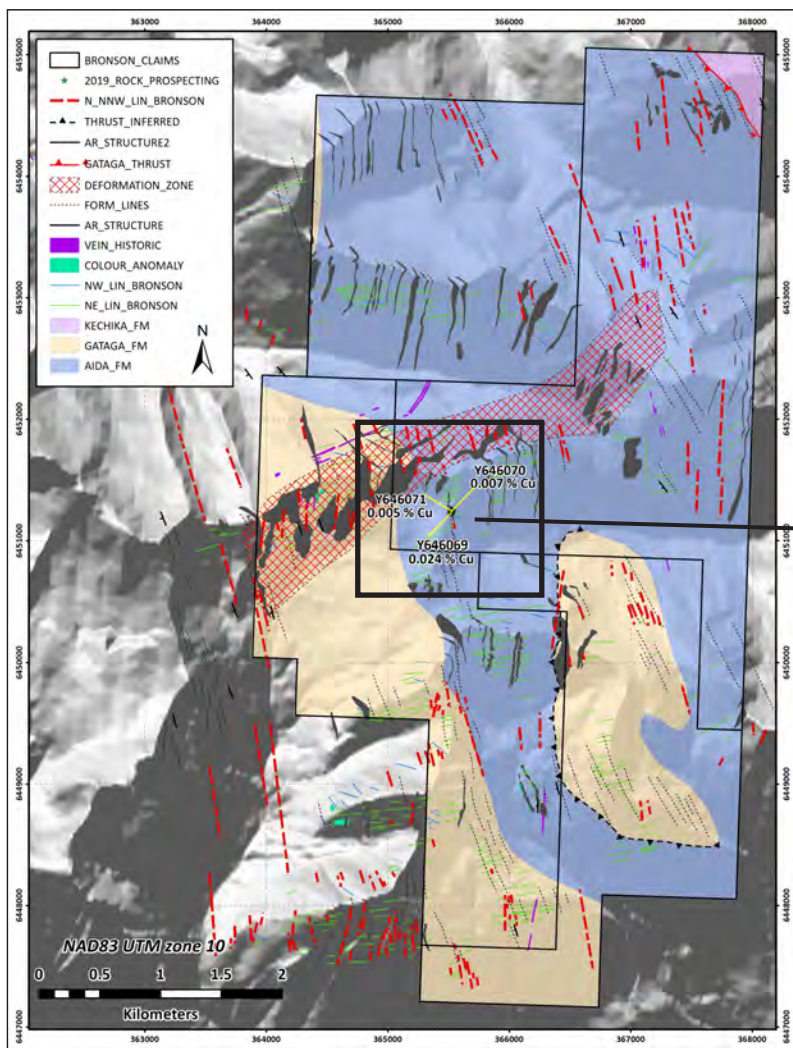


Figure 22: Location and Cu percent grades of 3 rock prospecting samples collected on the Bronson property. No appreciable Cu % values occurred in these samples



Figure 23: Photographs of Bronson diabase assay samples

6.0 HISTORICAL GEOCHEMICAL DATA AND ANALYSIS

Rock, silt and soil geochemical datasets were accessed from the 2005 assessment report completed by Archer Cathro and Associates for Twenty-Seven Capital Corp. A total of 50 rock prospecting samples, 135 rock samples collected at mineralized prospects, 170 regional silt samples and 761 soil samples over the Bronson prospect were available for analysis (**Figs. 24-26**). Thirty rock samples were sampled at various prospects on the Bronson claims and 17 silt samples cover the Bronson property watersheds.

Analytical packages used included:

- i) Regional rock sampling program: Aqua regia digest with 34 element ME-ICP41 (0.5 g volume sample); overlimit Cu was analyzed using Cu-AA46 – Aqua regia digest and AAS finish; Au, Pt and Pd were analysed using PGM-ICP23 which included a Fire Assay (30g volume) for Au and and ICPAES finish for Pt and Pd.
- ii) Prospect rock samples: 34 element ICP AES finish with Aqua regia digest (0.5 g volume sample); overlimit Cu was analyzed using Cu-AA46 – Aqua regia digest and AAS finish; Overlimit Zn was analyzed using Zn-AA46 with an AAS finish;
- iii) Silt samples: 34 element ICP AES finish with Aqua regia digest (0.5 g volume sample);
- iv) Toro Soil samples: 34 element ICP AES finish with Aqua regia digest; screened to 180 um (0.5 g volume sample);

Previous geochemical evaluation of these datasets was limited to anomalous threshold delineation for Cu and Co. Historical reports indicate that Co is predominantly structurally bound within pyrite grains. It is likely that the aqua regia digest used for these geochemical surveys was ineffective for liberating Co from within pyrite. A four acid digest is recommended for future geochemical surveys to better evaluate Co mineralization.

The datasets were accessed from MapInfo Tab files and assigned coordinate and elevation information (NAD83 UTM zone 10). The following geochemical analysis workflows were adopted to evaluate the datasets:

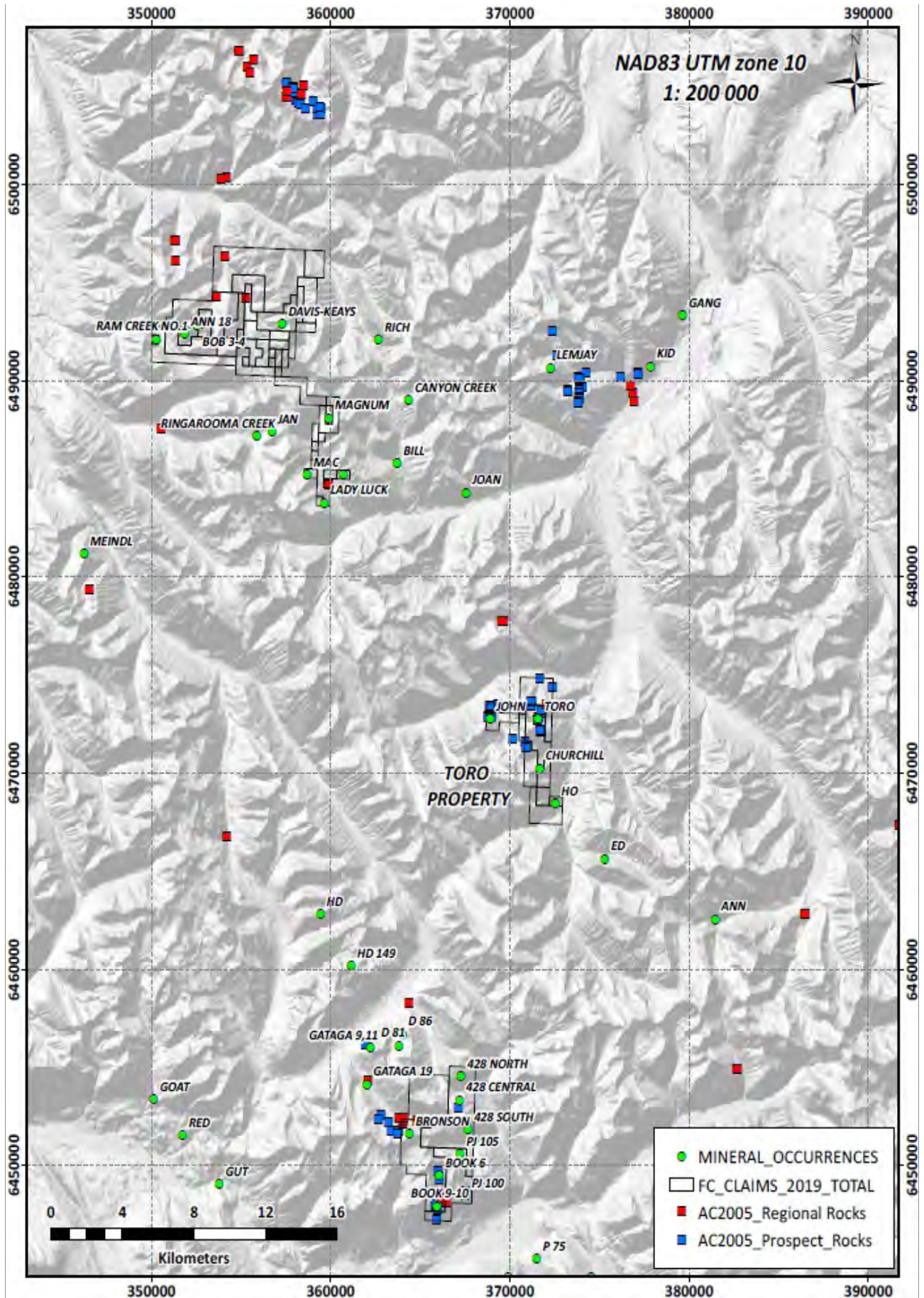


Figure 24: Location of 2005 rock prospecting samples.

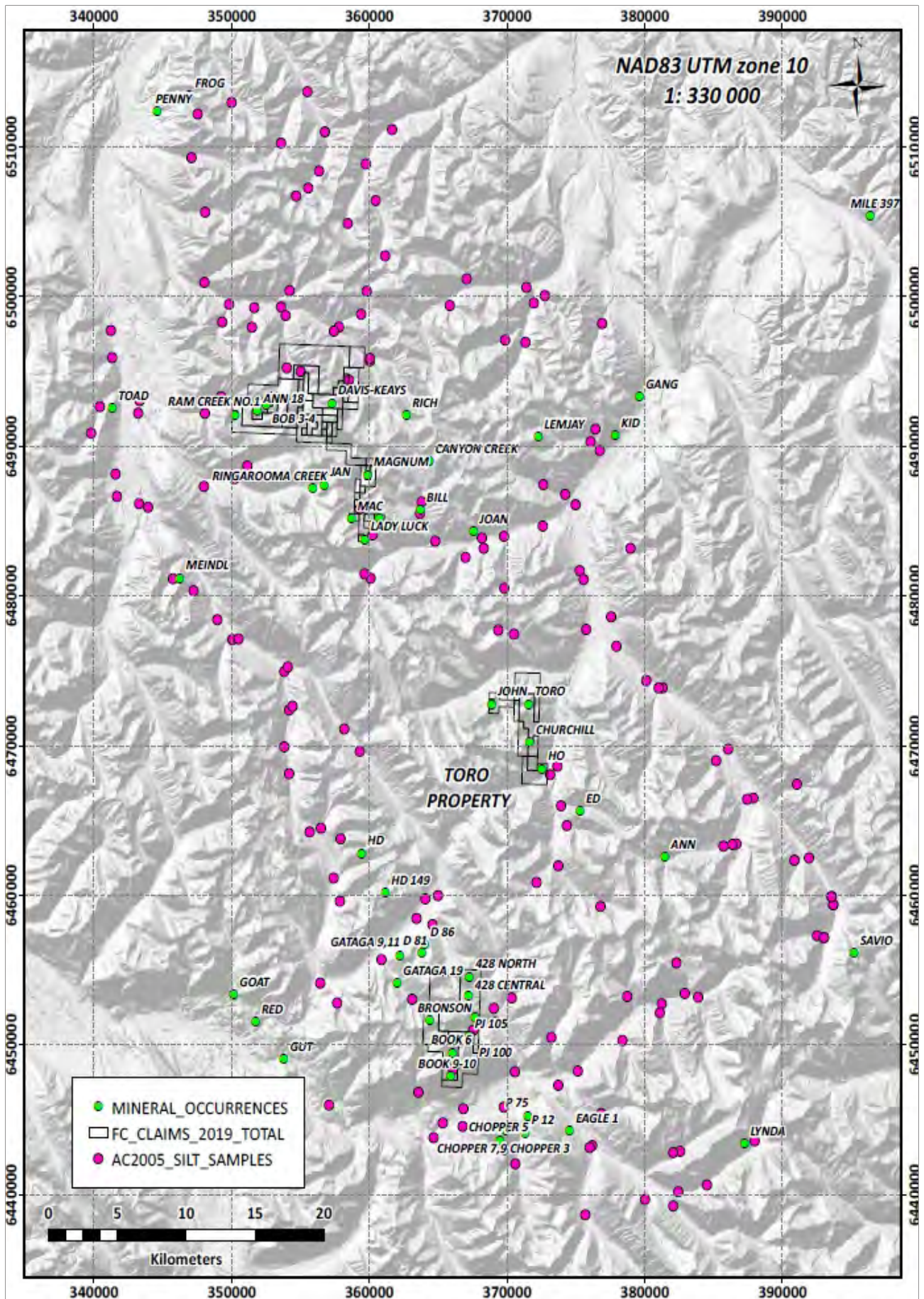


Figure 25: Location of 2005 regional silt samples.

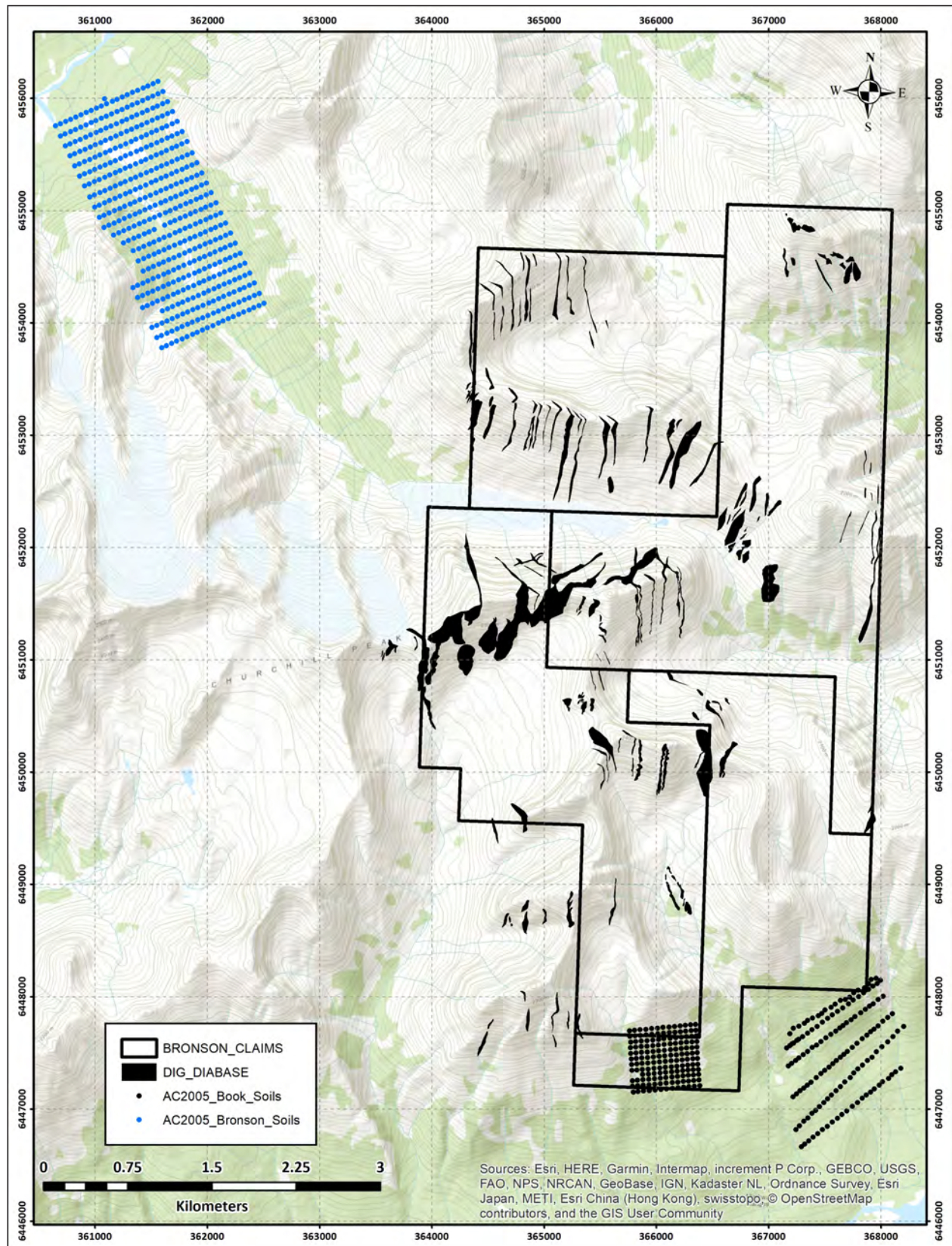


Figure 26: Location of 2005 Bronson and Book soil grids.

1. Treatment of left-censored data through imputation.
2. Univariate and multivariate analysis of rock data at known Cu prospects to establish **key pathfinder elements and other metals associated with mineralization** in the district. This information will then be used to assist interpretations of and targeting using the silt and soil exploration datasets.
3. Sample catchment basin analysis of regional silt samples collected within and adjacent to the Bronson claims.
4. Univariate and multivariate analysis of Bronson property soil data.

Treatment of Left Censored Data

A summary of the proportion of non-detects values for each geochemical package (rock, silt and Bronson soils) is presented in **Figures 27-29**. Several elements in the MEMS41 geochemical package have very high proportions of non-detects. Key pathfinder elements for IOCG systems include: Ag, As, Au, Ba, Bi, Ca, Cd, Ce, Co, Cr, Cs, Cu, Fe, K, La, Mn, Mo, Ni, S, Sb, Se, Sn, Te, U and W. Many of these pathfinders (e.g. **Ag, Bi, Cd, La, Sb, U, W, Mo**) have very high proportions of non-detects and cannot be used for targeting. It is recommended to use a more appropriate geochemical package for future geochemical surveys to improve targeting for IOCG mineralization in the district.

Current best practice (Palarea-Albaladejo and Martín-Fernández (2015), Grunsky and Caritat (2017), Filzmoser (2018)) in dealing with left-censored data includes:

1. If proportion of non-detects is <5-10%, a non-parametric replacement is acceptable (e.g. 0.5x DL; 0.65xDL, 0.33xDL).
2. If proportion of non-detects >50% of the total data points for the element in question, the element should be removed before any multivariate analysis.

3. If proportion of non-detects <50%, a suitable imputation method is required to minimize statistical bias, particularly when conducting multivariate analysis.

For all geochemical data reviewed, estimates of values below the detection limit were imputed using the “LrDA” function within the zCompositions package of the R statistical software

(<https://www.rdocumentation.org/packages/zCompositions/versions/1.1.2/topics/lrDA>).

This method respects the unique geometry of compositional data (i.e. non-euclidean) and better preserves ratios that exist among multi-part components in any given composition (Palarea-Albaladejo and Martín-Fernández 2015).

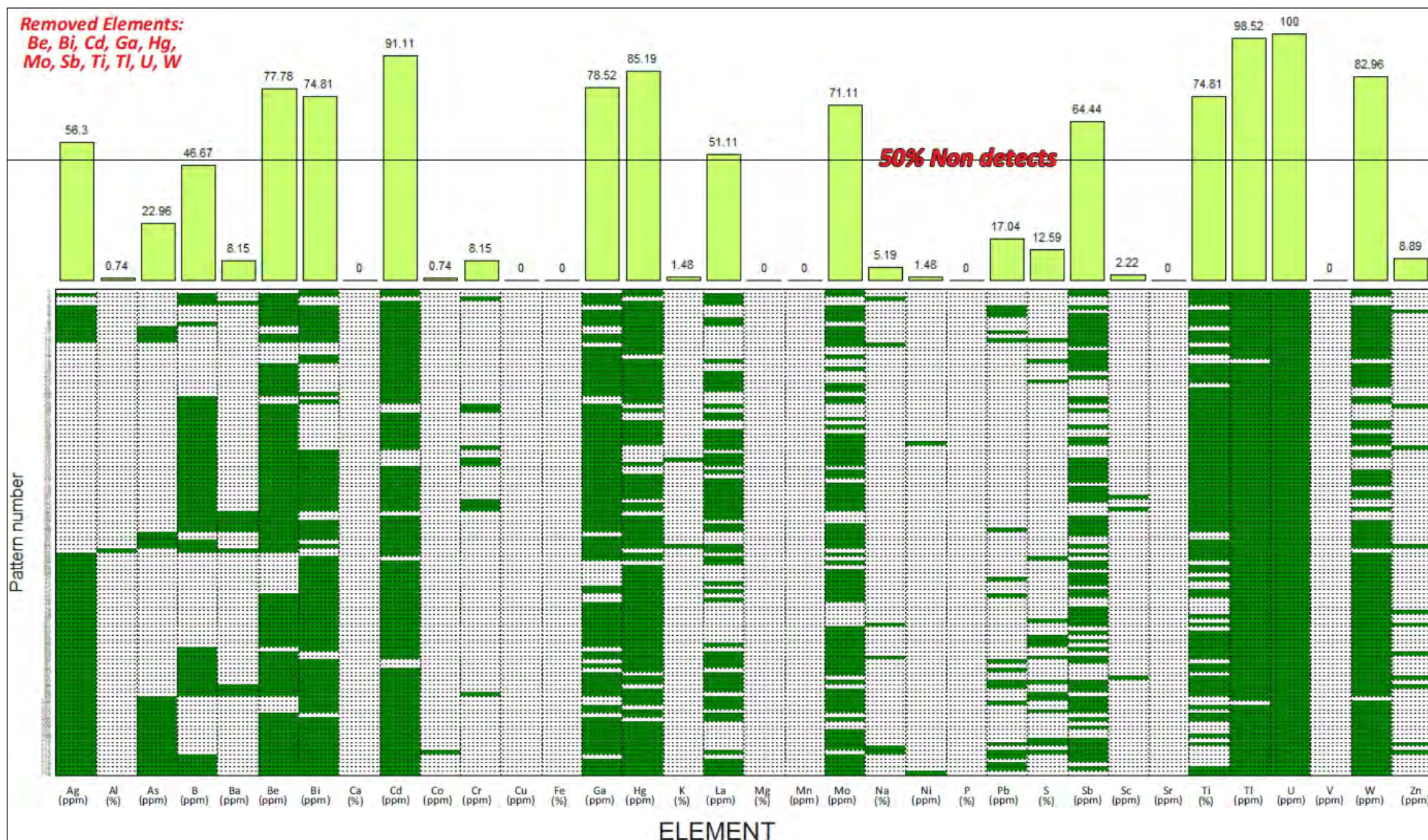


Figure 27: Proportion of non-detects (below detection level) for 2005 rock samples

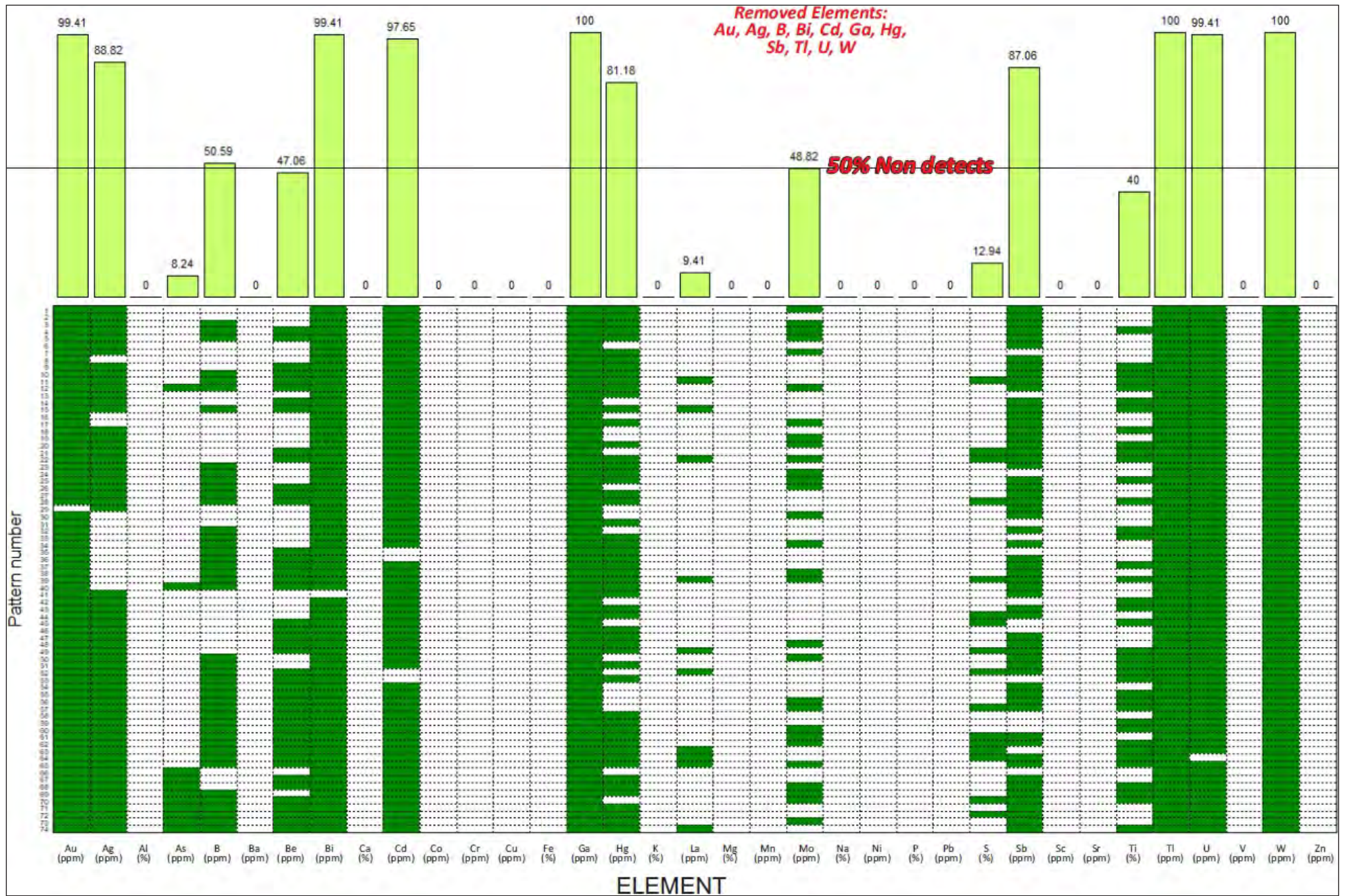


Figure 28: Proportion of non-detects (below detection level) for 2005 silt samples

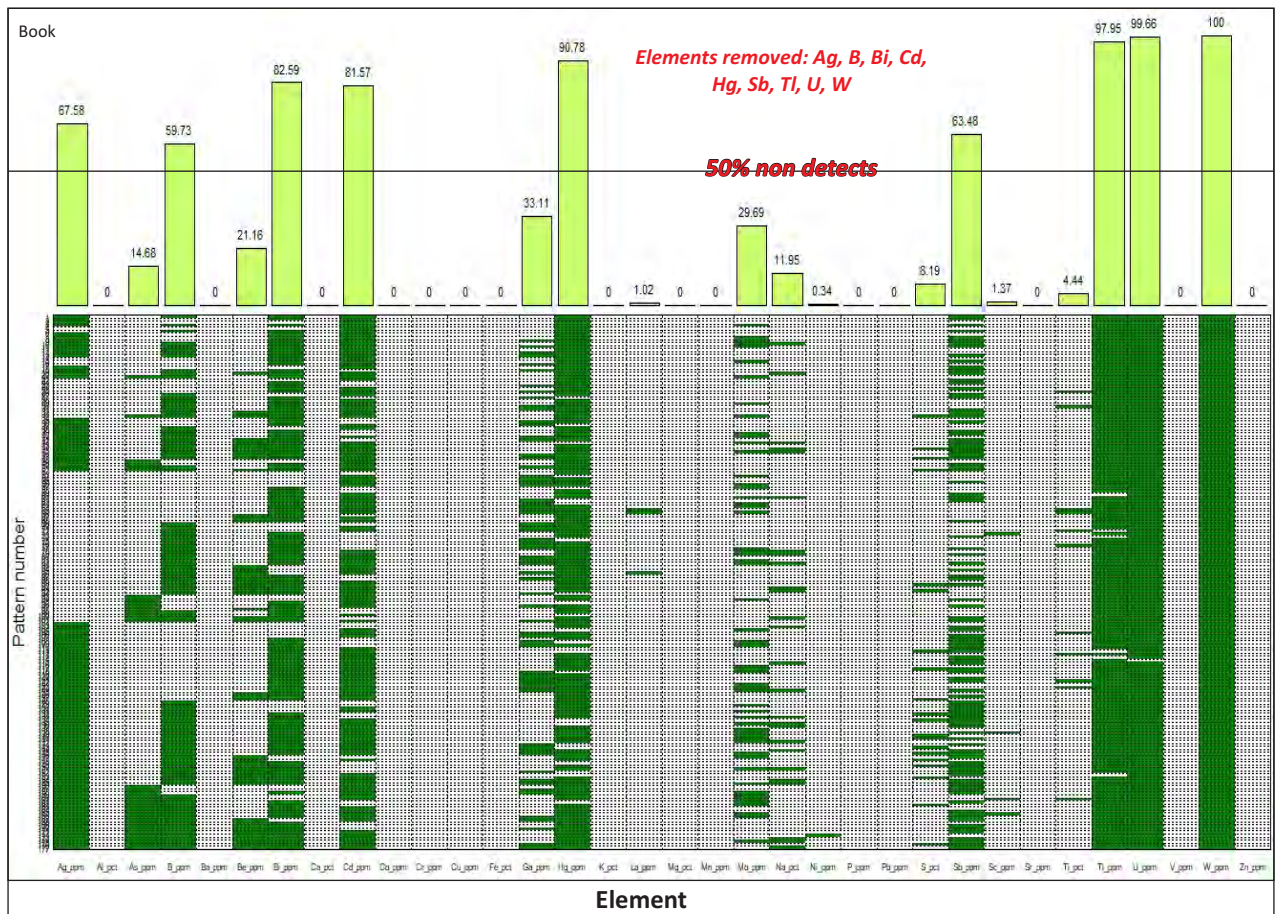
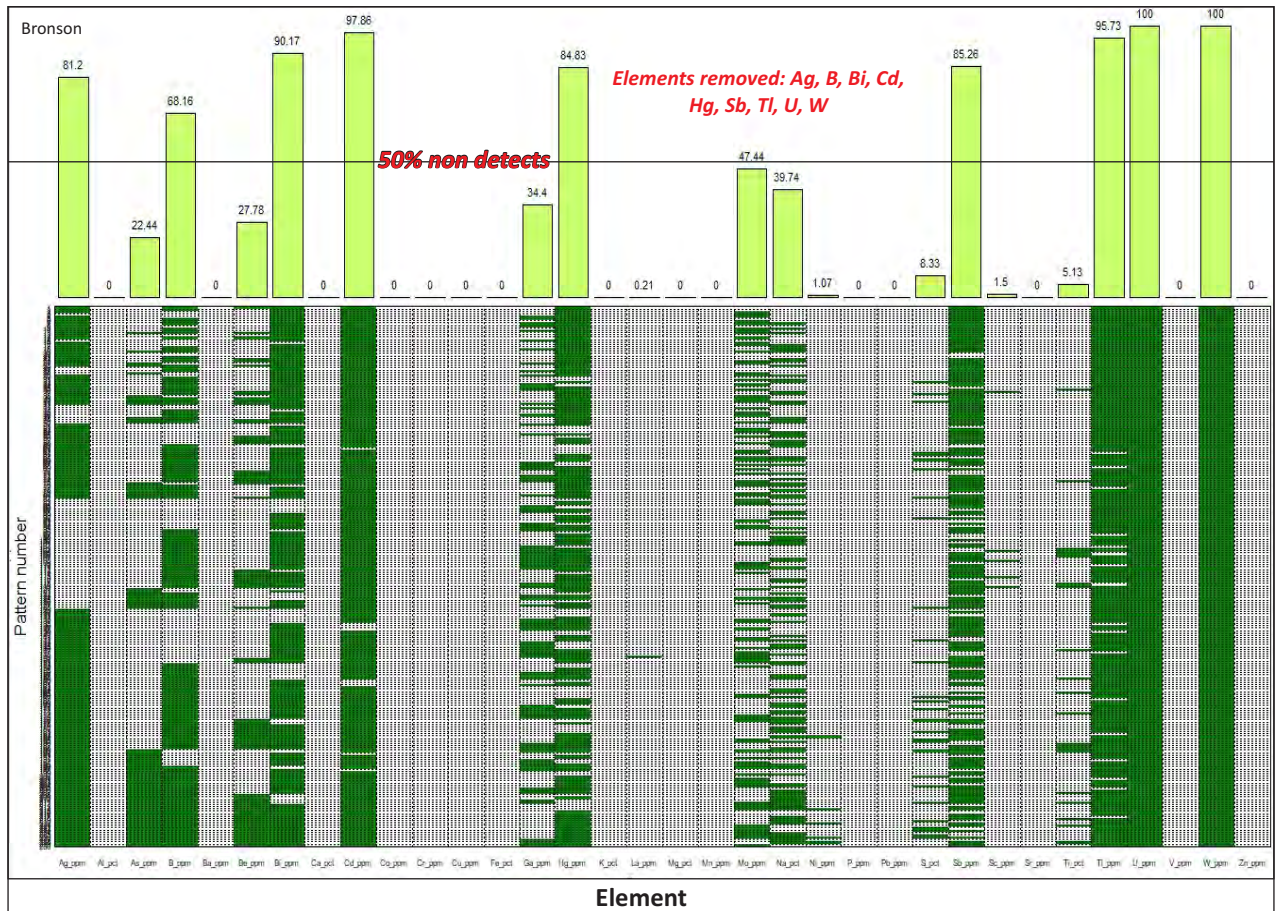


Figure 29: Proportion of non-detects (below detection level) for 2005 Bronson and Book soil grids.

Geochemical Data as Compositional Data (CoDa)

Geochemical data (compositional data or CoDa) are reported as proportions that always sum to a constant value (e.g. 100%; Grunsky and Caritat, 2017). The consequence of a constant sum is that no variable is free to vary independent of the others and thus, the information provided can only be relative (Filzmoser et al. 2009; Grunsky and Caritat, 2017). This is termed the 'closure' problem and affects all geochemical data. Closed data are also unique in that they are characterized by unique geometry (Aitchison geometry) that is inconsistent with geometry (Euclidean) that underlies most classical statistical analysis techniques. Closure can have significant effects on the results of any classic statistical methods applied to geochemical data. Aitchison (1986) developed the theory and methodology for analysis of CoDa using logratio transformations, of which there are three (additive log ratio, centre log ratio and isometric log ratio).

Application of these log ratio transformations effectively 'opens' up geochemical data and allows for safe application of univariate and multivariate statistical methods. The use of log ratio transformations has become common-place in evaluating exploration geochemical datasets (e.g. Carranza 2016; Shahrestani et al. 2019; Dmitrijeva et al, 2019; Reimann et al., 2017; Rezza et al. 2018). Several statistical packages have been developed specifically to evaluate compositional data. Where appropriate, evaluation of geochemical data from the Bronson property adopts the best practices presented in the body of current exploration literature that involves the use of log ratio transformations and application of robust statistical measures.

6.1 ROCK ANALYSIS

Univariate Analysis

Univariate geochemical characteristics are briefly evaluated, prior to analysis of the prospect datasets using the exploratory multivariate statistical techniques of clustering and robust principal component analysis.

Spearman correlation matrices were calculated for the 2005 rock prospects data (**Table 3**). The Spearman rank method is preferred because it provides a non-parametric (i.e. does not assume normal distribution) measure of correlation. The method estimates correlations between data rank values as opposed to actual data. Pearson correlations matrices can only be used when dataset in question has a multivariate normal distribution, which is rarely the case for geochemical datasets.

The rock prospects data is characterized by strong positive correlations between **Cu-S-As-Ag-Co and Ni** and moderate negative correlation between Cu and Mg. Other statistically significant correlations include:

- I) Strongly positive correlations between Ca-Sr-Mn-Mg-Na
- II) Moderately negative correlations between Ca and Ni-Cu-Co
- III) Moderately positive Pb-Ag-S correlations
- IV) Strong positive correlations between Ni-Co

Scatterplots of Cu versus S, As, Ag, Co and Ni confirm weak to moderate positive correlations (**Fig. 30**). A Cu versus Mg scatter plot illustrates a weak overall decrease in Mg concentrations with increasing Cu (**Fig. 31**). A similar observation is observed for Mn (**Fig 31**). Other important trends observed from scatterplots include (i) a positive correlation between Fe and Cu (**Fig. 31**) and (ii) a subtle trend of increasing Cu and Co with elevation suggesting some kind of vertical zonation may be present within the mineralizing system (**Fig. 32**).

KEY PATHFINDERS FROM UNIVARIATE ANALYSIS: Cu-S-As-Ag-Co-Fe and Ni

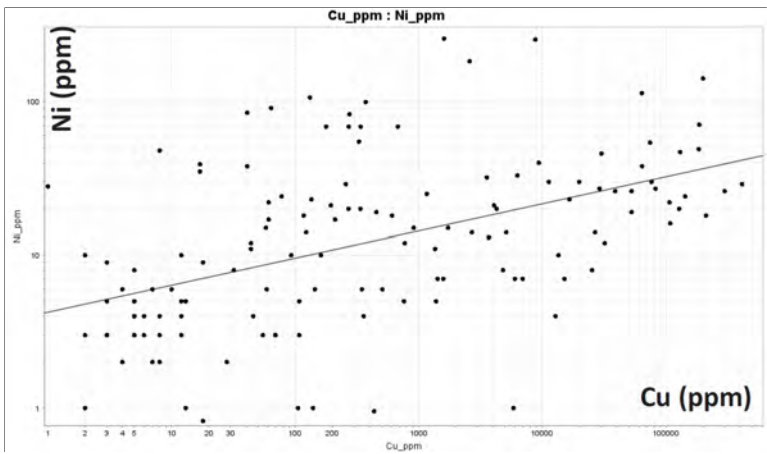
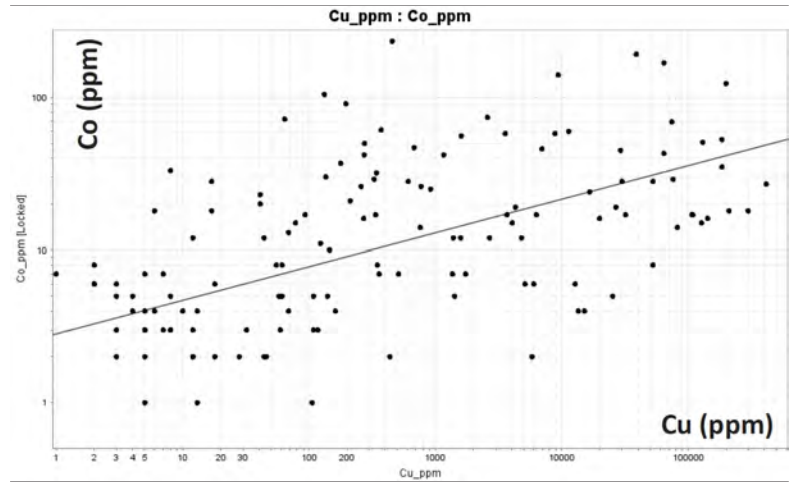
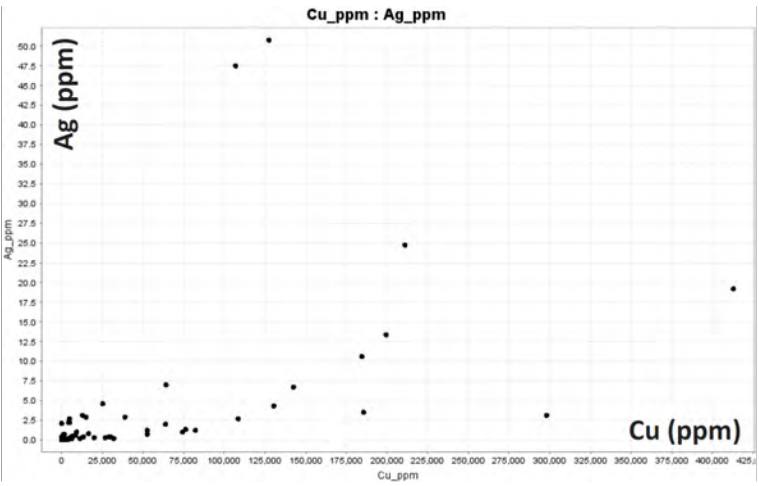
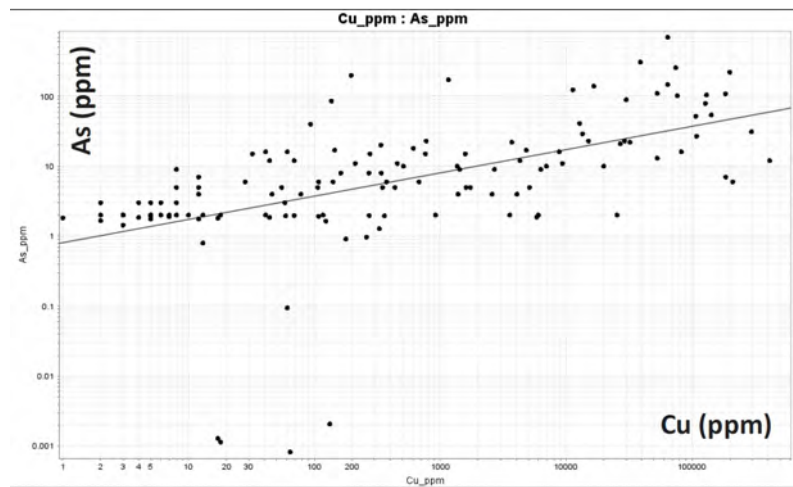
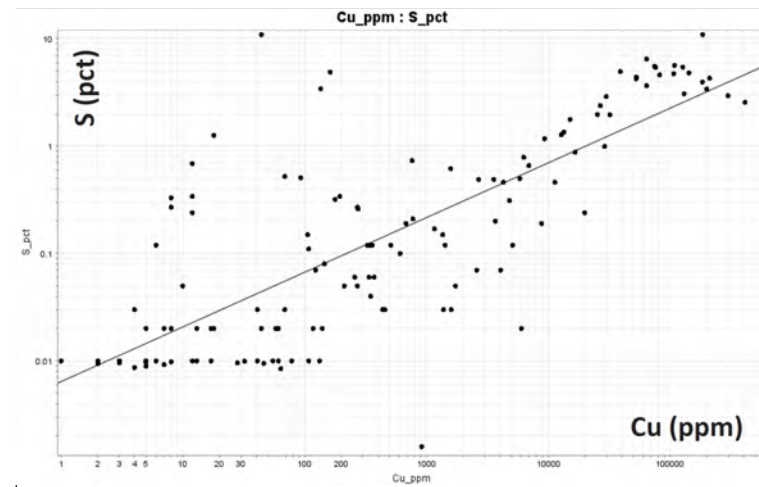


Figure 30: X-Y Scatter plot of Cu versus S, As, Ag, Co and Ni.

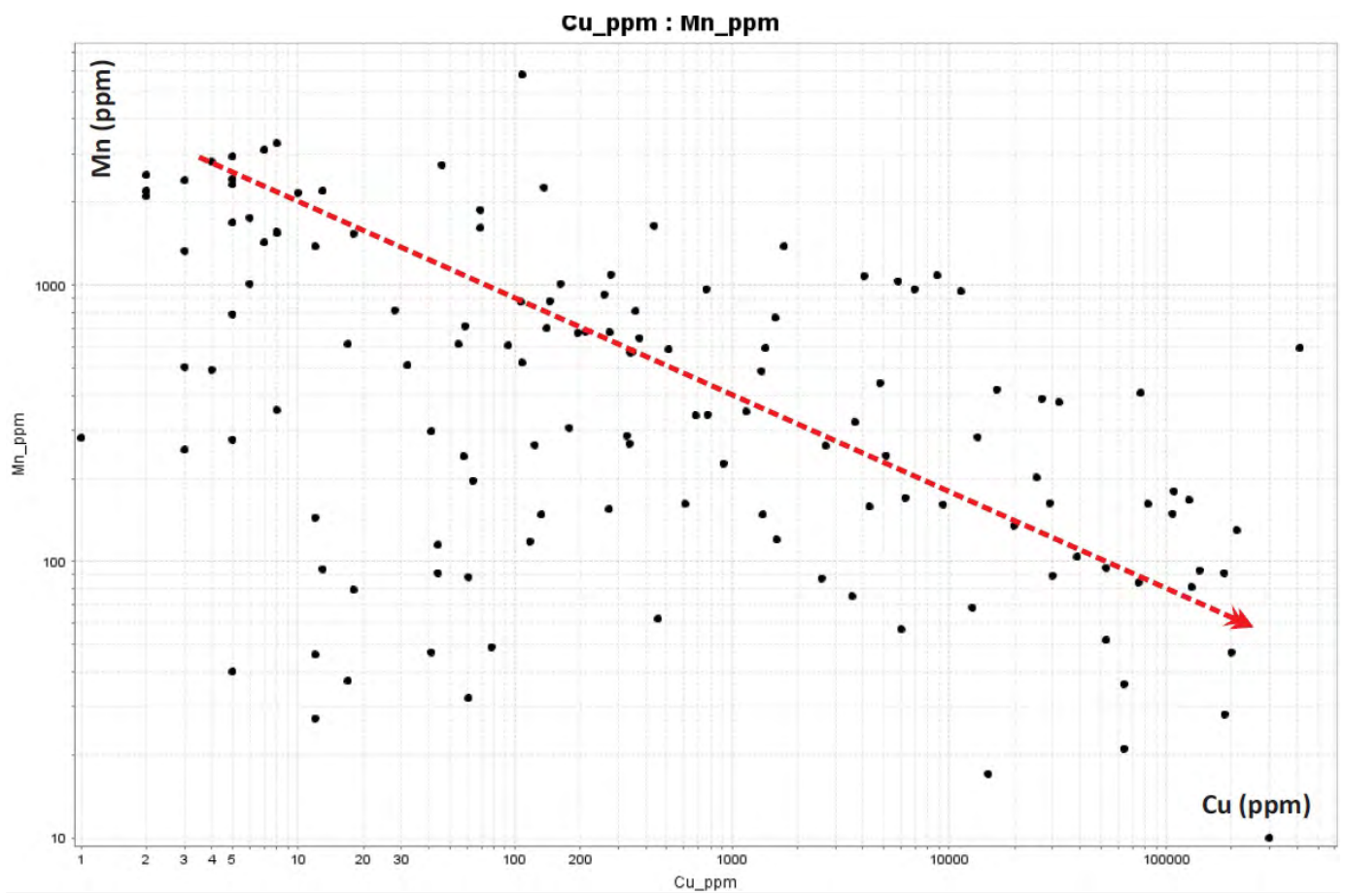
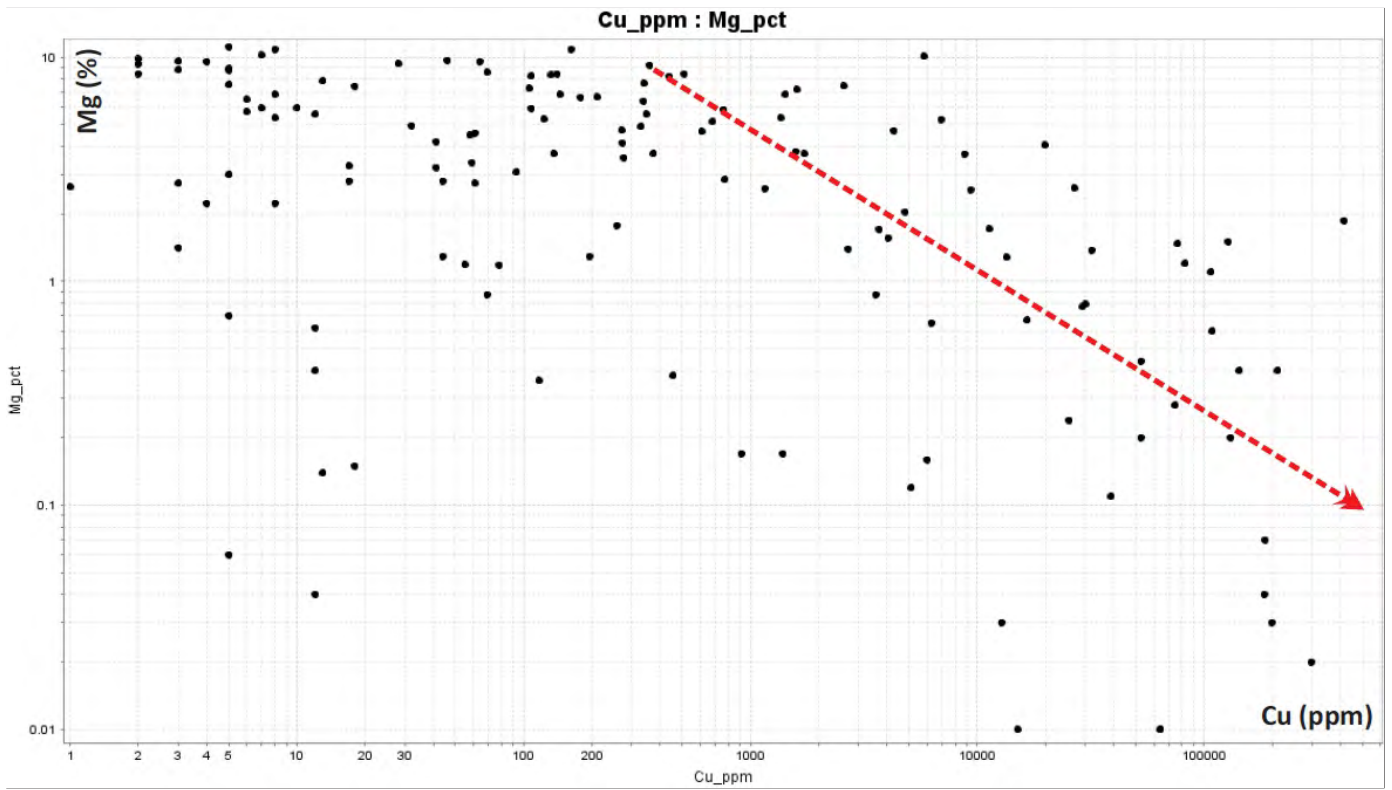


Figure 31: X-Y Scatter plot of Cu versus Mg and Mn.

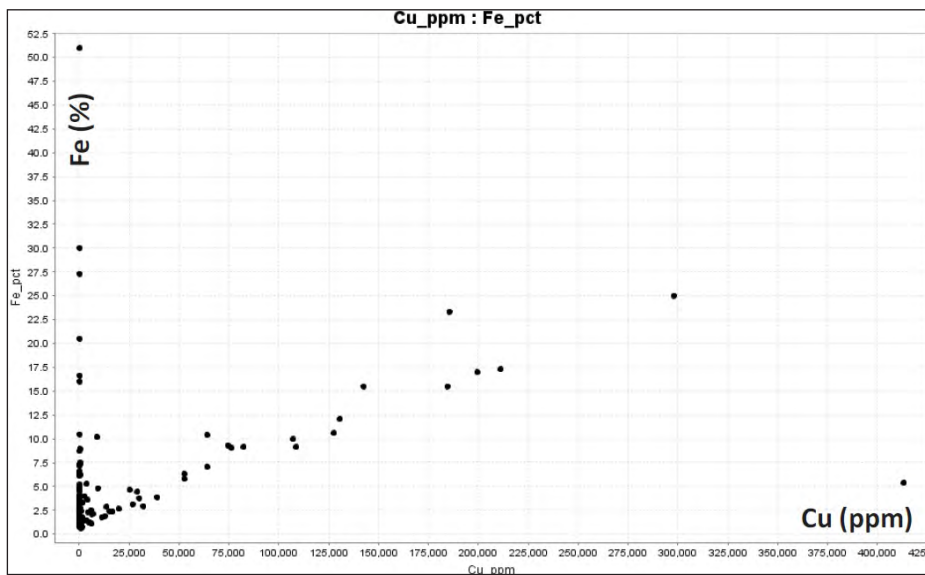
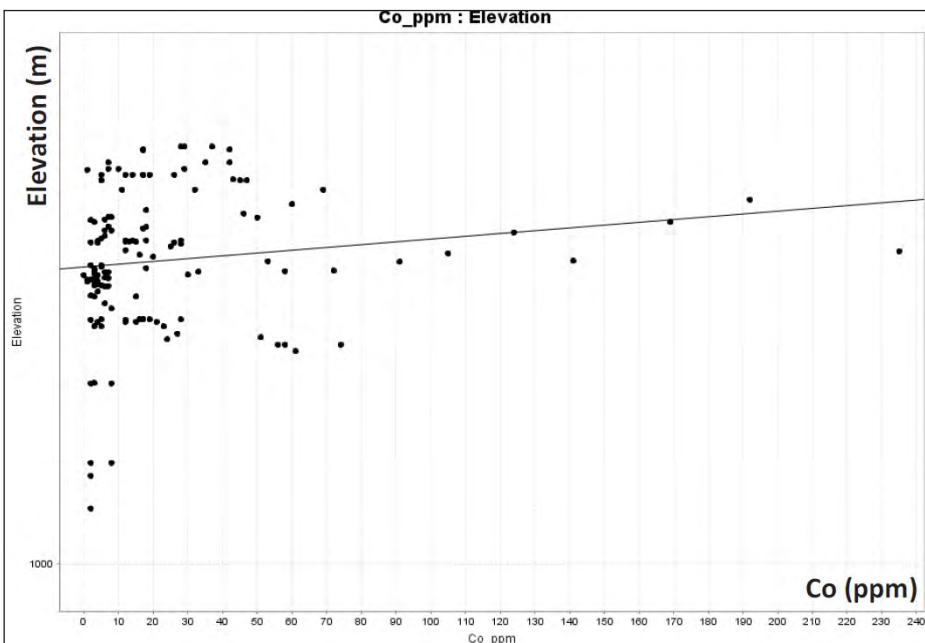
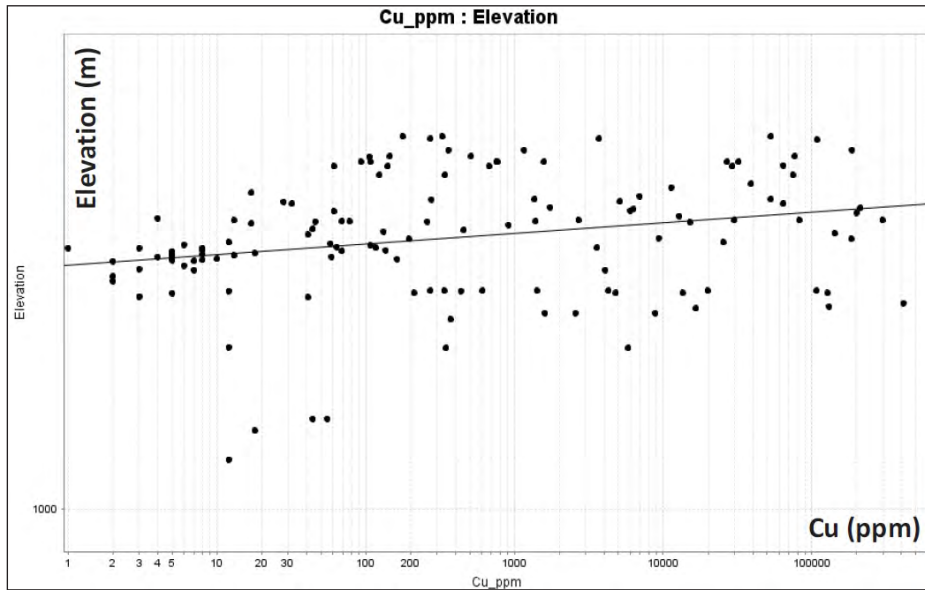


Figure 32: X-Y Scatter plot of Cu versus Fe and Elevation versus Cu and Co.

	Cu_ppm	Co_ppm	Ag_ppm	Al_pct	As_ppm	B_ppm	Ba_ppm	Ca_pct	Cr_ppm	Fe_pct	K_pct	La_ppm	Mg_pct	Mn_ppm	Na_pct	Ni_ppm	P_ppm	Pb_ppm	S_pct	Sc_ppm	Sr_ppm	V_ppm	Zn_ppm
Cu_ppm	1	0.57	0.62	-0.14	0.68	-0.47	-0.31	-0.46	-0.077	0.22	-0.22	-0.39	-0.51	-0.47	-0.34	0.53	0.19	0.48	0.78	0.022	-0.23	-0.25	0.43
Co_ppm	0.57	1	0.17	0.3	0.47	-0.19	-0.036	-0.42	0.18	0.24	0.062	-0.17	-0.23	-0.3	-0.19	0.83	0.34	0.2	0.41	0.29	-0.23	0.17	0.48
Ag_ppm	0.62	0.17	1	-0.39	0.56	-0.41	-0.27	-0.081	-0.33	0.25	-0.34	-0.29	-0.3	-0.13	-0.1	0.12	-0.11	0.53	0.57	-0.095	-0.006	-0.38	0.3
Al_pct	-0.14	0.3	-0.39	1	-0.24	0.44	0.2	-0.16	0.49	-0.034	0.53	0.4	0.22	-0.062	-0.15	0.43	0.6	-0.36	-0.23	0.51	-0.092	0.68	0.32
As_ppm	0.68	0.47	0.56	-0.24	1	-0.42	-0.39	-0.2	-0.13	0.099	-0.29	-0.31	-0.38	-0.26	-0.16	0.34	0.07	0.48	0.69	-0.095	-0.046	-0.38	0.25
B_ppm	-0.47	-0.19	-0.41	0.44	-0.42	1	0.32	0.31	0.23	0.0065	0.63	0.48	0.44	0.33	0.089	-0.079	0.14	-0.31	-0.44	0.3	0.19	0.42	-0.079
Ba_ppm	-0.31	-0.036	-0.27	0.2	-0.39	0.32	1	0.019	0.063	0.041	0.31	0.2	0.085	0.11	-0.04	-0.043	-0.088	-0.059	-0.28	0.046	0.025	0.27	0.055
Ca_pct	-0.46	-0.42	-0.081	-0.16	-0.2	0.31	0.019	1	-0.25	-0.046	-0.16	0.23	0.75	0.92	0.63	-0.58	-0.16	-0.11	-0.33	0.17	0.88	0.031	-0.31
Cr_ppm	-0.077	0.18	-0.33	0.49	-0.13	0.23	0.063	-0.25	1	-0.15	0.35	0.079	-0.031	-0.22	-0.1	0.31	0.47	-0.28	-0.14	0.26	-0.2	0.3	0.044
Fe_pct	0.22	0.24	0.25	-0.034	0.099	0.0065	0.041	-0.046	-0.15	1	-0.15	-0.27	-0.0054	-0.0065	0.043	0.35	-0.077	0.35	0.3	0.072	-0.049	0.24	0.53
K_pct	-0.22	0.062	-0.34	0.53	-0.29	0.63	0.31	-0.16	0.35	-0.15	1	0.49	0.046	-0.095	-0.28	0.19	0.3	-0.17	-0.22	0.26	-0.18	0.32	0.077
La_ppm	-0.39	-0.17	-0.29	0.4	-0.31	0.48	0.2	0.23	0.079	-0.27	0.49	1	0.34	0.29	0.11	-0.14	0.11	-0.4	-0.43	0.16	0.13	0.28	-0.13
Mg_pct	-0.51	-0.23	-0.3	0.22	-0.38	0.44	0.085	0.75	-0.031	-0.0054	0.046	0.34	1	0.73	0.51	-0.31	-0.026	-0.28	-0.52	0.35	0.62	0.31	-0.16
Mn_ppm	-0.47	-0.3	-0.13	-0.062	-0.26	0.33	0.11	0.92	-0.22	-0.0065	-0.095	0.29	0.73	1	0.61	-0.48	-0.15	-0.16	-0.39	0.23	0.8	0.13	-0.22
Na_pct	-0.34	-0.19	-0.1	-0.15	-0.16	0.089	-0.04	0.63	-0.1	0.043	-0.28	0.11	0.51	0.61	1	-0.36	-0.027	-0.2	-0.29	0.11	0.6	0.11	-0.16
Ni_ppm	0.53	0.83	0.12	0.43	0.34	-0.079	-0.043	-0.58	0.31	0.35	0.19	-0.14	-0.31	-0.48	-0.36	1	0.36	0.18	0.39	0.24	-0.43	0.24	0.54
P_ppm	0.19	0.34	-0.11	0.6	0.07	0.14	-0.088	-0.16	0.47	-0.077	0.3	0.11	-0.026	-0.15	-0.027	0.36	1	-0.21	0.065	0.5	-0.06	0.43	0.18
Pb_ppm	0.48	0.2	0.53	-0.36	0.48	-0.31	-0.059	-0.11	-0.28	0.35	-0.17	-0.4	-0.28	-0.16	-0.2	0.18	-0.21	1	0.57	-0.24	0.024	-0.4	0.36
S_pct	0.78	0.41	0.57	-0.23	0.69	-0.44	-0.28	-0.33	-0.14	0.3	-0.22	-0.43	-0.52	-0.39	-0.29	0.39	0.065	0.57	1	-0.018	-0.12	-0.35	0.38
Sc_ppm	0.022	0.29	-0.095	0.51	-0.095	0.3	0.046	0.17	0.26	0.072	0.26	0.16	0.35	0.23	0.11	0.24	0.5	-0.24	-0.018	1	0.28	0.59	0.15
Sr_ppm	-0.23	-0.23	-0.0058	-0.092	-0.046	0.19	0.025	0.88	-0.2	-0.049	-0.18	0.13	0.62	0.8	0.6	-0.43	-0.06	0.024	-0.12	0.28	1	0.039	-0.19
V_ppm	-0.25	0.17	-0.38	0.68	-0.38	0.42	0.27	0.031	0.3	0.24	0.32	0.28	0.31	0.13	0.11	0.24	0.43	-0.4	-0.35	0.59	0.039	1	0.11
Zn_ppm	0.43	0.48	0.3	0.32	0.25	-0.079	0.055	-0.31	0.044	0.53	0.077	-0.13	-0.16	-0.22	-0.16	0.54	0.18	0.36	0.38	0.15	-0.19	0.11	1

Table 3: Spearman Rank correlation matrix for 2005 rock prospects samples

Multivariate Analysis

Cluster analysis is an exploratory statistical tool that groups individual observations into homogeneous datasets or clusters based on compositional similarity (Filzmoser, 2018). Most clustering methods are based on the use of Euclidean distances, however as mentioned above, compositional datasets are better modelled using Aitchison geometry (Aitchison, 1986). Clustering methods for compositional data use what is termed the 'Aitchison distance' to calculate the metrics required and the use of a log ratio transformation is critical to generation of realistic results (Filzmoser, 2018).

Robust hierarchical clustering utilizing the complete linkage option was applied to the 2005 Archer Cathro rock prospects multi-element dataset. This method of clustering is an agglomerative method (i.e. sequential merging of clusters controlled by distance metrics) and results in the generation of a series of clustering partitions (Filzmoser, 2018). The use of the complete linkage option involves constructing the clusters based on the greatest distances between observations (Filzmoser, 2018).

Cluster analysis was performed in the R statistics software using the RobCompositions robust clustering algorithms. Isometric log ratio transformed data were used to calculate a variation matrix which was subsequently used for calculation of clusters using the Aitchison distance. A robust approach was adopted to minimize the effect of outliers that occur within the data. Clustering results are presented on the dendrogram in **Figure 33**.

Five distinct clusters are observed in the rock prospects data (**Fig. 33**) including:

- Group 1: Cu-S-As-Ag-Pb (mineralization)
- Group 2: Ca-Mg-Mn-Sr (carbonate alteration)
- Group 3: Zn-Co-Ni (mineralization)
- Group 4: Ba-Fe-B-Na (alteration ?)
- Group 5: La-Al-V-Cr-P-K-Sc (lithology related)

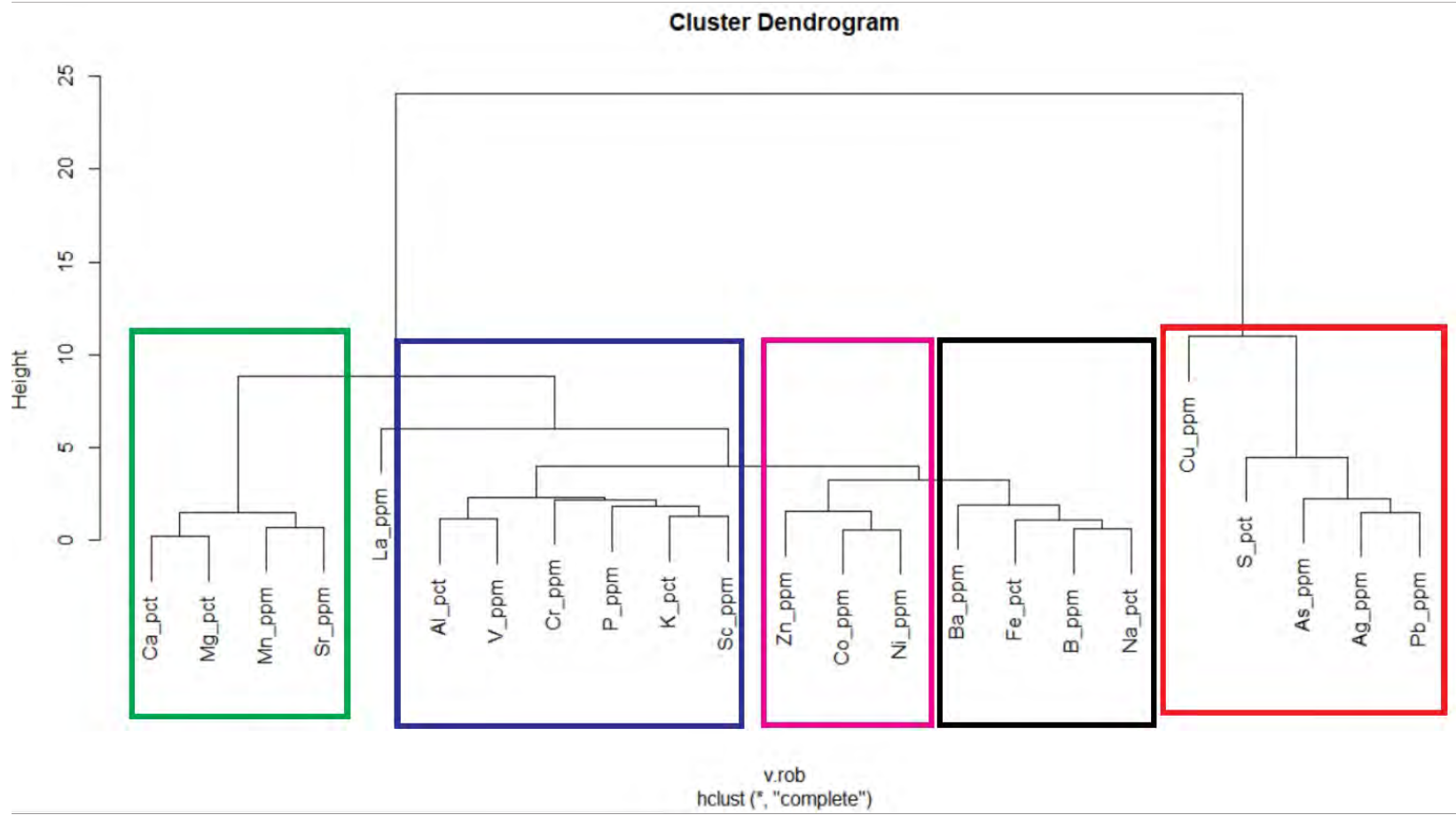


Figure 33: Hierarchical clustering dendrogram for 2005 rock prospecting samples

KEY PATHFINDERS FROM CLUSTER ANALYSIS: Cu-S-As-Ag-Pb

Alteration identified from clustering appears to be predominantly carbonate minerals.

Principal Component Analysis (PCA) is a mathematical procedure that transforms high dimensional correlated variables into a number of uncorrelated variables called principal components. The technique is very commonly used to identify important multivariate associations between elements in geochemical datasets and provide insight into controlling geological processes (Grunsky, 2010). The first principal component accounts for the majority of the variability in the dataset, with successive components accounting for remaining variability. The results of PCA are typically presented as a biplot of scores (PC1 vs PC2) and loadings (Gabriel, 1971).

Due to the unique geometry of compositional data (i.e. non-euclidean), classical PCA typically does not yield uncorrelated components largely due to the influence of outliers and non-normal population distributions. Robust principal component analysis (RPCA) using the minimum covariance determinant method (MCD) aims to subdue the influence of outlier data.

Robust principal component analysis (RPCA) was applied to the 2005 Archer Cathro rock prospect data. Analysis was completed in R statistics package RobCompositions (*pcaCoDA algorithm*). In this method, raw data are transformed into isometric log ratio (ILR) co-ordinates prior to application of RPCA. The results are then back-transformed into center-log transformed (CLR) data for interpretation purposes. The analysis generates eigenvalues (rankings or importance) and eigenvectors (element loadings). Eigenvalues > 1 are considered meaningful (Kaiser, 1960). Components < 1 represent noise in the data. Additional filtering of principal components (PC) is carried out using a component versus eigen value plot (**Fig. 34**). Meaningful components occur above eigenvalues where a significant change in angle can be marked (elbow method; **Fig. 34**). Positive eigenvector values (loadings) typically indicate that a particular

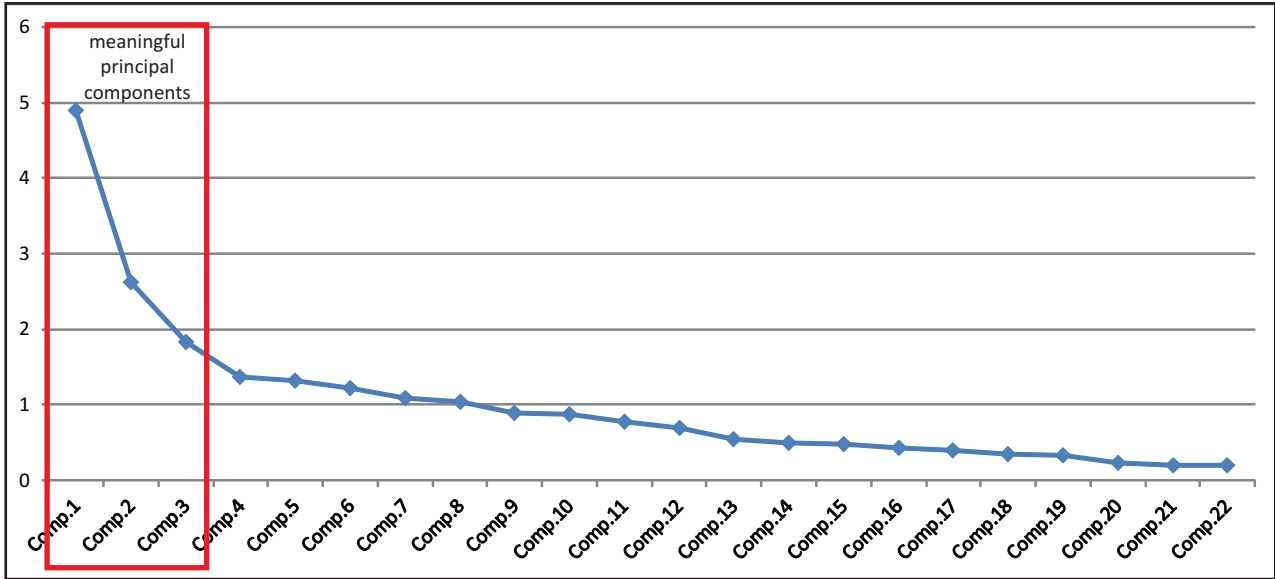


Figure 34: Eigenvalue versus number of principal component plot for 2005 rock prospect samples (elbow method)

variable contributes to a given PC. Negative loadings indicate no association between the variable and the PC.

Eigenvalues and eigenvector loadings for PCs with eigenvalues > 1 are presented in **Tables 4 and 5**, respectively. Graphical representation of the ordered loadings of principal components with eigenvalues > 1 for each geochemical package is presented in the **Figure 35**.

Three principal components are considered meaningful from ILR transformed RPCA for the rock prospect geochemical data (**Table 4**). PC 1 has moderate positive loadings for Cu-S-As, weak positive loadings for Ni-Ag-Co and is interpreted as the main Cu mineralizing system. PC2 has positive loadings for Ca-Mn-Ag-Sr-As-Pb-Mg and may represent a base metal component of mineralization associated with carbonate alteration. PC3 has positive loadings for Fe-Cr-Ag-V-Zn-Pb-Ba-Mn and is interpreted to represent geochemical associations related to host rocks.

Univariate and multivariate geochemical analysis of rock samples taken from existing zones of Cu-Co mineralization indicate the important element pathfinders are:

Cu-S-As-Fe-Ag-Ni-Co+/- Pb

Additionally, the presence of geochemical clusters and principal components associated Ca-Mn-Sr-Mg suggest carbonate minerals may represent an important component of the alteration system. These pathfinder elements as defined from both the univariate and multivariate geochemical analysis are consistent with pathfinders characteristic of well-known IOCG deposits.

	Eigenvalues	Proportion of Variance	Cumulative Proportion
PC 1	4.897	0.524	0.524
PC 2	2.625	0.151	0.675
PC 3	1.836	0.074	0.748
PC 4	1.376	0.041	0.790
PC 5	1.315	0.038	0.828
PC 6	1.221	0.033	0.860
PC 7	1.098	0.026	0.886
PC 8	1.037	0.024	0.910
PC 9	0.887	0.017	0.927
PC 10	0.870	0.017	0.944
PC 11	0.779	0.013	0.957
PC 12	0.700	0.011	0.968
PC 13	0.543	0.006	0.974
PC 14	0.499	0.005	0.980
PC 15	0.473	0.005	0.984
PC 16	0.425	0.004	0.988
PC 17	0.397	0.003	0.992
PC 18	0.351	0.003	0.995
PC 19	0.336	0.002	0.997
PC 20	0.237	0.001	0.998
PC 21	0.206	0.001	0.999
PC 22	0.199	0.001	1.000

Table 4: Summary of eigenvalues for each identified principal component of 2005 rock prospect samples.

	PC 1	PC 2	PC 3
Cu_ppm	0.660	0.078	-0.333
Zn_ppm	0.061	-0.128	0.127
V_ppm	-0.125	-0.415	0.165
Fe_pct	-0.030	0.009	0.284
Ag_ppm	0.088	0.258	0.170
Mg_pct	-0.192	0.141	0.004
Al_pct	-0.056	-0.392	-0.084
Mn_ppm	-0.199	0.265	0.109
Na_pct	-0.089	0.137	0.098
Ca_pct	-0.196	0.335	0.050
La_ppm	-0.411	-0.021	-0.772
Sr_ppm	-0.101	0.258	-0.002
B_ppm	-0.055	0.056	0.073
Sc_ppm	-0.037	-0.124	0.015
Ni_ppm	0.093	-0.258	0.053
Pb_ppm	0.037	0.142	0.122
P_ppm	0.089	-0.230	-0.065
K_pct	-0.070	-0.154	-0.060
Co_ppm	0.086	-0.102	-0.034
Ba_ppm	-0.153	0.013	0.114
As_ppm	0.177	0.219	-0.172
S_pct	0.374	0.117	-0.042
Cr_ppm	0.048	-0.204	0.180

Table 5: Resultant element loadings for statistically meaningful principal components (PC 1 – PC3).

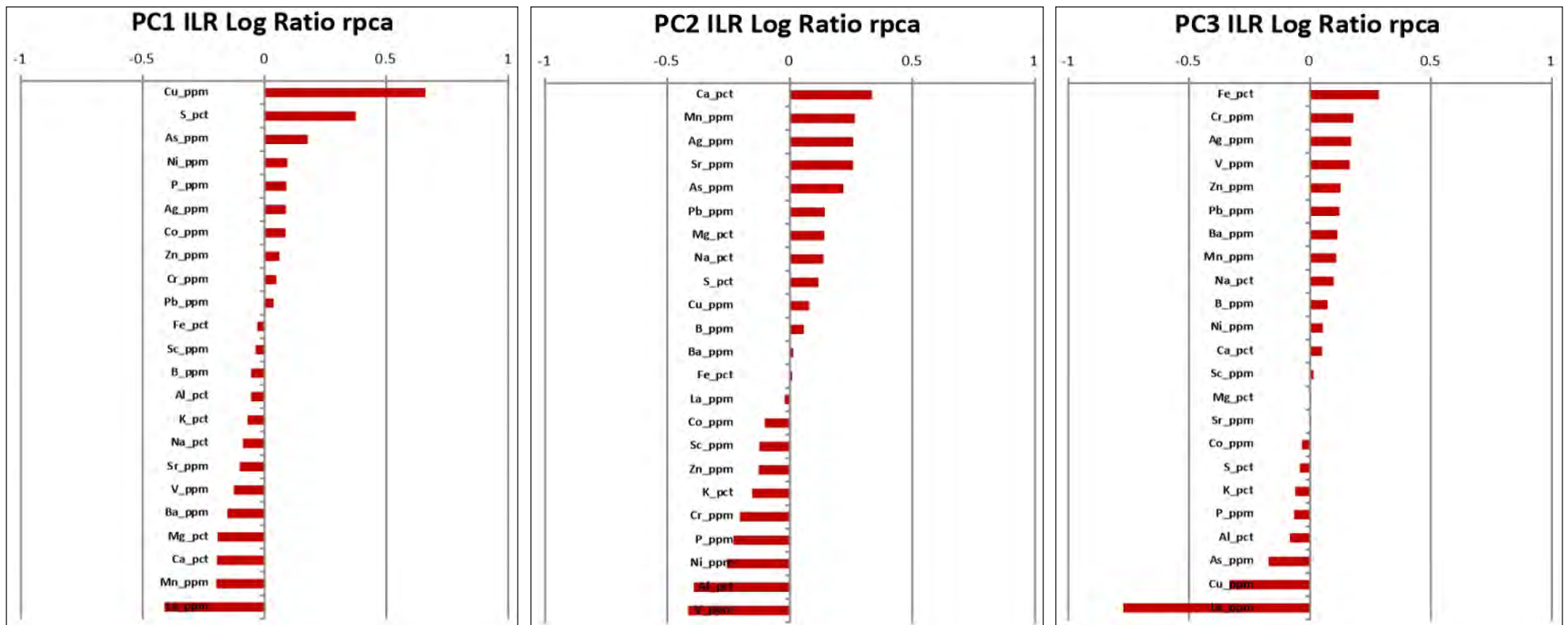


Figure 35: Graphical representation of loadings associated with PC 1 to PC3 of 2005 rock prospect samples.

6.2 SAMPLE CATCHMENT BASIN ANALYSIS

The 2005 Archer Cathro stream sediment dataset comprises a total of 170 samples. Seventeen of these samples occur within and adjacent to the Bronson property (**Figs. 36**). Subsequent to removal of elements with greater than 50 % non-detects and imputation of values below detection levels, the stream sediment data on the Bronson property were evaluated using the sample catchment basin analysis method.

Methodology

Stream sediment data can be analyzed using either interpolation of data points using techniques such as Kriging or Inverse Distance Weighting (IDW) calculations which yields continuous raster datasets or using the sample catchment basin analysis method (SCBA), where watersheds are delineated and stream sediment data are assigned to the derived watershed (discrete raster data).

The 2005 stream sediment dataset has large gaps in sampling in the central portion of the project area, such that use of interpolation methods would lead to significant artifacts in the derived raster data. As such, analysis was restricted to SCB methods to assess silt geochemical data.

Two major controls on stream sediment geochemistry include background lithology within the catchment area and transport-controlled dilution. It is important to correct for these factors in order to generate realistic geochemical anomalies. Upstream lithology controls a significant proportion of the geochemical variation present in any given stream sediment sample. The SCBA method attempts to correct for this by calculating background concentrations for each element as a weighted average using areal proportions of each lithological unit in every sample catchment basin (Bonham-Carter et al. 1987).

In this method, weighted mean concentration due to lithology (M_j) was calculated as:

$$M_j = (\sum_{i=1}^n Y_i X_{ij}) / (\sum_{i=1}^n X_{ij})$$

where Y_i represents measured elemental values per stream sediment sample i ($=1,2,\dots,n$), X_{ij} is the area of each of the j ($=1,2,\dots,m$) lithologic units in SCB i .

The local background elemental background concentration (Y'_i) due to j lithologic units per SCB is then estimated using:

$$Y'_i = (\sum_{j=1}^m M_j X_{ij}) / (\sum_{j=1}^m X_{ij})$$

The estimated background value is then removed from the stream sediment value to create residual values ($Y_i - Y'_i$), which can be either positive or negative.

Dilution of stream sediment geochemistry is corrected for using the following equation (Hawkes 1976, Carranza and Hale, 1997):

$$Y_a = 100A_i(Y_i - Y'_i)$$

where A_i is catchment basin area and can be determined by measuring area of known veins (exposed at surface within the MGP). Y_a denotes dilution-corrected residuals of elemental concentrations. Positive values of Y_a are of interest in mineral exploration because they most likely represent metal enrichment that is due to mineralization. Negative residuals may be interpreted as depletions and care should be taken to review these as many ore systems have distinctive element depletions (e.g. Y in orogenic gold systems).

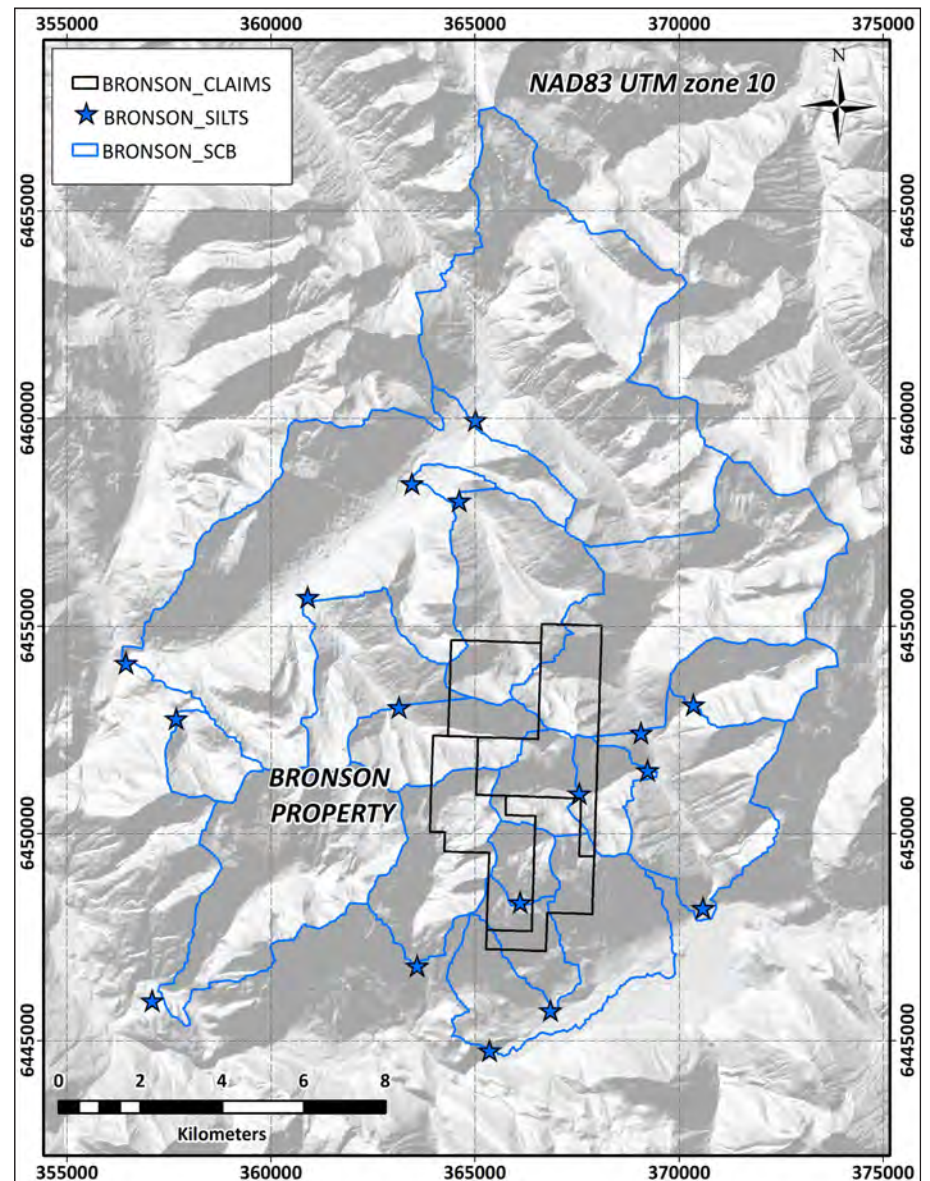
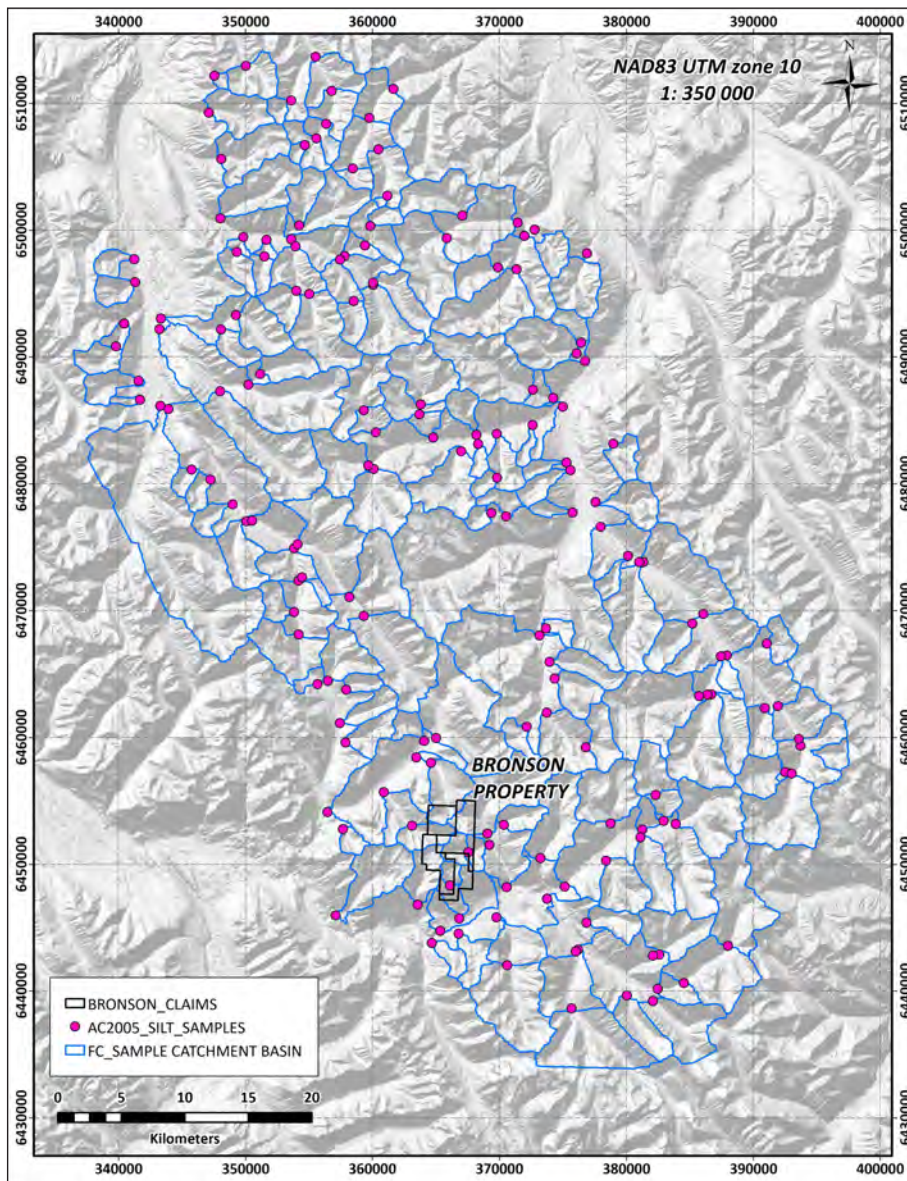


Figure 36: Total sample catchment basins for project area and seventeen sample catchment basins associated with the Bronson Property

An important objective of the analysis of stream sediment data is to define anomalous sample catchment basins using both univariate and multivariate geochemical data. Current best practice for defining anomalous element thresholds involves integration of frequency (i.e. statistical) and spatial techniques.

The concentration-area (C-A) technique is a multifractal analysis method (Cheng et al., 1994; Cheng, 2012), commonly used to establish population thresholds for the identification of anomalies in geochemical datasets. The term fractal describes the geometry of scale invariant properties that are characterized by self-similarity (Mandelbrot 1983). Geochemical data have been shown to represent multifractals (e.g. Agterberg et al., 1996, Cheng et al., 2000). Cheng (1994) proposed the C-A fractal model to identify geochemical anomalies from background populations. The model in 2D space consists of:

$$A(\rho) \propto \rho^{-\beta}$$

$A(\rho)$ represents the area delineated by the element concentration greater than or equal to ρ , and β denotes the fractal dimension. In a log-log plot of $A(\rho)$ vs ρ the data can be fitted into several lines (multi fractals) using the least-squares regression techniques. In order to define thresholds, a log-log plot of metal concentration versus area of metal contents greater than certain specified values (e.g. percentile breaks) defines a decreasing relationship (Shahrestani et al, 2019). Regression lines fitted through the log-log plot represent multiple populations for dataset in question. In the multifractal anomaly separation method, population thresholds are denoted by the line breaks.

The method takes into account spatial controls on geochemical variability and is considered to be superior to classic statistical (Mean + 2SD) and exploratory data analysis (Median + 2MAD) threshold derivation methods.

For the 2005 Archer Cathro stream sediment data in the Bronson property area, the following analysis workflow has been adopted:

- a. Sample catchment basin delineation using the regional 25 m DEM dataset.
- b. Calculation of background values and a dilution correction to generate geochemical residuals using formulas outlined above.
- c. Threshold delineation of background and dilution corrected residuals using the multifractal concentration area technique for the main pathfinder elements defined from geochemical analysis of rock samples.
- d. Robust principal component analysis.
- e. Evaluation of univariate and multivariate data and selection of anomalous sample catchment basins. Highest priority SCB's are those with Cu and pathfinder element anomalism. All SCB identified as anomalous warrant detailed evaluation of existing data and if merited additional groundwork working upstream.

Univariate Results

Univariate and multivariate analysis of rock prospect data indicate Cu is associated with the pathfinders S-As-Ag-Co-Fe and Ni. With the exception of Ag, which was removed due to the very high proportion of non-detects, these pathfinder elements were evaluated using the SCB analysis method.

Anomalous thresholds were defined on background and dilution corrected residuals using the multi-fractal C-A method of Cheng (1994) for Cu-S-As-Ni-Co. Sample catchment basin maps with anomalous and background populations of univariate data are presented for the

Bronson prospect in **Figures 37-42**. All SCB identified as anomalous warrant detailed evaluation of existing data and if merited additional groundwork in the watershed.

Figure 37 shows the background + dilution corrected Cu results. Six catchment basins are identified as anomalous for Cu. **Figure 38** shows the distribution of rock prospecting samples and occurrence of diabase dykes in comparison to the distribution of sample catchment basins anomalous in Cu.

Figure 39 shows the background + dilution corrected S results. Eleven catchment basins are identified as having a high background value for S, but no basins are significantly anomalous. Eight catchment basins show high background for As (**Fig 40**). Eleven sample catchment basins are characterized by high background for Ni, all clustered around the Bronson claims (**Fig. 41**). Thirteen catchment basins have high background values of Co (**Fig. 42**).

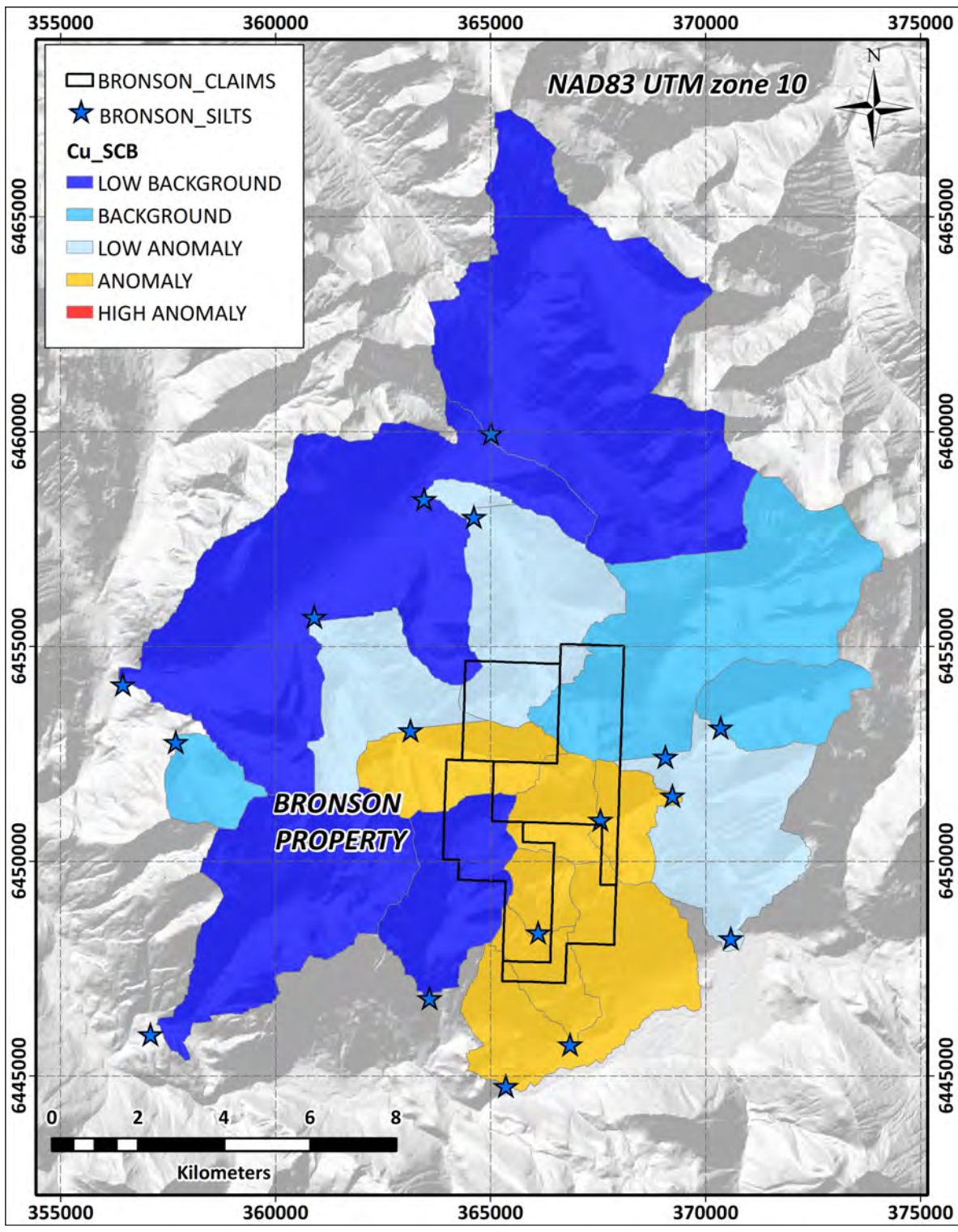


Figure 37: Bronson sample catchment basin results - Cu.

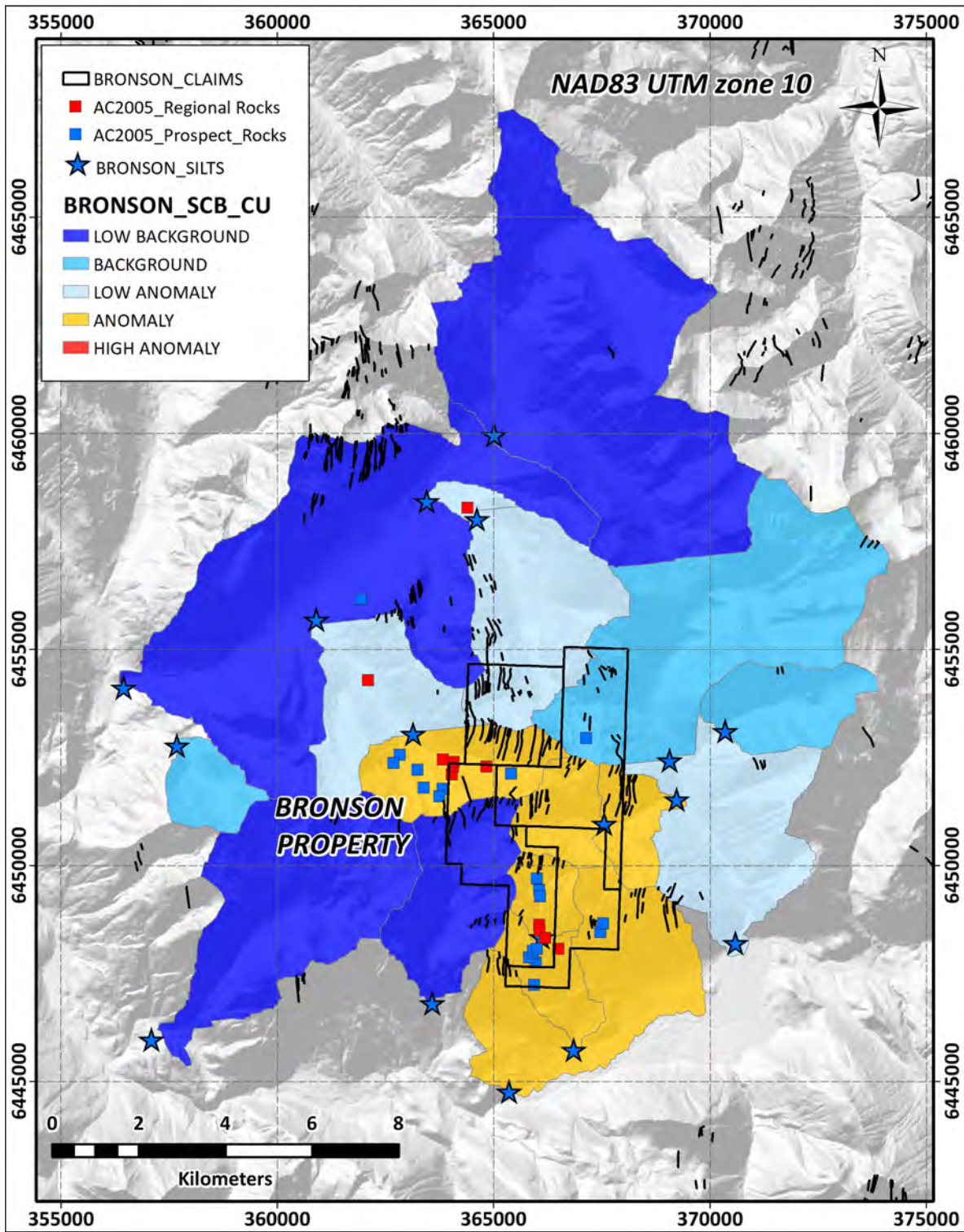


Figure 38: Bronson sample catchment basin results - Cu. Distribution of rock samples and diabase dykes superimposed

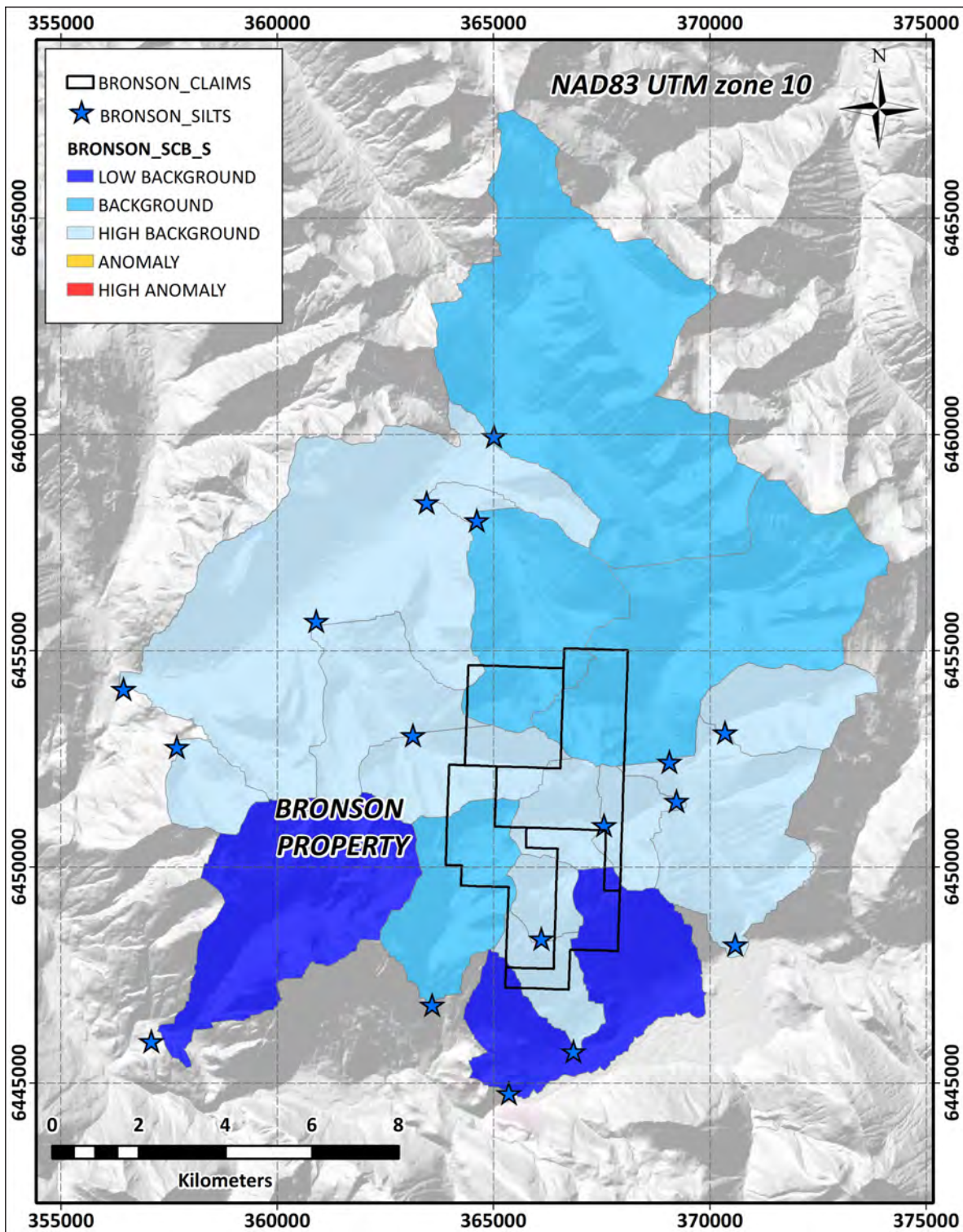


Figure 39: Bronson sample catchment basin results - S.

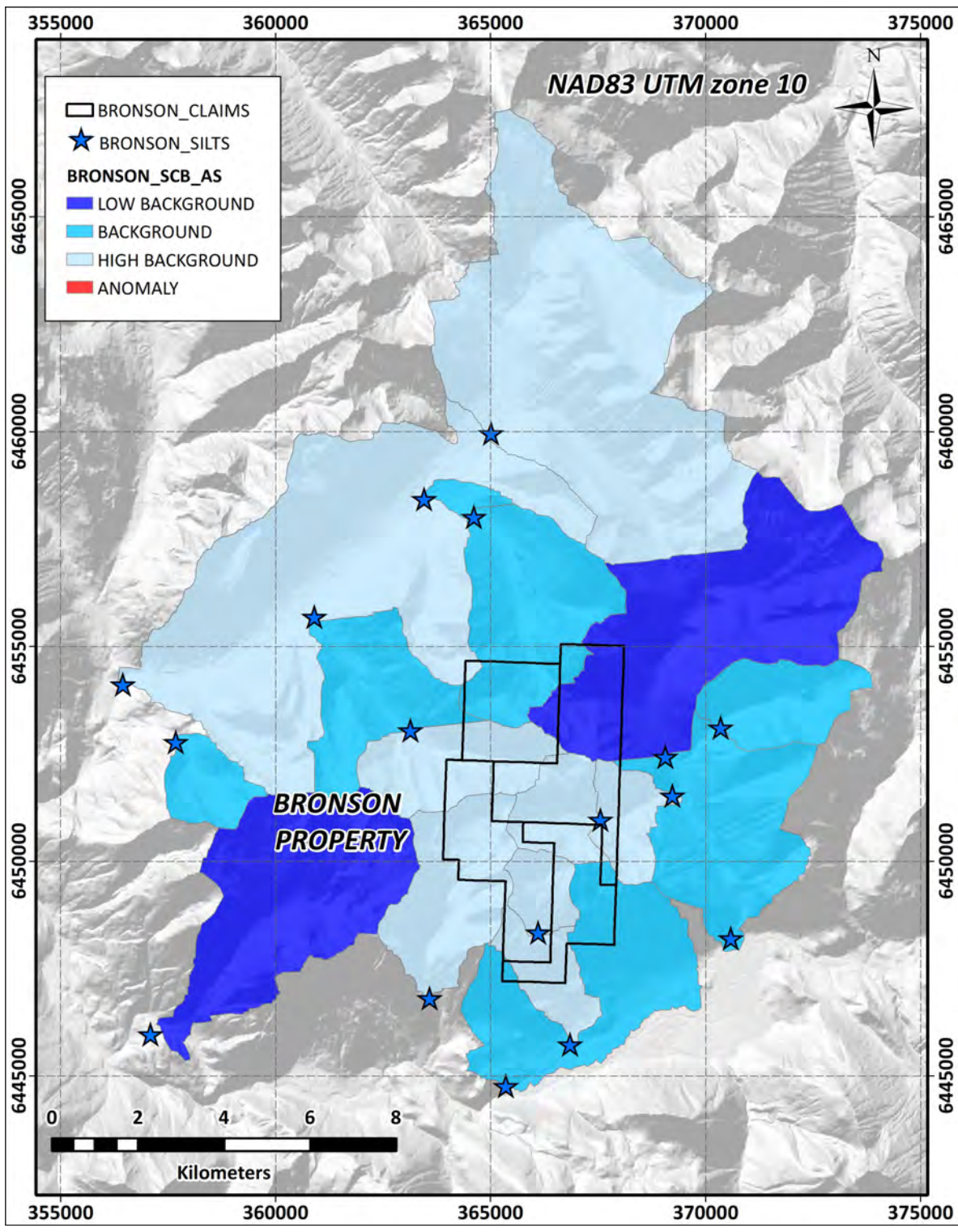


Figure 40: Bronson sample catchment basin results - As.

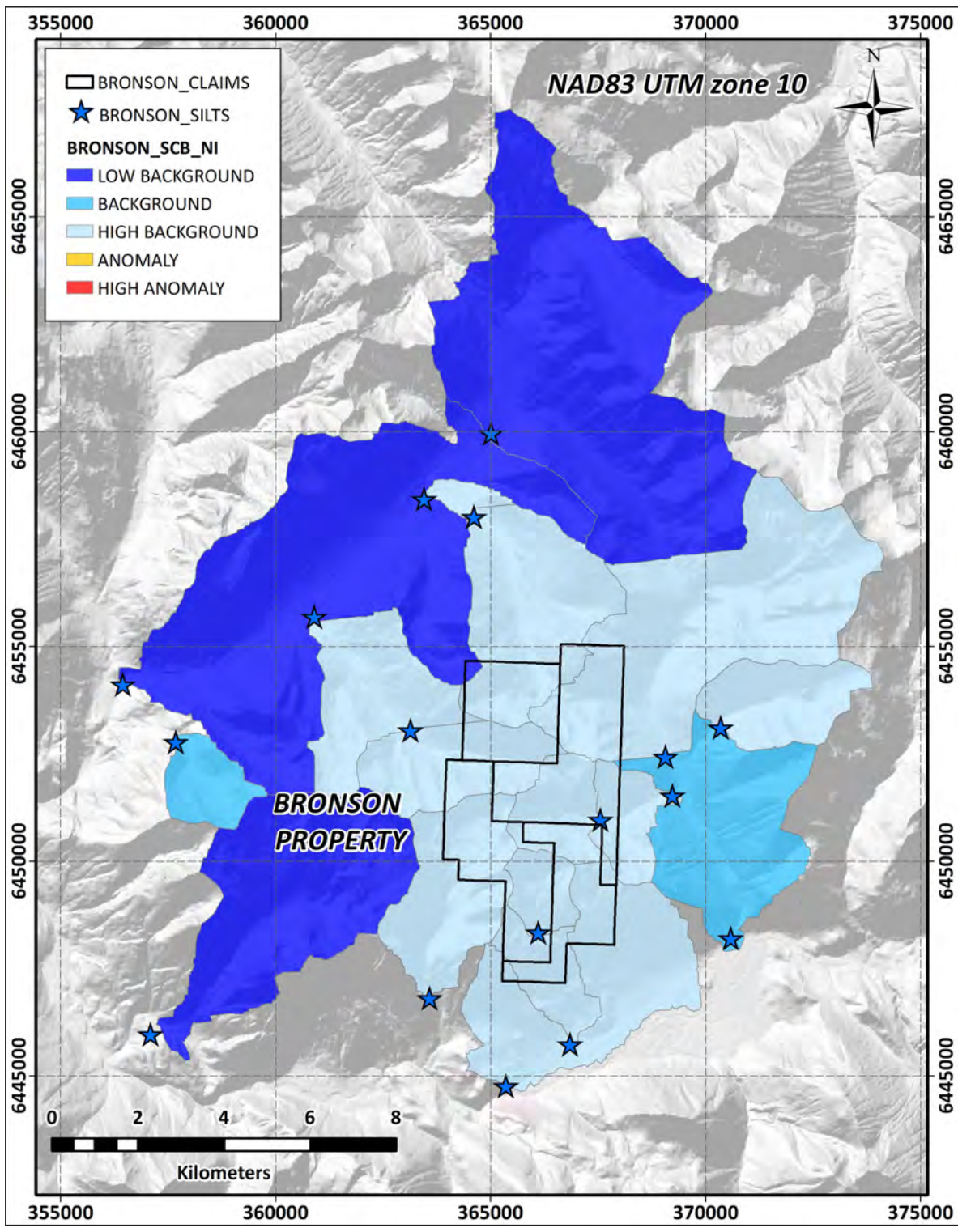


Figure 41: Bronson sample catchment basin results - Ni.

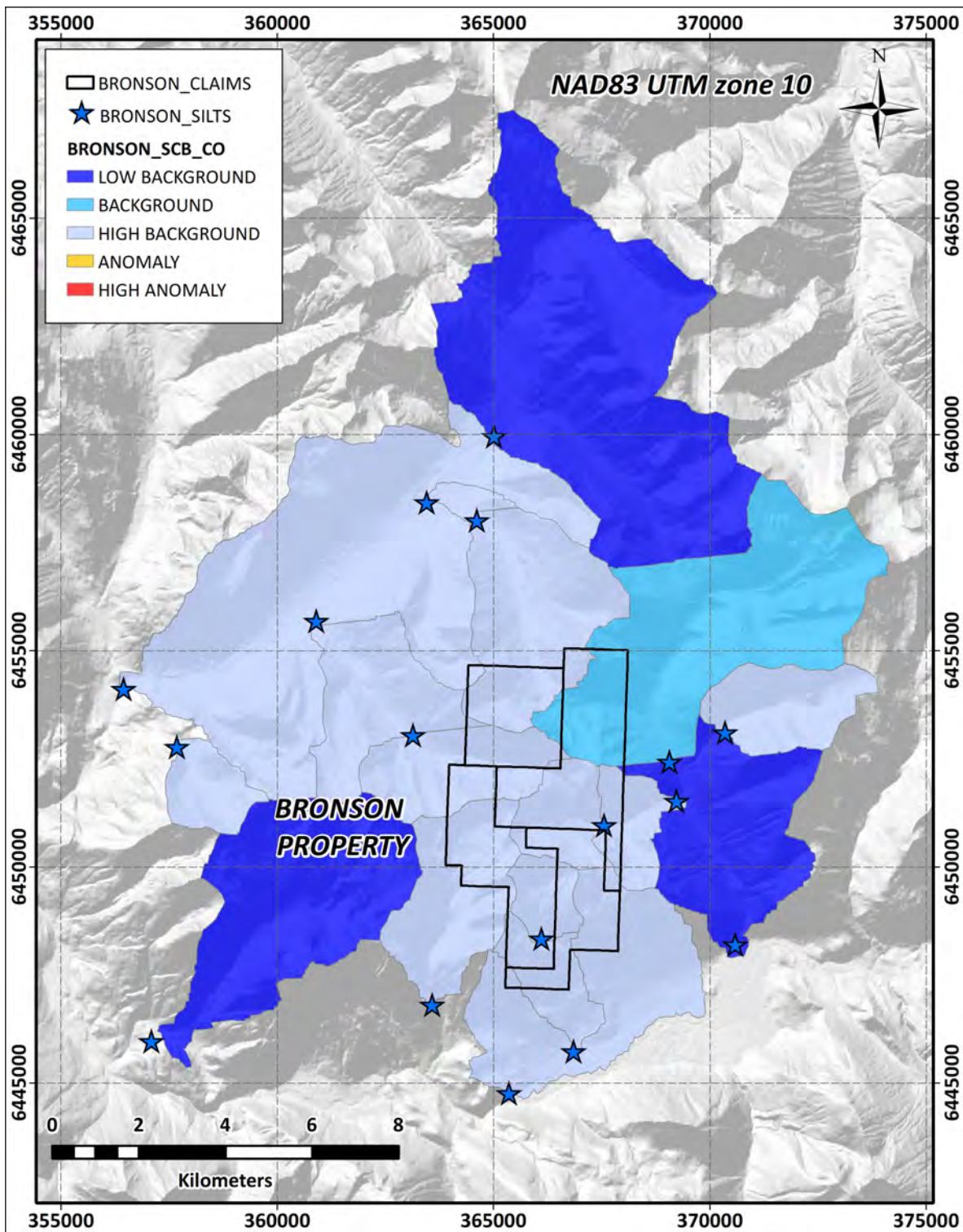


Figure 42: Bronson sample catchment basin results - Co.

Multivariate Results

Robust principal component analysis was carried out on the background + dilution corrected 24-element stream sediment data. Summary of resultant eigenvalues is presented in **Table 6**. Resulting element loadings for each principal component with an eigenvalue > 1 are presented in **Table 7**.

The first three principal components are considered meaningful and represent ~60% of the total variance within the stream sediment data. Principal component 1 has positive loadings for V-Cr-Ti-Al-Sc-Fe-Co-Be-Cu-K-Ni (**Table 7**) and is considered to represent mineralization. Principal component 2 has positive loadings for Ba-Sr-P-S and may represent the chemistry associated with the Proterozoic carbonate stratigraphy (**Table 7**). Principal component 3 has positive loadings for Ti-Sr-Ca-V-Na-Cr-Sc-Al-Mg and likely represents lithochemical contributions from both clastic and carbonate stratigraphy in the sampling area.

Principal Component 1 was used to identify multivariate anomalies with the sample catchment basins associated with the Bronson Prospect. Thresholds were defined using the multi-fractal C-A method of Cheng (1994). Anomalous multivariate (Cu+pathfinders) SCBs is presented in **Figure 43**. Two sample catchment basins were identified as anomalous for the first principal component. Six additional sample catchment basins were classified as having high multivariate geochemical backgrounds. **Figure 44** shows the distribution of sample catchment basins associated with multivariate anomalies in comparison to rock sampling and distribution of diabase dykes.

Component	Eigenvalues	Proportion of Variance	Cumulative Proportion
PC 1	0.392	0.284	0.284
PC 2	0.308	0.175	0.459
PC 3	0.276	0.140	0.600
PC 4	0.214	0.084	0.684
PC 5	0.200	0.074	0.758
PC 6	0.173	0.055	0.814
PC 7	0.140	0.036	0.850
PC 8	0.121	0.027	0.877
PC 9	0.116	0.025	0.902
PC 10	0.102	0.019	0.921
PC 11	0.090	0.015	0.936
PC 12	0.082	0.012	0.948
PC 13	0.078	0.011	0.959
PC 14	0.072	0.009	0.969
PC 15	0.066	0.008	0.977
PC 16	0.051	0.005	0.982
PC 17	0.049	0.004	0.986
PC 18	0.046	0.004	0.990
PC 19	0.037	0.003	0.993
PC 20	0.034	0.002	0.995
PC 21	0.032	0.002	0.997
PC 22	0.030	0.002	0.998
PC 23	0.025	0.001	0.999
PC 24	0.018	0.001	1.000

Table 6: Summary of eigenvalues for each identified principal component for the 2005 stream sediment data

	PC 1	PC 2	PC 3
Al_pct	0.1901	-0.0022	0.1064
As_ppm	-0.0509	-0.1264	-0.3148
B_ppmL	-0.0025	0.0324	-0.0048
Ba_ppm	0.0200	0.8578	-0.1775
Be_ppm	0.1200	-0.0285	0.0660
Ca_ppm	-0.5335	0.0008	0.2207
Co_ppm	0.1253	-0.0266	-0.0192
Cr_ppm	0.2522	0.0172	0.1192
Cu_ppm	0.0990	-0.0638	0.0206
Fe_pct	0.1654	-0.0337	0.0353
K_ppmL	0.0982	-0.0570	-0.0150
La_ppm	0.0342	-0.0560	0.0632
Mg_ppm	-0.3804	-0.1553	0.0956
Mn_ppm	-0.0077	-0.0031	0.0450
Mo_ppm	-0.0501	-0.0054	-0.6055
Na_ppm	-0.3152	-0.0949	0.1226
Ni_ppm	0.0966	-0.0136	-0.0776
P_ppmL	-0.0761	0.1193	0.0600
Pb_ppm	-0.0932	-0.1601	-0.3531
S_pctL	-0.0316	0.0788	0.0181
Sc_ppm	0.1732	0.0493	0.1166
Sr_ppm	-0.3087	0.1896	0.2627
Ti_ppm	0.2119	-0.1557	0.2682
V_ppmL	0.3024	-0.0679	0.1986
Zn_ppm	-0.0386	-0.2950	-0.2512

Table 7: Resultant element loadings for statistically meaningful principal components (PC 1 – PC3), stream sediment data.

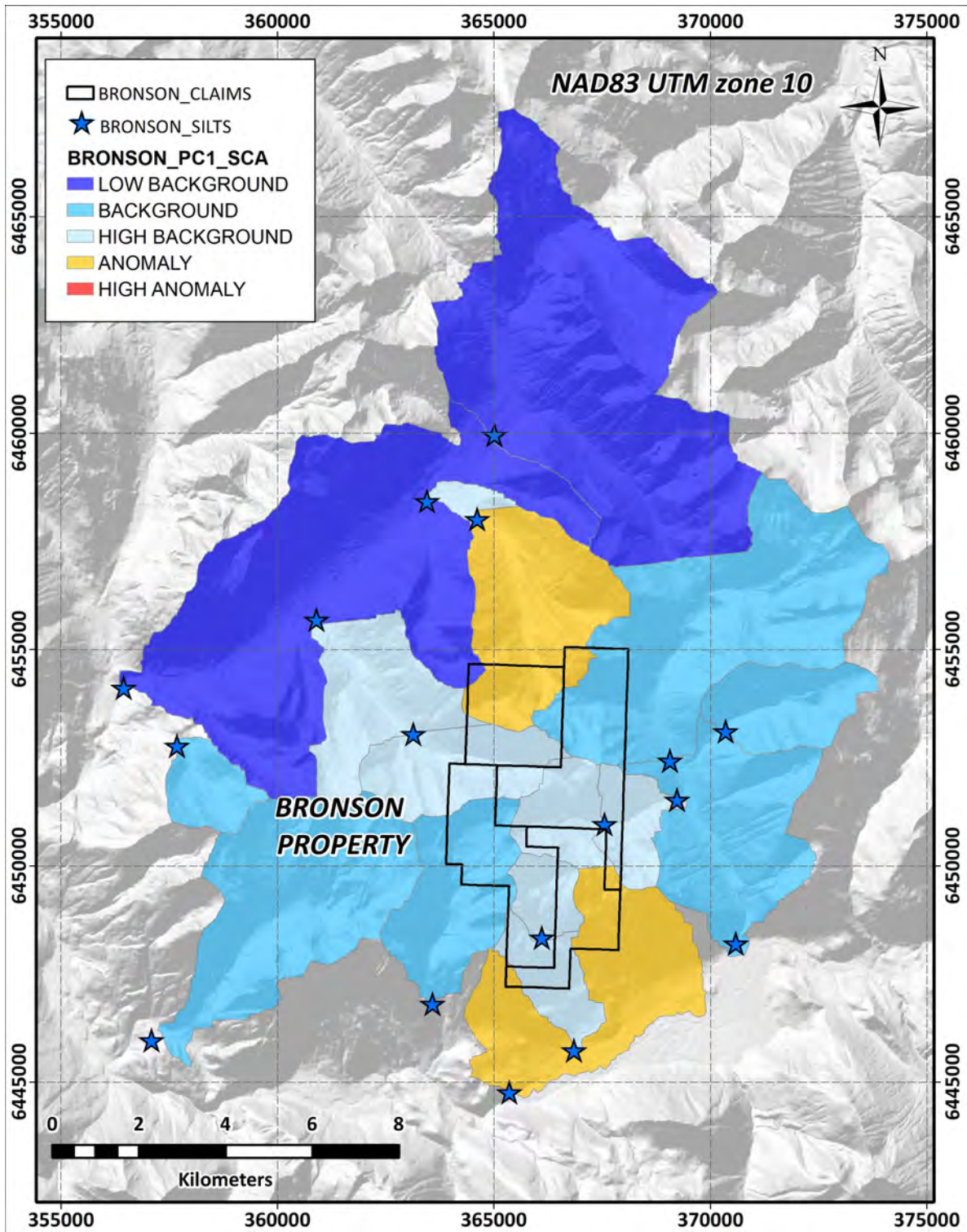


Figure 43: Bronson sample catchment basin results - Principal Component 1

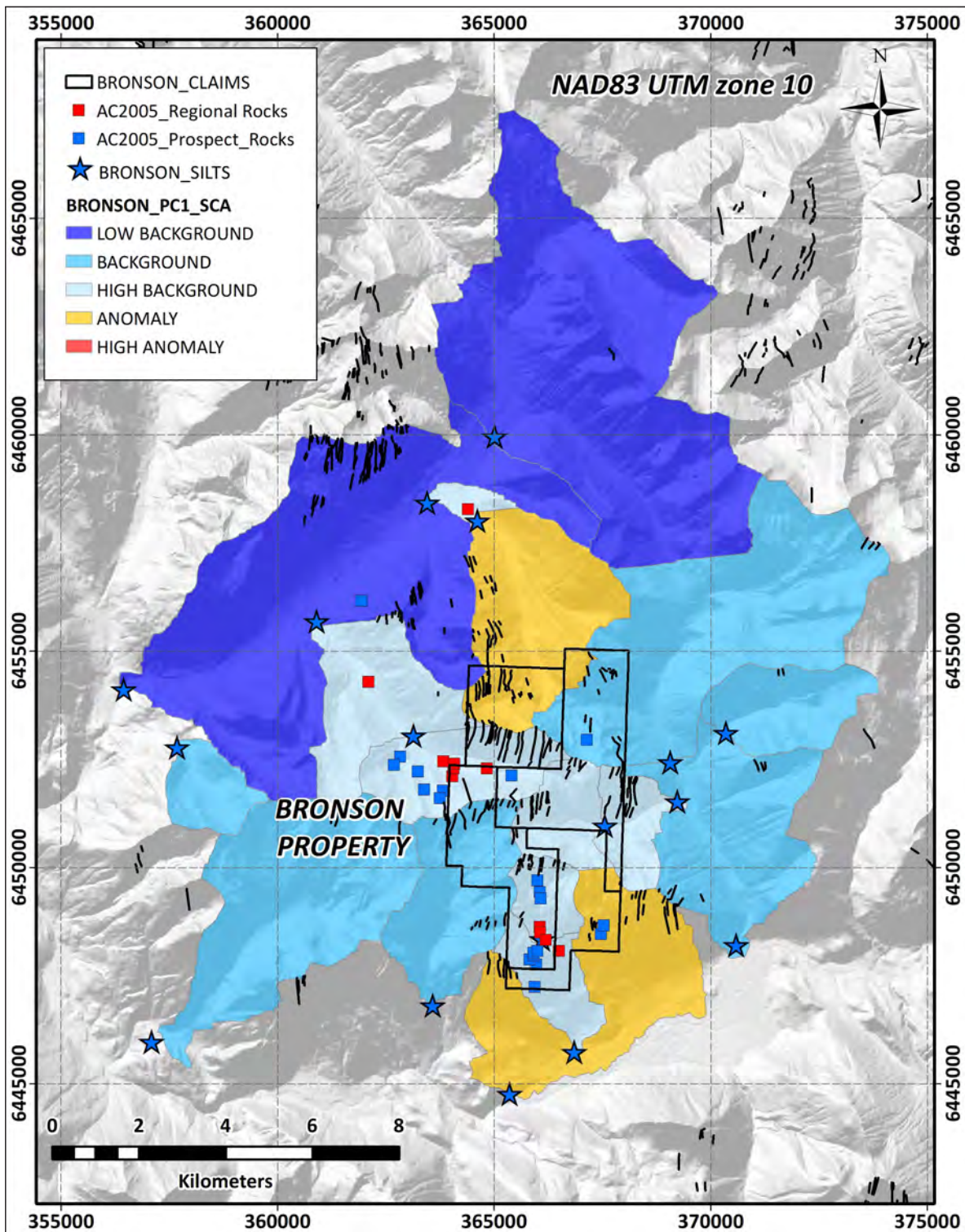


Figure 44: Bronson sample catchment basin results - Principal Component 1
Distribution of rock samples and diabase dykes superimposed

BRONSON PROPERTY HISTORIC SOIL ANALYSIS

Univariate and multivariate geochemical trends were evaluated for the Bronson soil dataset, which consists of 761 samples located in three spatially distinct grid surveys (Bronson, Book Grid 1, Book Grid 2; **FIG 26**). Anomalous thresholds for Cu and associated pathfinders were defined using (i) Tukey outliers, and (ii) the multifractal C-A method of Cheng (1994). Graduated symbol dot plots and Inverse Distance Weighted (IDW) interpolations raster images were generated to identify anomalous soil locations.

The multi-fractal C/A threshold determination method was used for interpretation and targeting. Robust hierarchical cluster analysis was also conducted on multi-element datasets prior to determination of anomalous sample populations using the C/A fractal method.

Univariate Results

Spearman rank correlation matrices and summary statistics for the three multi-element Bronson soil datasets are summarized in **Tables 8-13**. The three grids exhibit different pathfinder associations which and are discussed separately below.

The **Book 1** soil grid shows moderate strength correlations between **Cu-Be-Ca-P-Pb-S and Sr** and a moderate strength negative correlation between **Cu and V**. Scatterplot diagrams also indicate weaker positive correlations between Cu, As, Ni and Co (**Fig. 45**).

Univariate dot plots and IDW interpolations plots are presented in **Figures 46-52** for Cu, Co and key pathfinders (Ni-As-Ca-Pb-S). Only the economic metals of interest Cu and Co are presented as dot plots. Additionally only Cu dot plots are superimposed on IDW interpolation rasters for pathfinder elements. The anomalous thresholds for Cu and Co dot plots are defined using the Tukey far outlier statistic. The C/A fractal method is used to classify the IDW interpolation plots for anomalous thresholds. Significant observations from the Book 1 univariate soil geochemical data include:

154 rows - Univariate	Cu_ppm	Ag_ppm	As_ppm	Be_ppm	Ca_pct	Co_ppm	Cr_ppm	Ni_ppm	P_ppm	Pb_ppm	S_pct	Sr_ppm	V_ppm
[Visible] : Minimum	8	0.003847	0.238438	0.02976	0.03	3	4	4	140	6	0.00407	3	3
[Visible] : Maximum	835	0.8	46	2.9	2.79	51	34	33	1780	306	0.2	146	87
[Visible] : Mean	122.7987	0.1672	8.146488	0.924401	0.59026	17.49351	16.83766	14.65584	662.20779	28.11039	0.048722	24.91558	33.11039
[Visible] : Median	53	0.147652	7	0.85	0.4	14	17.5	14.5	625	24	0.04	18	32
[Visible] : Range	827.00	0.80	45.76	2.87	2.76	48.00	30.00	29.00	1640.00	300.00	0.20	143.00	84.00
[Visible] : Standard Deviation	161.95	0.14	6.97	0.50	0.53	9.68	5.75	5.42	338.97	27.33	0.04	21.60	14.87
[Visible] : Variance	26226.76	0.02	48.61	0.25	0.28	93.61	33.12	29.42	114900.98	746.88	0.00	466.40	221.14
[Visible] : Coefficient of Variation	131.88	82.79	85.59	54.13	89.97	55.31	34.18	37.01	51.19	97.22	82.00	86.68	44.91
[Visible] : Kurtosis	4.33	5.12	8.29	2.30	3.18	1.50	-0.19	0.30	0.71	73.36	2.51	8.25	1.58
[Visible] : Skewness	2.16	1.94	2.46	1.26	1.78	1.27	-0.29	0.52	0.95	7.79	1.54	2.48	0.60
[Visible] : Tukey Upper Outlier Threshold	299.125	0.394311	19	1.85	1.51875	36.625	31.875	28.5	1500	46.5	0.145	63.5	65.375
[Visible] : Tukey Upper Far Outlier Threshold	463	0.588621	28	2.6	2.2875	52	42.75	39	2160	63	0.22	95	89.75
[Visible] : 1 percentile	9.65	0.003924	0.405296	0.04117	0.041	3.55	4	4.55	151	7.1	0.004077	3.55	3.55
[Visible] : 5 percentile	13	0.018079	1.30039	0.245323	0.1175	6	6.75	6.75	245	12	0.00679	7	6
[Visible] : 10 percentile	16.5	0.034274	1.932138	0.400695	0.15	7.5	7.5	8	300	14	0.01	8	13.5
[Visible] : 20 percentile	21	0.061701	3	0.5	0.2	10	12	10	370	17	0.02	10	22
[Visible] : 30 percentile	29	0.083933	4	0.7	0.255	12	14	12	410	20	0.02	12	27
[Visible] : 40 percentile	39	0.110971	6	0.8	0.32	13	16	13	490	22	0.03	14	29
[Visible] : 50 percentile	53	0.147652	7	0.85	0.4	14	17.5	14.5	625	24	0.04	18	32
[Visible] : 60 percentile	74	0.180141	7	0.9	0.52	17	19	16	710	26	0.04	22	36
[Visible] : 70 percentile	107.5	0.2	8	1	0.68	20	20	17	795	28	0.06	26.5	38.5
[Visible] : 75 percentile	135.25	0.2	10	1.1	0.75	21.25	21	18	840	30	0.07	32	41
[Visible] : 80 percentile	182	0.2	11	1.3	0.89	25	22	19	930	31	0.08	35	43
[Visible] : 90 percentile	376	0.3	16.5	1.5	1.535	32	24	22	1160	40	0.1	50	51
[Visible] : 95 percentile	526	0.4	20.5	2.1	1.79	39.5	25	24	1310	48	0.1325	74.25	58.75
[Visible] : 99 percentile	745.9	0.745	40.5	2.68	2.713	49.35	30.7	30.8	1747	223.5	0.1945	129.5	86.45

Table 8: Book 1 Soil Grid summary statistics for Cu and pathfinders

Spearman Rank	Cu_ppm	Ag_ppm	Al_pct	As_ppm	B_ppm	Ba_ppm	Be_ppm	Ca_pct	Co_ppm	Cr_ppm	Fe_pct	Ga_ppm	K_pct	La_ppm	Mg_pct	Mn_ppm	Mo_ppm	Na_pct	Ni_ppm	P_ppm	Pb_ppm	S_pct	Sb_ppm	Sc_ppm	Sr_ppm	Ti_pct	V_ppm	Zn_ppm
Cu_ppm	1	0.19	-0.14	0.5	0.069	0.24	0.56	0.7	0.47	-0.21	-0.3	-0.34	-0.21	-0.35	0.036	0.37	0.075	0.23	0.37	0.51	0.21	0.65	0.11	0.32	0.67	-0.38	-0.51	0.037
Ag_ppm	0.19	1	-6.80E-05	0.14	0.081	-0.022	0.19	0.12	0.16	0.0031	0.011	0.099	-0.14	-0.12	-0.035	0.099	0.2	0.079	0.09	0.17	0.054	0.19	0.32	0.062	0.13	-0.13	-0.14	-0.11
Al_pct	-0.14	-6.80E-05	1	-0.0064	0.29	0.16	0.44	-0.16	-0.072	0.92	0.62	0.47	0.64	0.27	0.86	-0.044	-0.16	-0.13	0.68	-0.24	0.23	-0.32	-0.06	0.66	-0.075	0.49	0.51	0.31
As_ppm	0.5	0.14	-0.0064	1	0.0069	-0.1	0.4	0.24	0.49	-0.013	0.098	-0.13	-0.005	-0.19	0.11	0.31	0.17	0.043	0.23	0.25	0.33	0.3	0.21	0.21	0.18	-0.18	-0.23	0.16
B_ppm	0.069	0.081	0.29	0.0069	1	-0.005	0.26	0.1	0.15	0.29	0.14	0.16	0.31	-0.073	0.42	0.11	-0.14	-0.041	0.22	0.081	0.12	0.13	0.075	0.33	0.081	0.07	0.05	0.057
Ba_ppm	0.24	-0.022	0.16	-0.1	-0.005	1	0.2	0.33	0.049	0.14	0.0036	0.1	0.24	0.033	0.015	0.29	0.25	0.057	0.18	0.22	0.028	0.14	-0.014	0.15	0.46	-0.088	0.11	0.22
Be_ppm	0.56	0.19	0.44	0.4	0.26	0.2	1	0.41	0.47	0.32	0.19	-0.036	0.16	-0.18	0.46	0.48	-0.08	0.14	0.66	0.49	0.54	0.48	0.24	0.66	0.36	-0.18	-0.21	0.14
Ca_pct	0.7	0.12	-0.16	0.24	0.1	0.33	0.41	1	0.25	-0.21	-0.45	-0.34	-0.23	-0.59	-0.0095	0.29	0.053	0.28	0.27	0.46	0.078	0.63	0.08	0.21	0.93	-0.27	-0.4	0.017
Co_ppm	0.47	0.16	-0.072	0.49	0.15	0.049	0.47	0.25	1	-0.095	0.12	-0.18	0.099	-0.35	0.06	0.79	0.088	0.12	0.19	0.52	0.66	0.52	0.32	0.18	0.16	-0.27	-0.35	0.2
Cr_ppm	-0.21	0.0031	0.92	-0.013	0.29	0.14	0.32	-0.21	-0.095	1	0.74	0.53	0.59	0.23	0.75	-0.072	-0.06	-0.14	0.56	-0.24	0.28	-0.32	-0.093	0.53	-0.12	0.58	0.62	0.38
Fe_pct	-0.3	0.011	0.62	0.098	0.14	0.0036	0.19	-0.45	0.12	0.74	1	0.53	0.51	0.24	0.45	0.072	0.085	-0.12	0.29	-0.085	0.48	-0.22	0.012	0.19	-0.4	0.46	0.58	0.32
Ga_ppm	-0.34	0.099	0.47	-0.13	0.16	0.1	-0.036	-0.34	-0.18	0.53	0.53	1	0.46	0.17	0.28	-0.19	0.018	-0.13	0.028	-0.29	-0.014	-0.38	0.077	0.11	-0.23	0.29	0.59	0.15
K_pct	-0.21	-0.14	0.64	-0.005	0.31	0.24	0.16	-0.23	0.099	0.59	0.51	0.46	1	0.31	0.62	0.14	-0.099	-0.14	0.36	-0.23	0.18	-0.32	0.026	0.34	-0.16	0.43	0.47	0.34
La_ppm	-0.35	-0.12	0.27	-0.19	-0.073	0.033	-0.18	-0.59	-0.35	0.23	0.24	0.17	0.31	1	0.2	-0.3	-0.17	-0.21	0.01	-0.48	-0.18	-0.57	-0.11	0.081	-0.49	0.32	0.36	-0.039
Mg_pct	0.036	-0.035	0.86	0.11	0.42	0.015	0.46	-0.0095	0.06	0.75	0.45	0.28	0.62	0.2	1	0.01	-0.3	-0.04	0.75	-0.21	0.2	-0.18	-0.1	0.7	0.027	0.5	0.31	0.28
Mn_ppm	0.37	0.099	-0.044	0.31	0.11	0.29	0.48	0.29	0.79	-0.072	0.072	-0.19	0.14	-0.3	0.01	1	0.12	0.2	0.18	0.62	0.57	0.55	0.25	0.16	0.24	-0.24	-0.27	0.3
Mo_ppm	0.075	0.2	-0.16	0.17	-0.14	0.25	-0.08	0.053	0.088	-0.06	0.085	0.018	-0.099	-0.17	-0.3	0.12	1	-0.08	-0.21	0.054	-1.50E-04	0.087	0.056	-0.15	0.16	-0.12	0.024	0.011
Na_pct	0.23	0.079	-0.13	0.043	-0.041	0.057	0.14	0.28	0.12	-0.14	-0.12	-0.13	-0.14	-0.21	-0.04	0.2	-0.08	1	0.025	0.21	0.068	0.28	0.14	0.021	0.27	-0.11	-0.18	-0.11
Ni_ppm	0.37	0.09	0.68	0.23	0.22	0.18	0.66	0.27	0.19	0.56	0.29	0.028	0.36	0.01	0.75	0.18	-0.21	0.025	1	0.062	0.3	0.057	0.041	0.68	0.29	0.22	0.059	0.2
P_ppm	0.51	0.17	-0.24	0.25	0.081	0.22	0.49	0.46	0.52	-0.24	-0.085	-0.29	-0.23	-0.48	-0.21	0.62	0.054	0.21	0.062	1	0.38	0.82	0.22	-0.044	0.38	-0.53	-0.54	0.077
Pb_ppm	0.21	0.054	0.23	0.33	0.12	0.028	0.54	0.078	0.66	0.28	0.48	-0.014	0.18	-0.18	0.2	0.57	-1.50E-04	0.068	0.3	0.38	1	0.37	0.14	0.28	0.01	-0.019	0.033	0.31
S_pct	0.65	0.19	-0.32	0.3	0.13	0.14	0.48	0.63	0.52	-0.32	-0.22	-0.38	-0.32	-0.57	-0.18	0.55	0.087	0.28	0.057	0.82	0.37	1	0.18	0.024	0.52	-0.5	-0.6	-0.063
Sb_ppm	0.11	0.32	-0.06	0.21	0.075	-0.014	0.24	0.08	0.32	-0.093	0.012	0.077	0.026	-0.11	-0.1	0.25	0.056	0.14	0.041	0.22	0.14	0.18	1	0.07	-0.013	-0.29	-0.17	-0.099
Sc_ppm	0.32	0.062	0.66	0.21	0.33	0.15	0.66	0.21	0.18	0.53	0.19	0.11	0.34	0.081	0.7	0.16	-0.15	0.021	0.68	-0.044	0.28	0.024	0.07	1	0.2	0.16	0.11	0.14
Sr_ppm	0.67	0.13	-0.075	0.18	0.081	0.46	0.36	0.93	0.16	-0.12	-0.4	-0.23	-0.16	-0.49	0.027	0.24	0.16	0.27	0.29	0.38	0.01	0.52	-0.013	0.2	1	-0.21	-0.3	0.073
Ti_pct	-0.38	-0.13	0.49	-0.18	0.07	-0.088	-0.18	-0.27	-0.27	0.58	0.46	0.29	0.43	0.32	0.5	-0.24	-0.12	-0.11	0.22	-0.53	-0.019	-0.5	-0.29	0.16	-0.21	1	0.71	0.3
V_ppm	-0.51	-0.14	0.51	-0.23	0.05	0.11	-0.21	-0.4	-0.35	0.62	0.58	0.59	0.47	0.36	0.31	-0.27	0.024	-0.18	0.059	-0.54	0.033	-0.6	-0.17	0.11	-0.3	0.71	1	0.28
Zn_ppm	0.037	-0.11	0.31	0.16	0.057	0.22	0.14	0.017	0.2	0.38	0.32	0.15	0.34	-0.039	0.28	0.3	0.011	-0.11	0.2	0.077	0.31	-0.063	-0.099	0.14	0.073	0.3	0.28	1

Table 9: Spearman Rank correlation matrix results - Book 1 Soil Grid

139 rows - Univariate	Cu_ppm	Ag_ppm	As_ppm	Be_ppm	Ca_pct	Co_ppm	Cr_ppm	Ni_ppm	P_ppm	Pb_ppm	S_pct	Sr_ppm	V_ppm
[Visible] : Minimum	4.00	0.01	0.28	0.06	0.02	2.00	5.00	0.00	120.00	4.00	0.00	3.00	12.00
[Visible] : Maximum	142.00	0.80	15.00	1.30	2.52	28.00	34.00	26.00	1650.00	82.00	0.12	101.00	134.00
[Visible] : Mean	21.85	0.17	4.40	0.63	0.36	9.50	16.36	11.22	433.53	17.45	0.02	17.45	36.54
[Visible] : Median	18.00	0.15	4.00	0.60	0.21	9.00	16.00	11.00	360.00	16.00	0.02	12.00	35.00
[Visible] : Range	138.00	0.79	14.72	1.24	2.50	26.00	29.00	26.00	1530.00	78.00	0.12	98.00	122.00
[Visible] : Standard Deviation	17.49	0.12	3.03	0.27	0.41	4.39	5.29	4.88	258.75	9.28	0.02	17.82	18.47
[Visible] : Variance	305.96	0.02	9.16	0.07	0.16	19.31	28.00	23.78	66949.08	86.09	0.00	317.42	341.21
[Visible] : Coefficient of Variation	80.06	73.40	68.84	42.75	112.40	46.27	32.34	43.48	59.68	53.18	91.97	102.12	50.55
[Visible] : Kurtosis	16.53	6.25	0.76	-0.64	7.65	1.75	0.64	0.16	3.60	16.00	6.14	7.43	8.02
[Visible] : Skewness	3.27	2.07	1.05	0.08	2.55	1.03	0.50	0.32	1.60	2.76	2.35	2.65	2.29
[Visible] : Tukey Upper Outlier Threshold	43	0.376355	12	1.318714	0.79	19.5	30.5	24.5	1000	34.5	0.06	39.5	71.5
[Visible] : Tukey Upper Far Outlier Threshold	61	0.55271	18	1.837427	1.18	27	41	35	1450	48	0.09	59	100
[Visible] : 1 percentile	4.00	0.01	0.36	0.08	0.02	2.00	5.40	0.80	124.00	4.40	0.00	3.40	12.80
[Visible] : 5 percentile	6.00	0.04	0.72	0.21	0.06	4.00	8.00	3.00	150.00	6.00	0.01	5.00	17.00
[Visible] : 10 percentile	8.00	0.05	1.14	0.26	0.07	4.00	9.00	5.00	170.00	8.00	0.01	5.00	19.00
[Visible] : 20 percentile	11.00	0.07	1.94	0.37	0.10	6.00	12.00	7.00	220.00	11.00	0.01	6.00	22.00
[Visible] : 30 percentile	13.00	0.09	2.00	0.50	0.14	7.00	14.00	9.00	270.00	13.00	0.01	8.00	26.00
[Visible] : 40 percentile	15.00	0.12	3.00	0.50	0.18	8.00	15.00	10.00	310.00	14.00	0.01	10.00	31.00
[Visible] : 50 percentile	18.00	0.15	4.00	0.60	0.21	9.00	16.00	11.00	360.00	16.00	0.02	12.00	35.00
[Visible] : 60 percentile	20.00	0.18	4.00	0.70	0.25	10.00	17.00	12.00	430.00	18.00	0.02	14.00	38.00
[Visible] : 70 percentile	23.00	0.20	6.00	0.80	0.35	11.00	18.00	14.00	520.00	19.00	0.03	18.00	41.00
[Visible] : 75 percentile	25.00	0.20	6.00	0.80	0.40	12.00	20.00	14.00	550.00	21.00	0.03	20.00	43.00
[Visible] : 80 percentile	28.00	0.20	7.00	0.90	0.51	12.00	20.00	15.00	630.00	24.00	0.03	23.00	45.00
[Visible] : 90 percentile	42.00	0.30	8.00	1.00	0.91	16.00	23.00	17.00	810.00	29.00	0.06	37.00	52.00
[Visible] : 95 percentile	60.00	0.40	11.00	1.10	1.33	18.00	26.00	20.00	890.00	33.00	0.07	65.00	63.00
[Visible] : 99 percentile	116.40	0.72	13.80	1.26	2.20	25.60	32.80	25.20	1502.00	65.20	0.12	95.00	124.40

Table 10: Book 2 Soil Grid summary statistics for Cu and pathfinders

Spearman Rank	Cu_ppm	Ag_ppm	Al_pct	As_ppm	B_ppm	Ba_ppm	Be_ppm	Ca_pct	Co_ppm	Cr_ppm	Fe_pct	Ga_ppm	K_pct	La_ppm	Mg_pct	Mn_ppm	Mo_ppm	Na_pct	Ni_ppm	P_ppm	Pb_ppm	S_pct	Sb_ppm	Sc_ppm	Sr_ppm	Ti_pct	V_ppm	Zn_ppm
Cu_ppm	1	0.15	0.4	0.3	0.43	0.23	0.65	0.62	0.65	0.52	0.32	-0.027	0.25	-0.36	0.59	0.53	0.043	0.25	0.63	0.61	0.46	0.66	0.15	0.71	0.53	0.14	0.11	0.27
Ag_ppm	0.15	1	0.3	0.11	0.33	0.088	0.13	0.034	0.16	0.3	0.27	0.2	0.15	0.016	0.24	0.031	0.11	0.1	0.17	0.078	0.045	-0.035	0.35	0.23	0.039	0.089	0.15	0.033
Al_pct	0.4	0.3	1	0.37	0.52	0.21	0.69	0.22	0.67	0.85	0.72	0.37	0.6	-0.026	0.86	0.35	0.031	0.27	0.74	0.25	0.38	0.2	0.2	0.68	0.22	0.13	0.17	0.41
As_ppm	0.3	0.11	0.37	1	0.31	0.03	0.42	0.23	0.38	0.25	0.23	0.083	0.39	-0.02	0.42	0.23	-0.0084	-0.046	0.39	0.13	0.46	0.17	-0.0096	0.36	0.29	0.033	-0.094	0.24
B_ppm	0.43	0.33	0.52	0.31	1	0.025	0.55	0.4	0.47	0.51	0.34	0.14	0.47	-0.13	0.63	0.25	0.24	0.32	0.46	0.34	0.38	0.36	0.19	0.57	0.36	-0.017	-0.084	0.28
Ba_ppm	0.23	0.088	0.21	0.03	0.025	1	0.19	0.37	0.26	0.16	-0.0044	0.07	0.29	-0.15	0.085	0.41	0.0092	0.19	0.13	0.24	0.29	0.27	0.041	0.14	0.44	-0.3	-0.16	0.3
Be_ppm	0.65	0.13	0.69	0.42	0.55	0.19	1	0.53	0.68	0.56	0.39	-0.0049	0.48	-0.13	0.78	0.51	-0.029	0.22	0.74	0.4	0.61	0.48	0.2	0.82	0.5	-0.11	-0.2	0.29
Ca_pct	0.62	0.034	0.22	0.23	0.4	0.37	0.53	1	0.46	0.21	-0.013	-0.23	0.24	-0.53	0.43	0.55	-0.0095	0.25	0.39	0.48	0.56	0.75	0.13	0.57	0.89	-0.19	-0.32	0.36
Co_ppm	0.65	0.16	0.67	0.38	0.47	0.26	0.68	0.46	1	0.65	0.59	0.077	0.37	-0.2	0.66	0.75	0.026	0.26	0.69	0.48	0.53	0.45	0.23	0.7	0.36	0.087	0.11	0.39
Cr_ppm	0.52	0.3	0.85	0.25	0.51	0.16	0.56	0.21	0.65	1	0.8	0.4	0.49	-0.16	0.77	0.35	0.11	0.34	0.73	0.39	0.25	0.3	0.25	0.6	0.18	0.33	0.42	0.4
Fe_pct	0.32	0.27	0.72	0.23	0.34	-0.0044	0.39	-0.013	0.59	0.8	1	0.38	0.33	-0.034	0.53	0.29	0.079	0.27	0.55	0.37	0.2	0.14	0.22	0.38	-0.072	0.34	0.49	0.31
Ga_ppm	-0.027	0.2	0.37	0.083	0.14	0.07	-0.0049	-0.23	0.077	0.4	0.38	1	0.16	0.25	0.16	-0.094	0.14	0.01	0.079	-0.079	-0.12	-0.17	0.12	0.032	-0.15	0.36	0.47	0.1
K_pct	0.25	0.15	0.6	0.39	0.47	0.29	0.48	0.24	0.37	0.49	0.33	0.16	1	-0.02	0.65	0.23	0.082	0.36	0.5	0.27	0.35	0.2	0.16	0.39	0.32	-0.18	-0.2	0.4
La_ppm	-0.36	0.016	-0.026	-0.02	-0.13	-0.15	-0.13	-0.53	-0.2	-0.16	-0.034	0.25	-0.02	1	-0.17	-0.26	0.08	-0.18	-0.19	-0.41	-0.25	-0.5	-0.12	-0.2	-0.44	-0.038	0.045	-0.3
Mg_pct	0.59	0.24	0.86	0.42	0.63	0.085	0.78	0.43	0.66	0.77	0.53	0.16	0.65	-0.17	1	0.39	-0.012	0.33	0.81	0.41	0.5	0.42	0.24	0.8	0.39	0.082	-0.024	0.45
Mn_ppm	0.53	0.031	0.35	0.23	0.25	0.41	0.51	0.55	0.75	0.35	0.29	-0.094	0.23	-0.26	0.39	1	-0.15	0.2	0.45	0.57	0.49	0.53	0.15	0.44	0.42	-0.2	-0.12	0.4
Mo_ppm	0.043	0.11	0.031	-0.0084	0.24	0.0092	-0.029	-0.0095	0.026	0.11	0.079	0.14	0.082	0.08	-0.012	-0.15	1	0.3	-0.094	-0.037	-0.054	-0.14	0.11	0.0064	0.025	0.12	0.11	-0.015
Na_pct	0.25	0.1	0.27	-0.046	0.32	0.19	0.22	0.25	0.26	0.34	0.27	0.01	0.36	-0.18	0.33	0.2	0.3	1	0.2	0.34	0.23	0.19	0.31	0.21	0.2	-0.089	-0.086	0.26
Ni_ppm	0.63	0.17	0.74	0.39	0.46	0.13	0.74	0.39	0.69	0.73	0.55	0.079	0.5	-0.19	0.81	0.45	-0.094	0.2	1	0.39	0.43	0.4	0.17	0.73	0.35	0.14	0.047	0.41
P_ppm	0.61	0.078	0.25	0.13	0.34	0.24	0.4	0.48	0.48	0.39	0.37	-0.079	0.27	-0.41	0.41	0.57	-0.037	0.34	0.39	1	0.41	0.76	0.2	0.3	0.33	-0.14	-0.034	0.53
Pb_ppm	0.46	0.045	0.38	0.46	0.38	0.29	0.61	0.56	0.53	0.25	0.2	-0.12	0.35	-0.25	0.5	0.49	-0.054	0.23	0.43	0.41	1	0.51	0.2	0.49	0.59	-0.16	-0.28	0.52
S_pct	0.66	-0.035	0.2	0.17	0.36	0.27	0.48	0.75	0.45	0.3	0.14	-0.17	0.2	-0.5	0.42	0.53	-0.14	0.19	0.4	0.76	0.51	1	0.12	0.43	0.64	-0.13	-0.17	0.4
Sb_ppm	0.15	0.35	0.2	-0.0096	0.19	0.041	0.2	0.13	0.23	0.25	0.22	0.12	0.16	-0.12	0.24	0.15	0.11	0.31	0.17	0.2	0.2	0.12	1	0.2	0.15	-0.0032	-0.013	0.14
Sc_ppm	0.71	0.23	0.68	0.36	0.57	0.14	0.82	0.57	0.7	0.6	0.38	0.032	0.39	-0.2	0.8	0.44	0.0064	0.21	0.73	0.3	0.49	0.43	0.2	1	0.49	0.073	-0.053	0.27
Sr_ppm	0.53	0.039	0.22	0.29	0.36	0.44	0.5	0.89	0.36	0.18	-0.072	-0.15	0.32	-0.44	0.39	0.42	0.025	0.2	0.35	0.33	0.59	0.64	0.15	0.49	1	-0.17	-0.34	0.37
Ti_pct	0.14	0.089	0.13	0.033	-0.017	-0.3	-0.11	-0.19	0.087	0.33	0.34	0.36	-0.18	-0.038	0.082	-0.2	0.12	-0.089	0.14	-0.14	-0.16	-0.13	-0.0032	0.073	-0.17	1	0.79	-0.074
V_ppm	0.11	0.15	0.17	-0.094	-0.084	-0.16	-0.2	-0.32	0.11	0.42	0.49	0.47	-0.2	0.045	-0.024	-0.12	0.11	-0.086	0.047	-0.034	-0.28	-0.17	-0.013	-0.053	-0.34	0.79	1	-0.091
Zn_ppm	0.27	0.033	0.41	0.24	0.28	0.3	0.29	0.36	0.39	0.4	0.31	0.1	0.4	-0.3	0.45	0.4	-0.015	0.26	0.41	0.53	0.52	0.4	0.14	0.27	0.37	-0.074	-0.091	1

Table 11: Spearman Rank correlation matrix results - Book 2 Soil Grid

468 rows - Univariate	Cu_ppm	As_ppm	Be_ppm	Ca_pct	Co_ppm	Cr_ppm	Ni_ppm	P_ppm	Pb_ppm	S_pct	Sr_ppm	V_ppm
[Visible] : Minimum	2.00	0.03	0.00	0.01	1.00	5.00	0.15	130.00	5.00	0.00	2.00	7.00
[Visible] : Maximum	274.00	16.00	4.20	7.64	54.00	32.00	46.00	2990.00	73.00	0.17	127.00	155.00
[Visible] : Mean	26.14	4.25	0.74	0.57	11.62	14.65	11.98	626.24	17.58	0.03	13.25	30.27
[Visible] : Median	20.00	4.00	0.70	0.25	10.00	15.00	12.00	560.00	16.00	0.03	10.00	27.00
[Visible] : Range	272.00	15.97	4.20	7.63	53.00	27.00	45.85	2860.00	68.00	0.17	125.00	148.00
[Visible] : Standard Deviation	26.31	3.05	0.45	0.92	7.16	4.36	5.59	341.99	8.37	0.03	12.00	17.50
[Visible] : Variance	692.17	9.32	0.21	0.85	51.31	19.00	31.29	116960.13	70.05	0.00	144.10	306.28
[Visible] : Coefficient of Variation	100.65	71.86	61.82	162.06	61.63	29.75	46.68	54.61	47.62	78.97	90.60	57.81
[Visible] : Kurtosis	40.73	1.37	8.29	20.30	5.49	-0.10	4.42	8.11	9.62	2.76	23.79	13.49
[Visible] : Skewness	5.35	1.06	1.77	3.98	1.95	0.09	1.07	2.17	2.31	1.56	3.46	2.99
[Visible] : Tukey Upper Outlier Threshold	55.50	12.00	1.82	1.59	24.50	28.50	25.50	1296.25	34.50	0.11	37.50	55.00
[Visible] : Tukey Upper Far Outlier Threshold	81.00	18.00	2.64	2.49	35.00	39.00	36.00	1832.50	48.00	0.17	57.00	76.00
[Visible] : 1 percentile	5.00	0.07	0.01	0.01	2.00	6.00	0.90	173.80	5.00	0.00	2.00	8.00
[Visible] : 5 percentile	8.00	0.36	0.12	0.02	4.00	7.00	4.00	244.50	8.00	0.01	3.00	12.00
[Visible] : 10 percentile	9.00	0.70	0.23	0.03	5.00	9.00	5.00	300.00	9.90	0.01	3.00	14.90
[Visible] : 20 percentile	12.00	1.54	0.39	0.06	6.80	11.00	7.00	378.00	12.00	0.01	4.00	19.00
[Visible] : 30 percentile	14.00	2.00	0.50	0.11	8.00	12.00	9.00	430.00	13.00	0.02	6.00	22.00
[Visible] : 40 percentile	17.00	3.00	0.60	0.18	9.00	13.00	11.00	480.00	14.60	0.02	7.00	25.00
[Visible] : 50 percentile	20.00	4.00	0.70	0.25	10.00	15.00	12.00	560.00	16.00	0.03	10.00	27.00
[Visible] : 60 percentile	24.00	5.00	0.80	0.39	11.00	16.00	13.00	630.00	18.00	0.03	13.00	30.00
[Visible] : 70 percentile	27.30	6.00	0.90	0.56	13.00	17.00	14.30	700.00	20.00	0.04	16.00	32.00
[Visible] : 75 percentile	30.00	6.00	1.00	0.69	14.00	18.00	15.00	760.00	21.00	0.05	18.00	34.00
[Visible] : 80 percentile	33.00	6.00	1.10	0.82	15.00	18.20	16.00	820.00	22.00	0.05	20.00	37.00
[Visible] : 90 percentile	45.00	8.00	1.20	1.28	20.00	20.00	18.00	1013.00	27.10	0.07	28.00	46.00
[Visible] : 95 percentile	61.00	10.00	1.50	2.30	27.55	21.55	20.00	1235.50	32.00	0.09	33.55	58.00
[Visible] : 99 percentile	151.62	15.00	2.16	5.65	36.24	24.31	32.00	2129.30	50.03	0.12	48.31	111.48

Table 12: Bronson Soil Grid summary statistics for Cu and pathfinders

Spearman Rank	Cu_ppm	Al_pct	As_ppm	B_ppm	Ba_ppm	Be_ppm	Ca_pct	Co_ppm	Cr_ppm	Fe_pct	Ga_ppm	K_pct	La_ppm	Mg_pct	Mn_ppm	Mo_ppm	Na_pct	Ni_ppm	P_ppm	Pb_ppm	S_pct	Sc_ppm	Sr_ppm	Ti_pct	V_ppm	Zn_ppm
Cu_ppm	1	0.35	0.46	0.5	0.1	0.77	0.64	0.71	0.38	0.36	-0.28	0.17	-0.49	0.45	0.49	0.22	0.32	0.63	0.48	0.43	0.58	0.61	0.67	0.17	-0.058	0.22
Al_pct	0.35	1	0.21	0.33	0.37	0.56	0.26	0.46	0.83	0.66	0.29	0.65	0.16	0.66	0.3	-0.13	0.16	0.67	-0.03	0.23	0.015	0.68	0.34	0.49	0.44	0.63
As_ppm	0.46	0.21	1	0.23	0.035	0.37	0.27	0.38	0.27	0.3	-0.18	0.021	-0.24	0.15	0.19	0.2	0.29	0.33	0.18	0.25	0.25	0.24	0.31	0.094	0.084	0.088
B_ppm	0.5	0.33	0.23	1	0.19	0.48	0.61	0.42	0.27	0.086	-0.2	0.36	-0.29	0.5	0.29	-0.065	0.3	0.43	0.17	0.19	0.34	0.56	0.59	0.13	-0.11	0.25
Ba_ppm	0.1	0.37	0.035	0.19	1	0.23	0.25	0.2	0.35	0.22	0.075	0.3	-0.072	0.074	0.38	-0.0064	0.048	0.14	0.23	0.29	0.22	0.3	0.32	0.11	0.15	0.54
Be_ppm	0.77	0.56	0.37	0.48	0.23	1	0.55	0.8	0.52	0.46	-0.23	0.36	-0.27	0.51	0.56	0.085	0.25	0.74	0.39	0.52	0.47	0.69	0.6	0.14	-0.062	0.36
Ca_pct	0.64	0.26	0.27	0.61	0.25	0.55	1	0.45	0.26	-0.019	-0.38	0.31	-0.51	0.6	0.36	-0.057	0.37	0.47	0.28	0.14	0.57	0.68	0.93	0.22	-0.16	0.27
Co_ppm	0.71	0.46	0.38	0.42	0.2	0.8	0.45	1	0.47	0.58	-0.23	0.26	-0.32	0.43	0.76	0.13	0.28	0.71	0.42	0.62	0.45	0.54	0.47	0.13	-0.011	0.4
Cr_ppm	0.38	0.83	0.27	0.27	0.35	0.52	0.26	0.47	1	0.65	0.21	0.53	0.081	0.55	0.28	-0.0027	0.23	0.73	0.015	0.3	0.062	0.57	0.34	0.6	0.51	0.67
Fe_pct	0.36	0.66	0.3	0.086	0.22	0.46	-0.019	0.58	0.65	1	0.23	0.25	-0.0075	0.29	0.42	0.14	0.091	0.51	0.2	0.54	0.082	0.33	0.06	0.32	0.46	0.51
Ga_ppm	-0.28	0.29	-0.18	-0.2	0.075	-0.23	-0.38	-0.23	0.21	0.23	1	0.15	0.4	-0.1	-0.21	-0.052	-0.014	-0.15	-0.31	-0.13	-0.37	-0.11	-0.29	0.3	0.58	0.13
K_pct	0.17	0.65	0.021	0.36	0.3	0.36	0.31	0.26	0.53	0.25	0.15	1	0.25	0.67	0.2	-0.28	0.12	0.48	-0.12	0.06	-0.0025	0.59	0.3	0.35	0.18	0.48
La_ppm	-0.49	0.16	-0.24	-0.29	-0.072	-0.27	-0.51	-0.32	0.081	-0.0075	0.4	0.25	1	-0.049	-0.27	-0.21	-0.21	-0.08	-0.52	-0.19	-0.62	-0.15	-0.49	0.15	0.25	0.033
Mg_pct	0.45	0.66	0.15	0.5	0.074	0.51	0.6	0.43	0.55	0.29	-0.1	0.67	-0.049	1	0.23	-0.26	0.25	0.73	-0.12	0.05	0.1	0.79	0.53	0.44	0.055	0.42
Mn_ppm	0.49	0.3	0.19	0.29	0.38	0.56	0.36	0.76	0.28	0.42	-0.21	0.2	-0.27	0.23	1	0.059	0.17	0.39	0.56	0.51	0.52	0.39	0.37	-0.023	-0.042	0.4
Mo_ppm	0.22	-0.13	0.2	-0.065	-0.0064	0.085	-0.057	0.13	-0.0027	0.14	-0.052	-0.28	-0.21	-0.26	0.059	1	0.036	-0.0072	0.31	0.2	0.21	-0.13	0.0065	-0.15	-0.0014	-0.058
Na_pct	0.32	0.16	0.29	0.3	0.048	0.25	0.37	0.28	0.23	0.091	-0.014	0.12	-0.21	0.25	0.17	0.036	1	0.24	0.12	0.0099	0.29	0.27	0.35	0.23	0.12	0.1
Ni_ppm	0.63	0.67	0.33	0.43	0.14	0.74	0.47	0.71	0.73	0.51	-0.15	0.48	-0.08	0.73	0.39	-0.0072	0.24	1	0.096	0.37	0.17	0.69	0.49	0.41	0.082	0.51
P_ppm	0.48	-0.03	0.18	0.17	0.23	0.39	0.28	0.42	0.015	0.2	-0.31	-0.12	-0.52	-0.12	0.56	0.31	0.12	0.096	1	0.42	0.74	0.091	0.3	-0.29	-0.16	0.12
Pb_ppm	0.43	0.23	0.25	0.19	0.29	0.52	0.14	0.62	0.3	0.54	-0.13	0.06	-0.19	0.05	0.51	0.2	0.0099	0.37	0.42	1	0.35	0.2	0.18	-0.053	-0.042	0.37
S_pct	0.58	0.015	0.25	0.34	0.22	0.47	0.57	0.45	0.062	0.082	-0.37	-0.0025	-0.62	0.1	0.52	0.21	0.29	0.17	0.74	0.35	1	0.26	0.58	-0.16	-0.21	0.087
Sc_ppm	0.61	0.68	0.24	0.56	0.3	0.69	0.68	0.54	0.57	0.33	-0.11	0.59	-0.15	0.79	0.39	-0.13	0.27	0.69	0.091	0.2	0.26	1	0.67	0.39	0.084	0.46
Sr_ppm	0.67	0.34	0.31	0.59	0.32	0.6	0.93	0.47	0.34	0.06	-0.29	0.3	-0.49	0.53	0.37	0.0065	0.35	0.49	0.3	0.18	0.58	0.67	1	0.28	-0.078	0.31
Ti_pct	0.17	0.49	0.094	0.13	0.11	0.14	0.22	0.13	0.6	0.32	0.3	0.35	0.15	0.44	-0.023	-0.15	0.23	0.41	-0.29	-0.053	-0.16	0.39	0.28	1	0.69	0.44
V_ppm	-0.058	0.44	0.084	-0.11	0.15	-0.062	-0.16	-0.011	0.51	0.46	0.58	0.18	0.25	0.055	-0.042	-0.0014	0.12	0.082	-0.16	-0.042	-0.21	0.084	-0.078	0.69	1	0.34
Zn_ppm	0.22	0.63	0.088	0.25	0.54	0.36	0.27	0.4	0.67	0.51	0.13	0.48	0.033	0.42	0.4	-0.058	0.1	0.51	0.12	0.37	0.087	0.46	0.31	0.44	0.34	1

Table 13: Spearman Rank correlation matrix results - Bronson Soil Grid

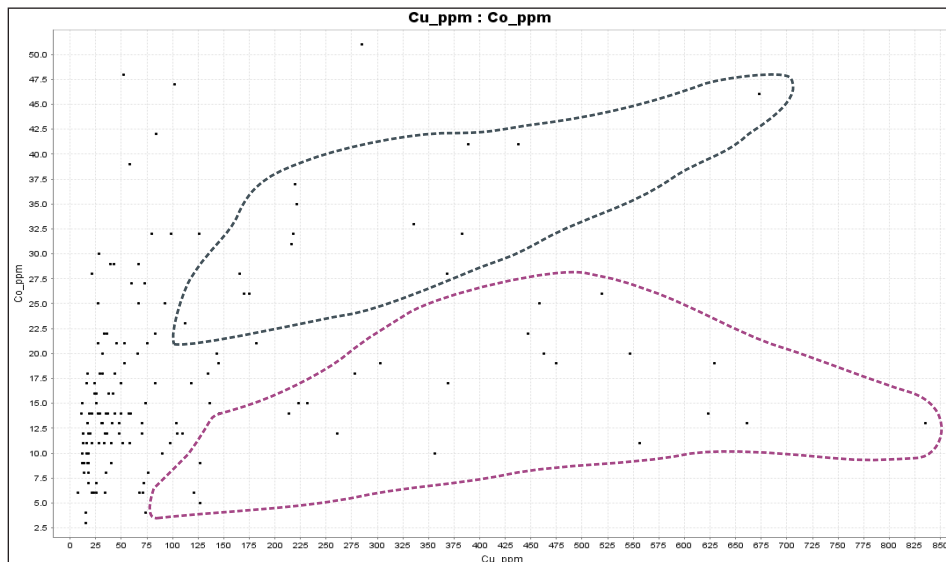
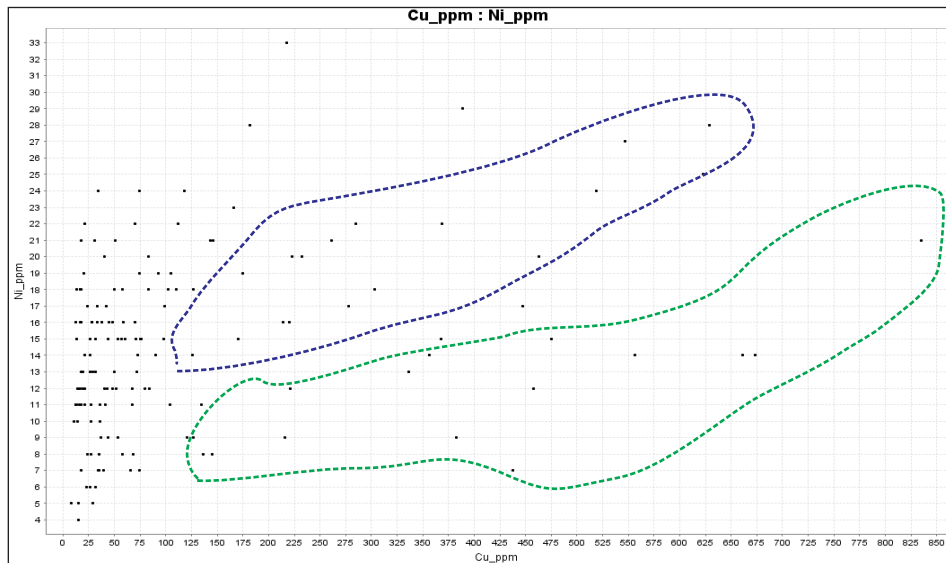
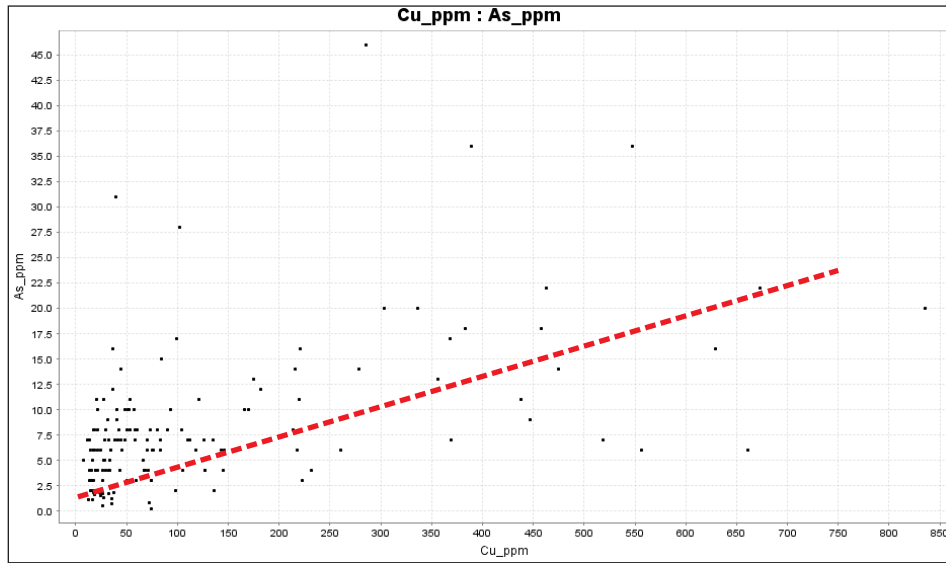


Figure 45: Scatterplots for Book 1 soil grid showing weak correlations between Cu, As, Ni and Co

- Two main NNW trending zone of anomalous Cu and Co (**Fig. 46, 47**), the strike-length of the stronger anomaly is in excess of 500 m. Cobalt anomalism is spatially coincident with Cu anomalism.
- A spatially coincident, but dispersed and larger low-level As anomaly enveloping Cu-Co anomalism (**Fig. 48**).
- Broader zones of Ca and S anomalism associated with Cu-Co anomalism (**Figs. 49, 50**).
- Wide zones of low level Ni and Pb anomalism exhibiting poor spatial coincidence with Cu-Co anomalism (i.e. on local spatial overlap) suggesting other geochemical processes control anomalism of these metals (**Figs. 51, 52**).

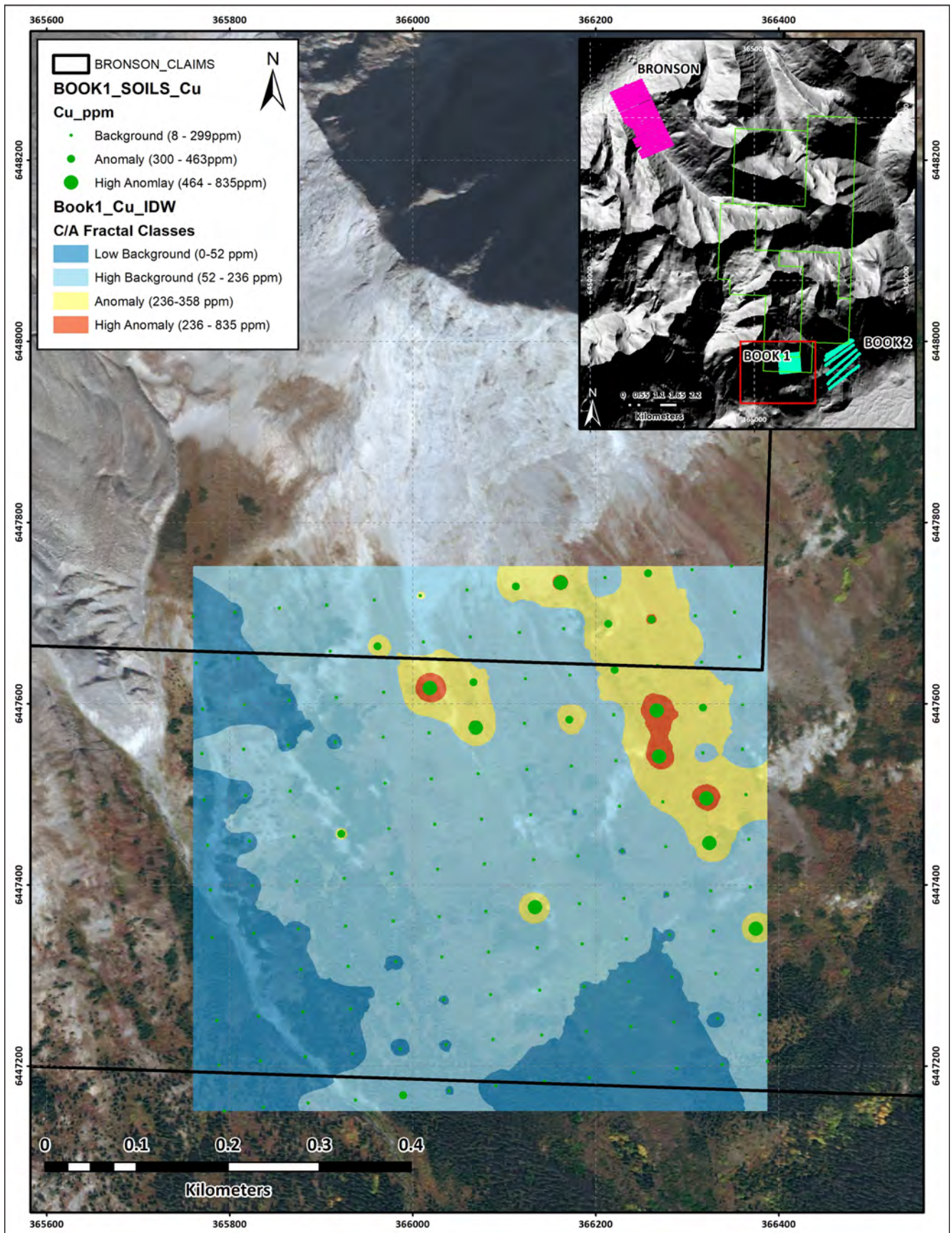


Figure 46: Graduated dot plots superimposed on IDW interpolation raster for Cu, Book 1 soil grid

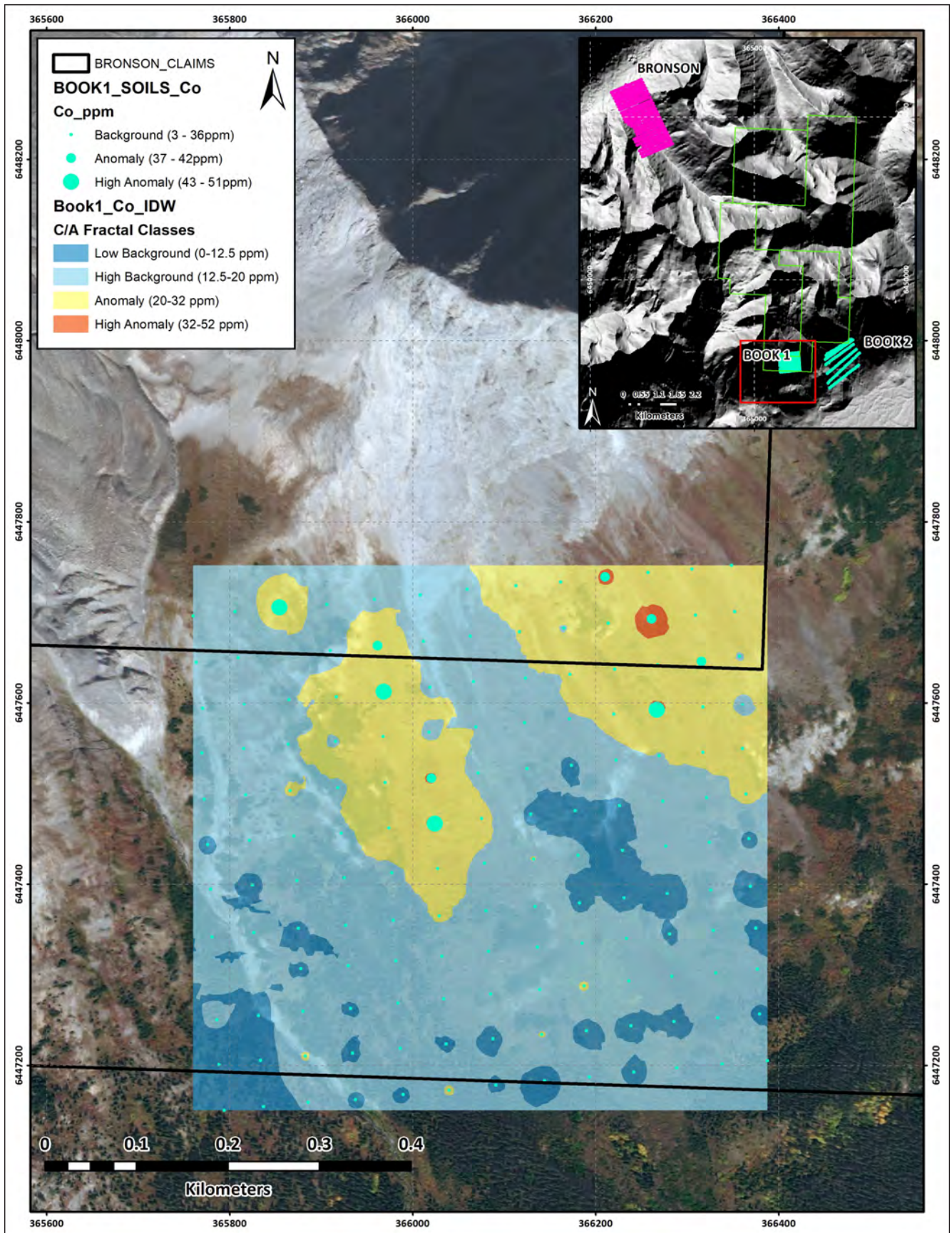


Figure 47: Graduated dot plots superimposed on IDW interpolation raster for Co, Book 1 soil grid

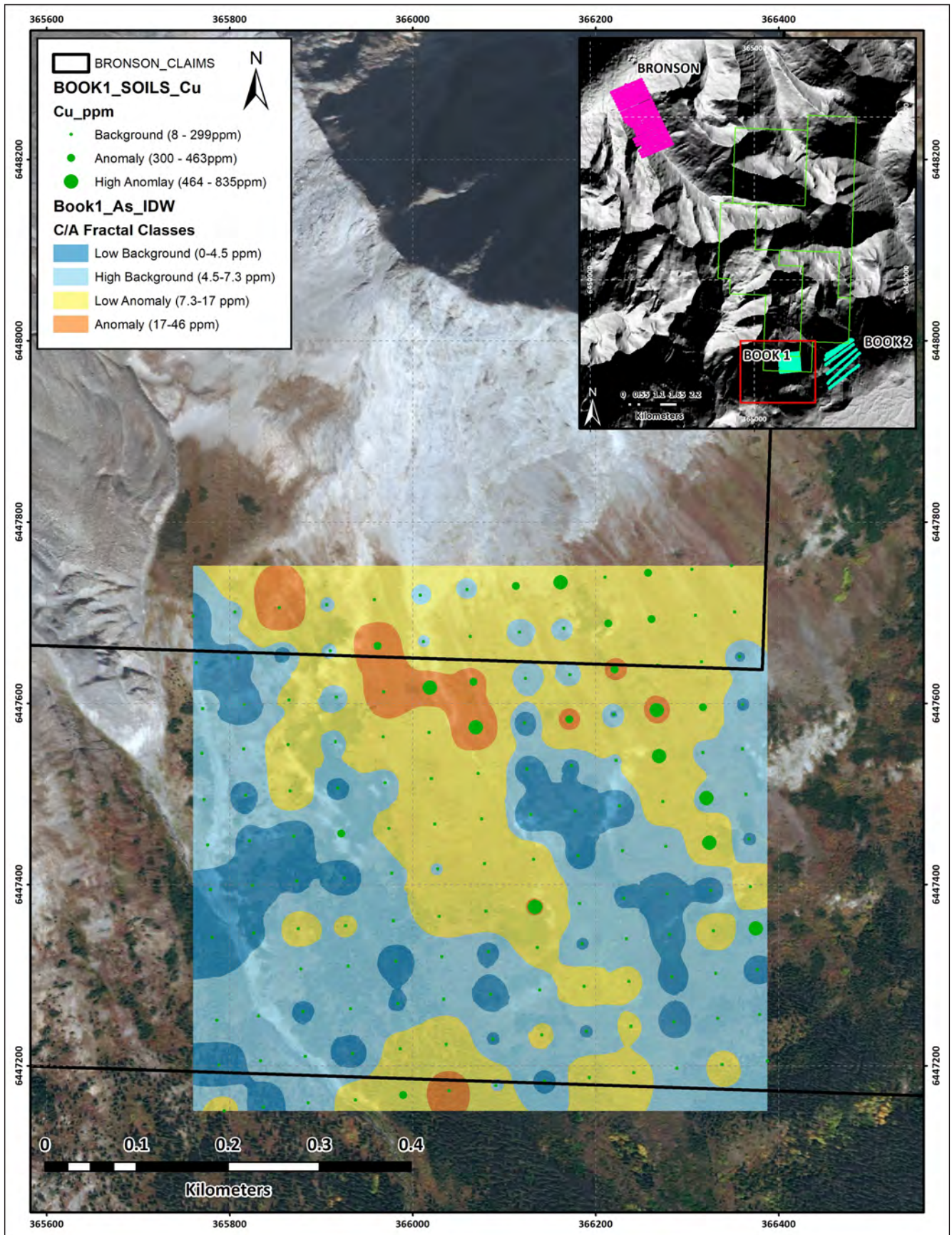


Figure 48: Graduated dot plots (As) superimposed on Cu IDW interpolation raster, Book 1 soil grid.

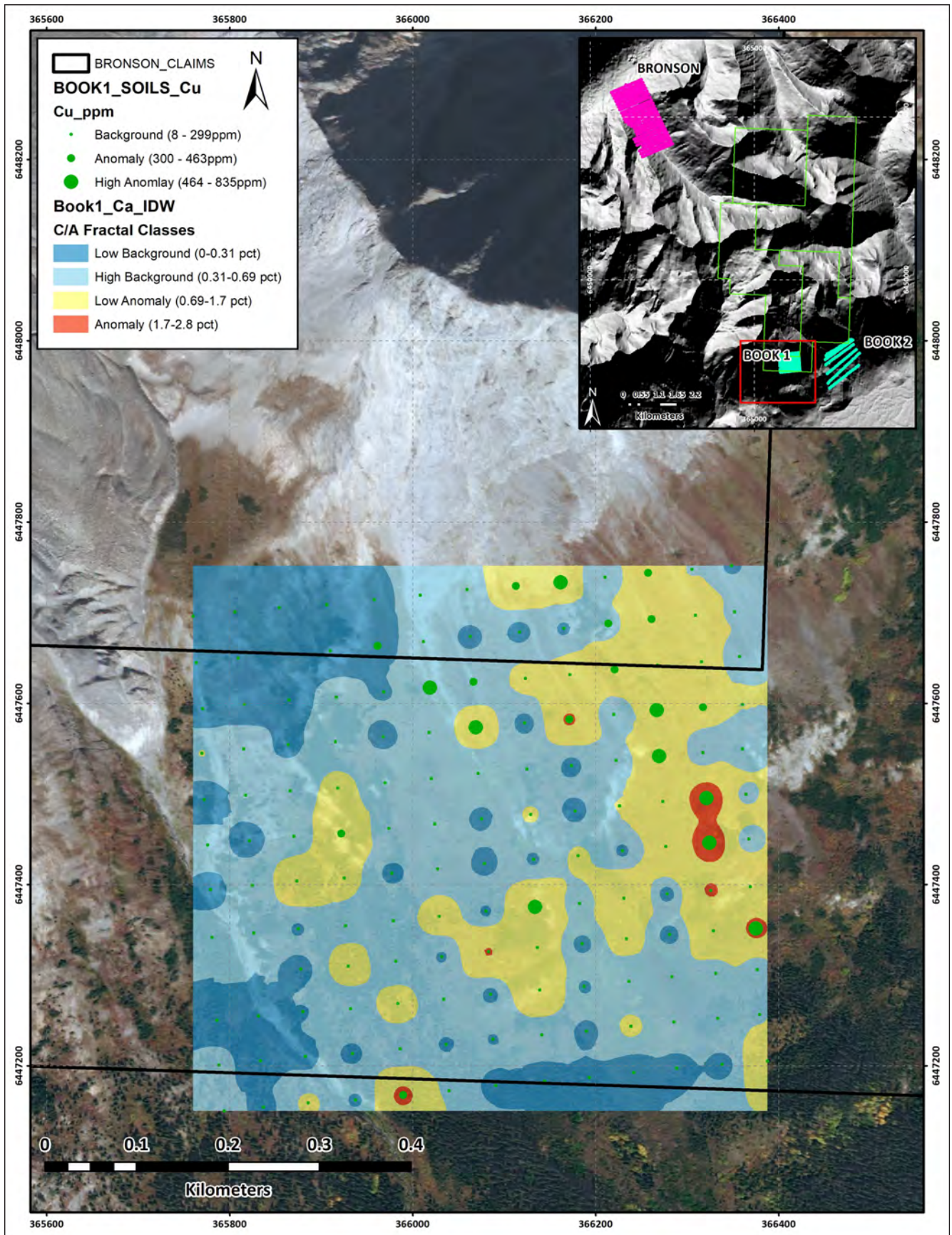


Figure 49: Graduated dot plots (Ca) superimposed on Cu IDW interpolation raster, Book 1 soil grid.

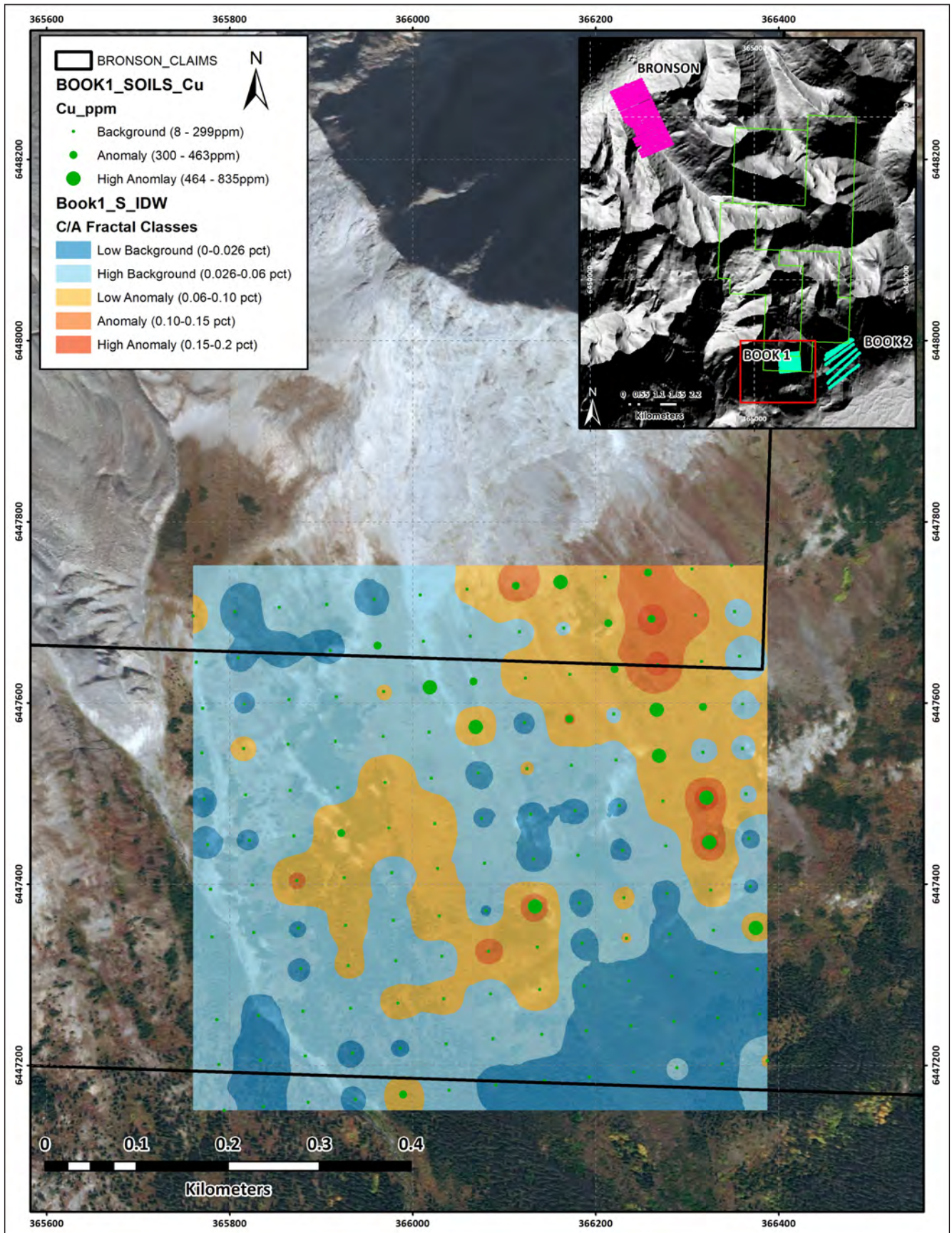


Figure 50: Graduated dot plots (S) superimposed on Cu IDW interpolation raster, Book 1 soil grid.

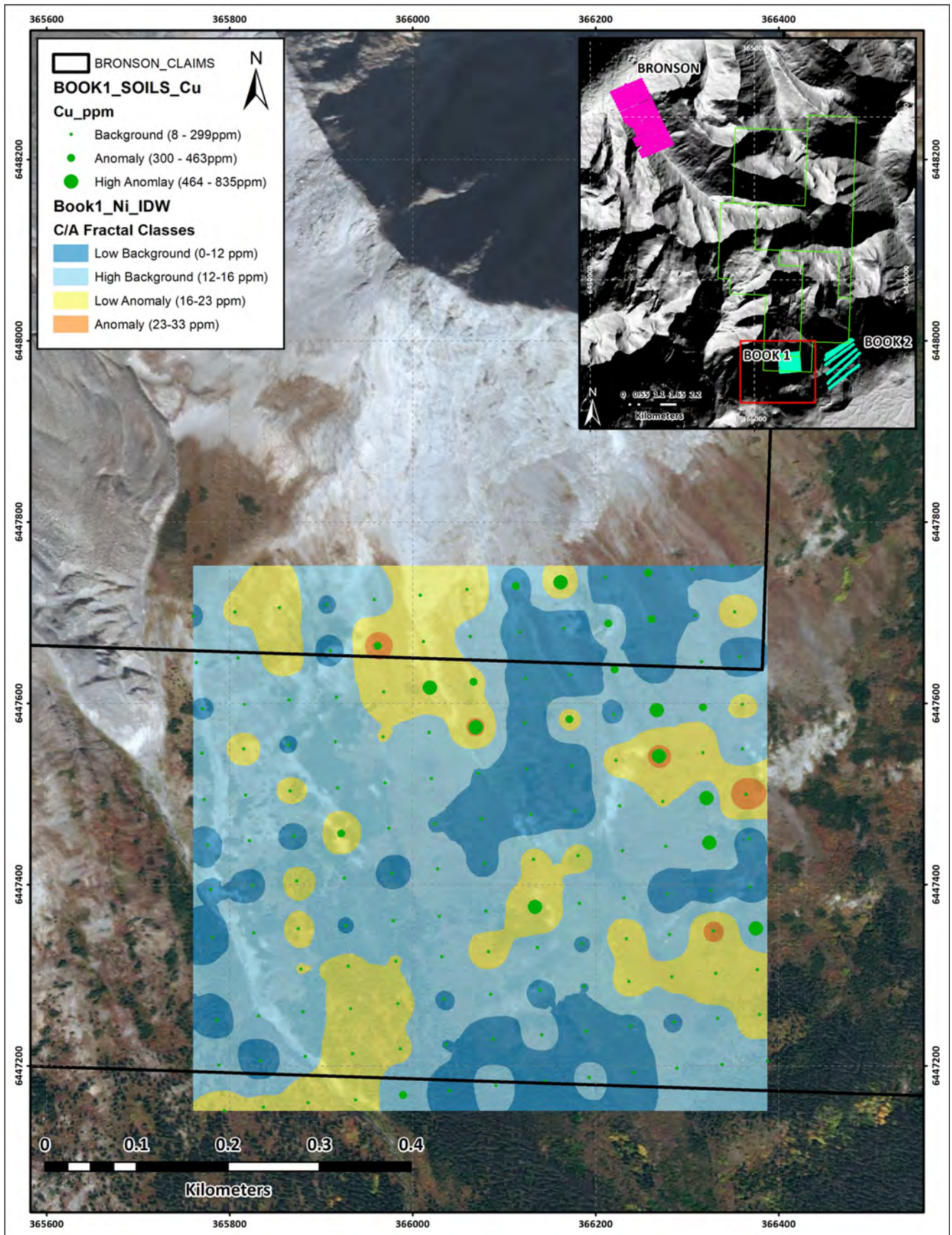


Figure 51: Graduated dot plots (Ni) superimposed on Cu IDW interpolation raster, Book 1 soil grid.

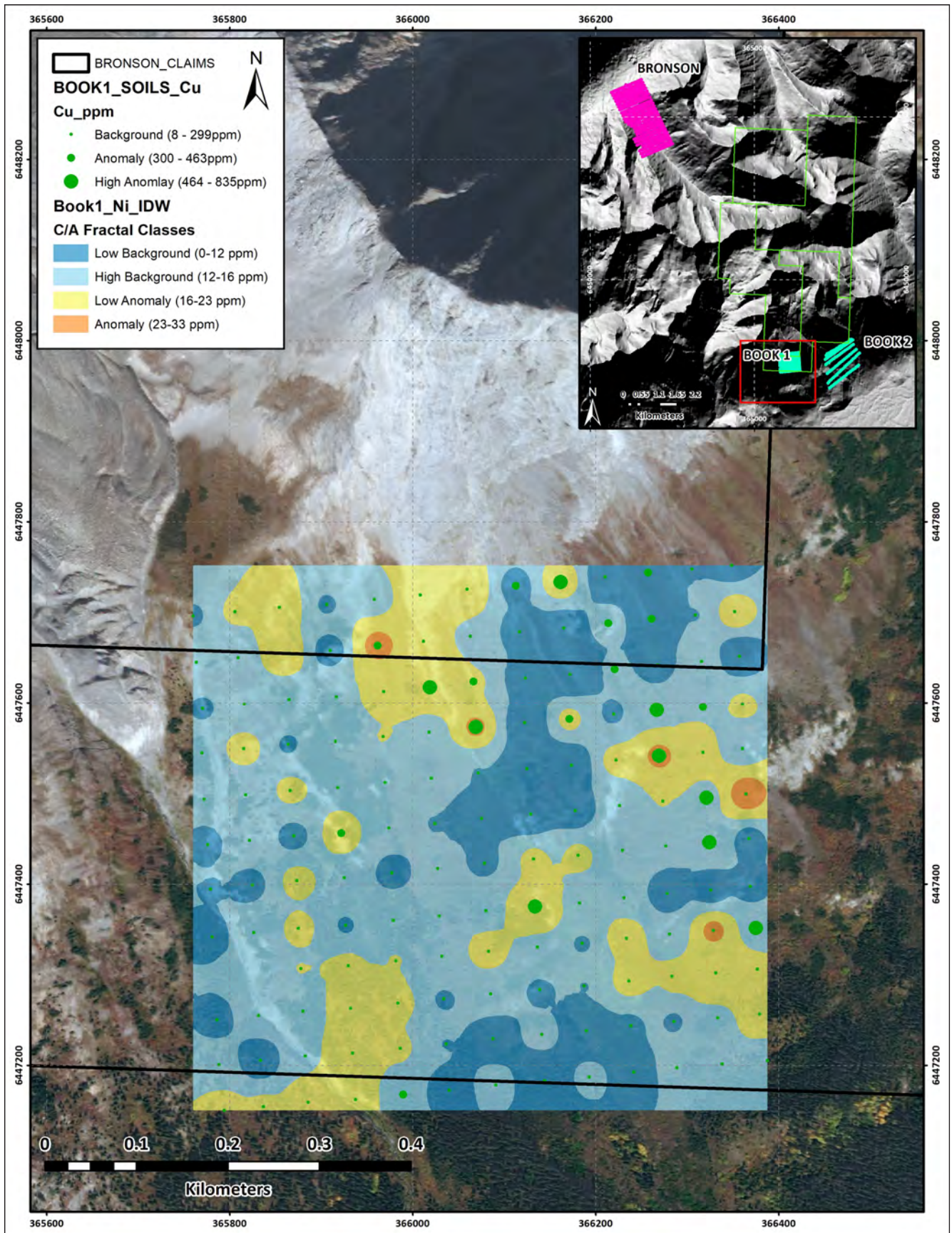


Figure 52: Graduated dot plots (Pb) superimposed on Cu IDW interpolation raster, Book 1 soil grid.

The **Book 2** soil grid is characterized by moderate strength correlations between **Cu-Be-Ca-Co-Cr-Mg-Mn-Ni-P-Sc and Sr**. Scatterplot diagrams (**Fig. 53**) also indicate weaker positive correlations between Cu, K and Pb. In general the strength of Cu-Co and pathfinder anomalism in this grid is weak. Univariate dot plots and IDW interpolation rasters are presented in **Figures 54-60** for Cu, Co and key pathfinders (**Ni-Ca-Cr-Mn-K**). Significant observations from the Book 2 univariate soil geochemical data include:

- Small, localized zones of Cu-Co anomalism, spatially coincident with Ca anomalism (**Figs. 54-56**).
- Broader low-level haloes of Ni, Cr and Mn anomalism enveloping the Cu-Co anomalies (**Figs. 57-59**). These haloes may represent distal zonation metals.
- Spatially disparate, broad zones of K anomalism trending northeasterly (**Fig. 60**).

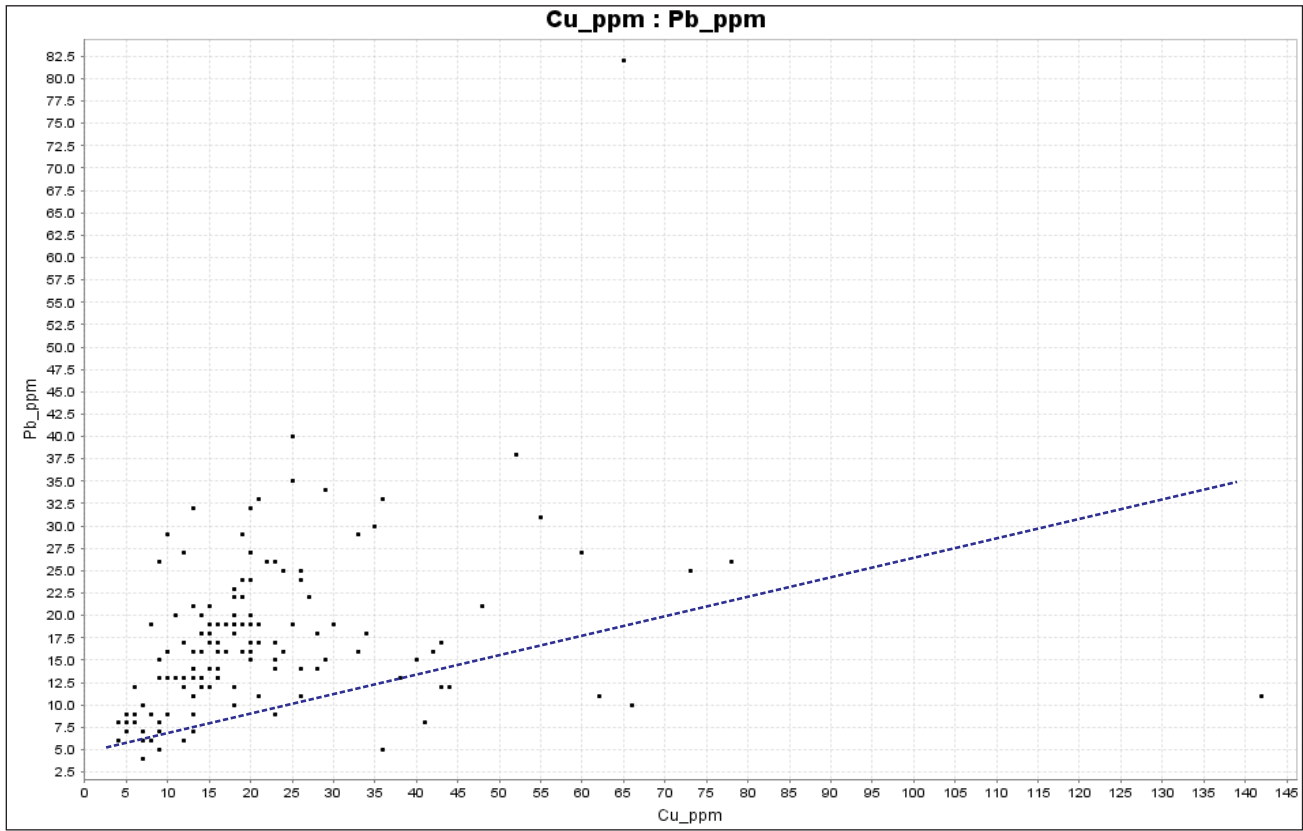
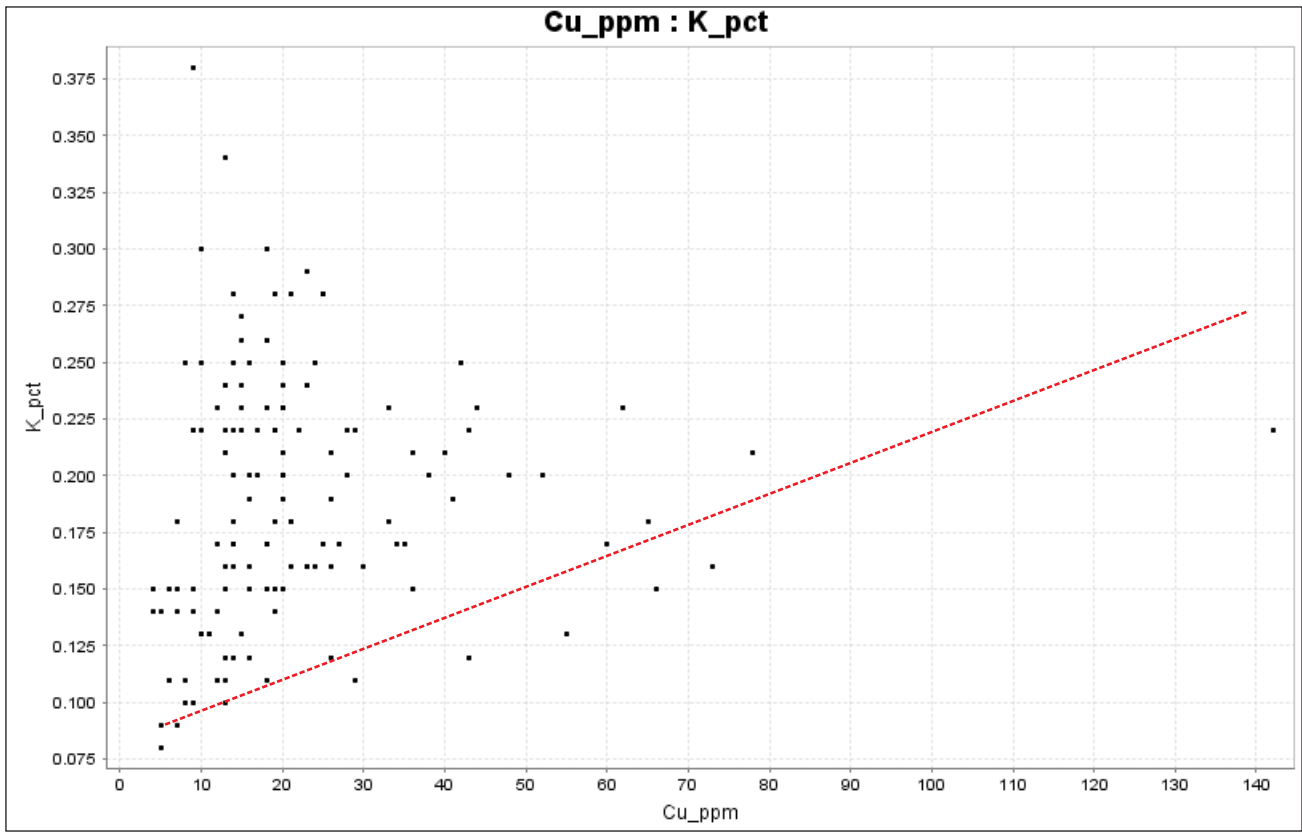


Figure 53: Scatterplots for Book2 soil grid showing weak correlations between Cu, K and Pb.

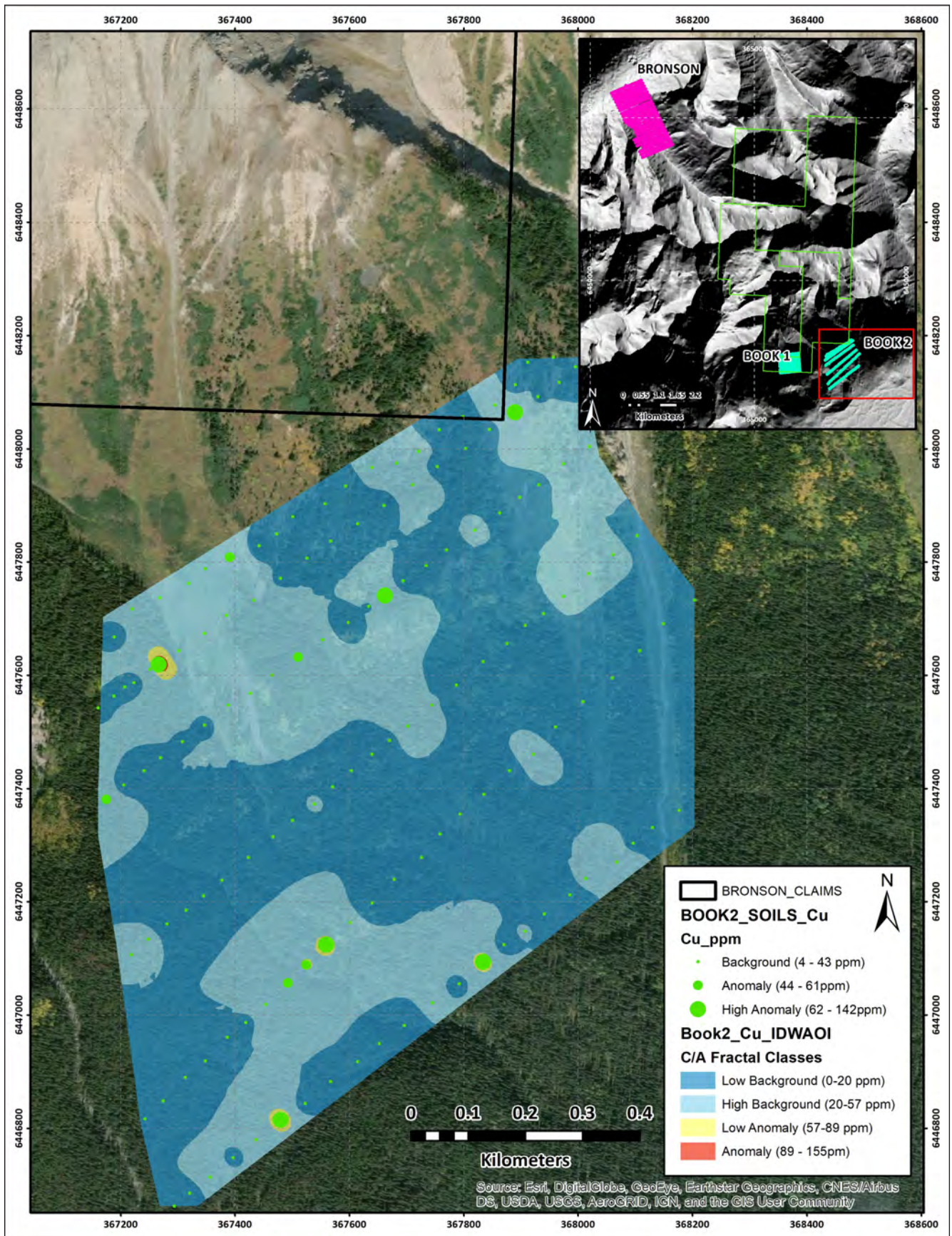


Figure 54: Graduated dot plots superimposed on IDW interpolation raster for Cu, Book 2 soil grid

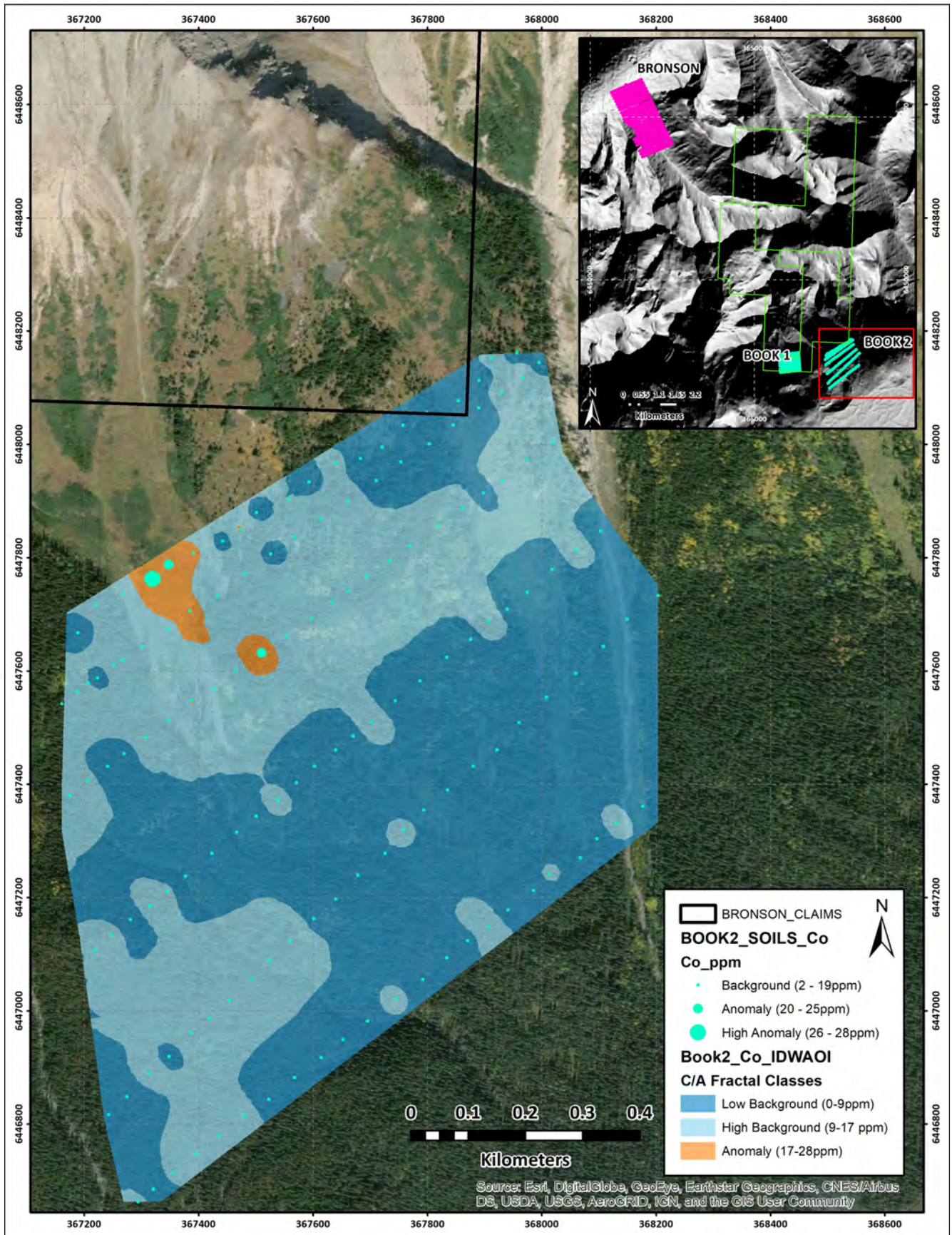


Figure 55: Graduated dot plots superimposed on IDW interpolation raster for Co, Book 2 soil grid

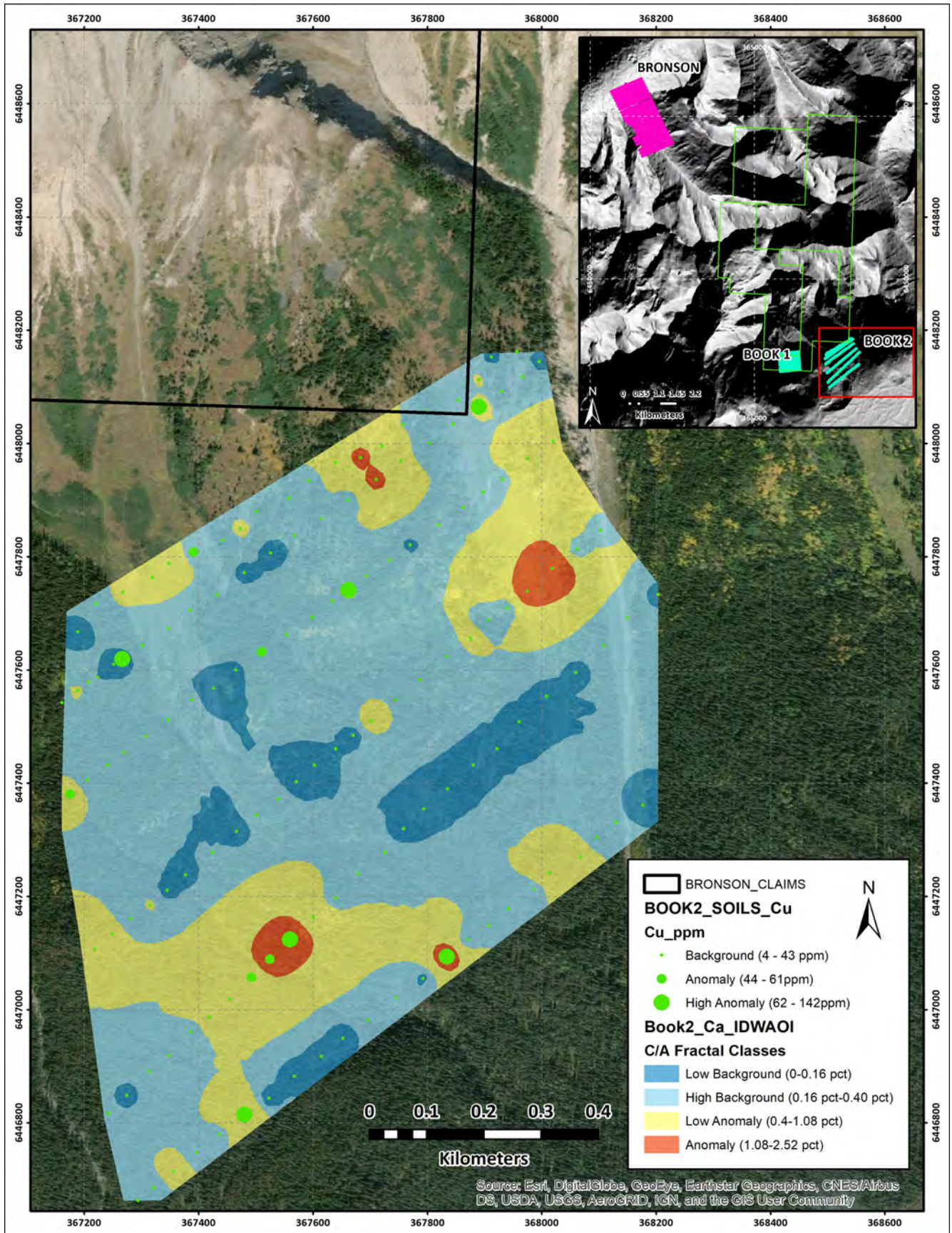


Figure 56: Graduated dot plots (Ca) superimposed on Cu IDW interpolation raster, Book 2 soil grid.

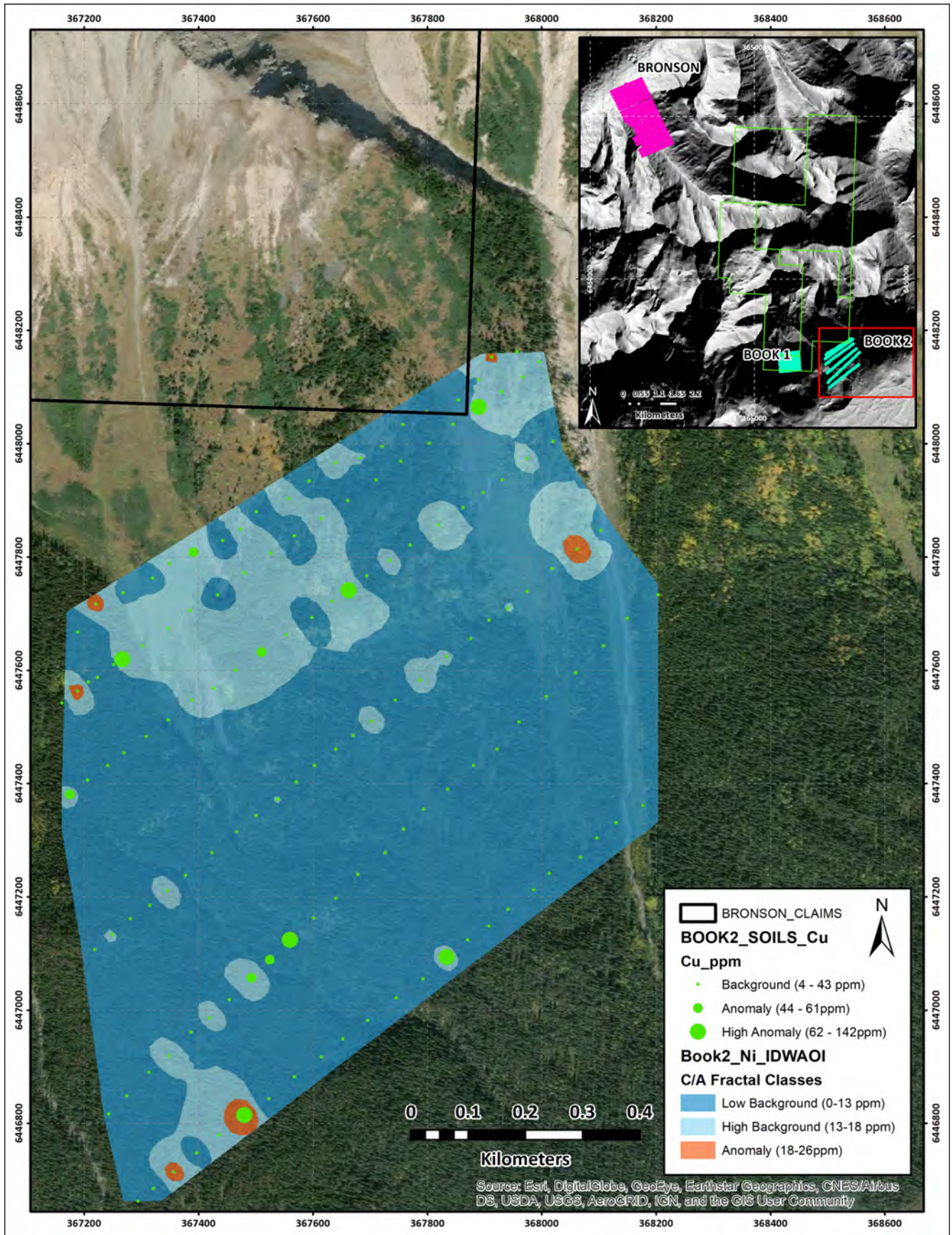


Figure 57: Graduated dot plots (Ni) superimposed on Cu IDW interpolation raster, Book 2 soil grid.

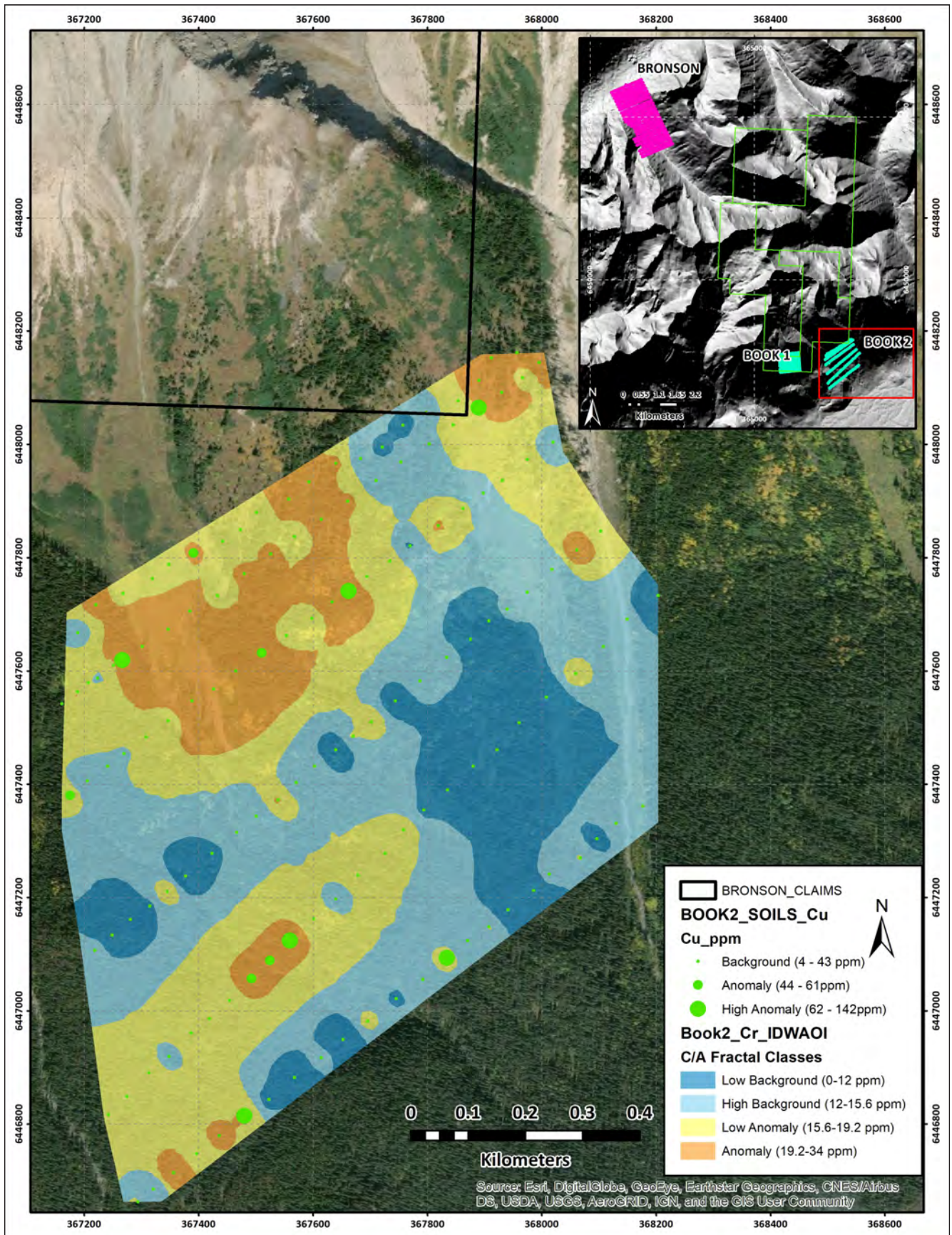


Figure 58: Graduated dot plots (Cr) superimposed on Cu IDW interpolation raster, Book 2 soil grid.

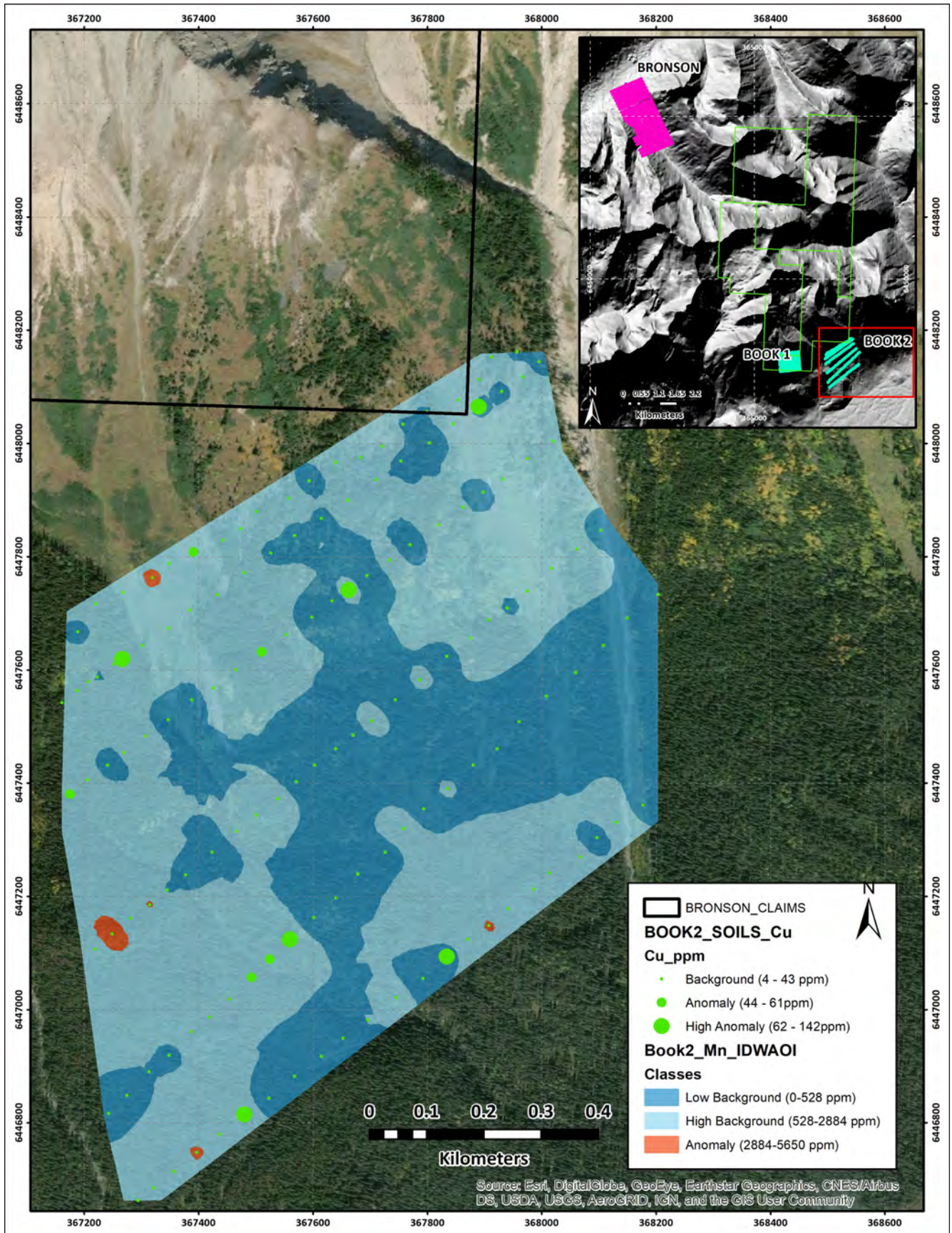


Figure 59: Graduated dot plots (Mn) superimposed on Cu IDW interpolation raster, Book 2 soil grid.

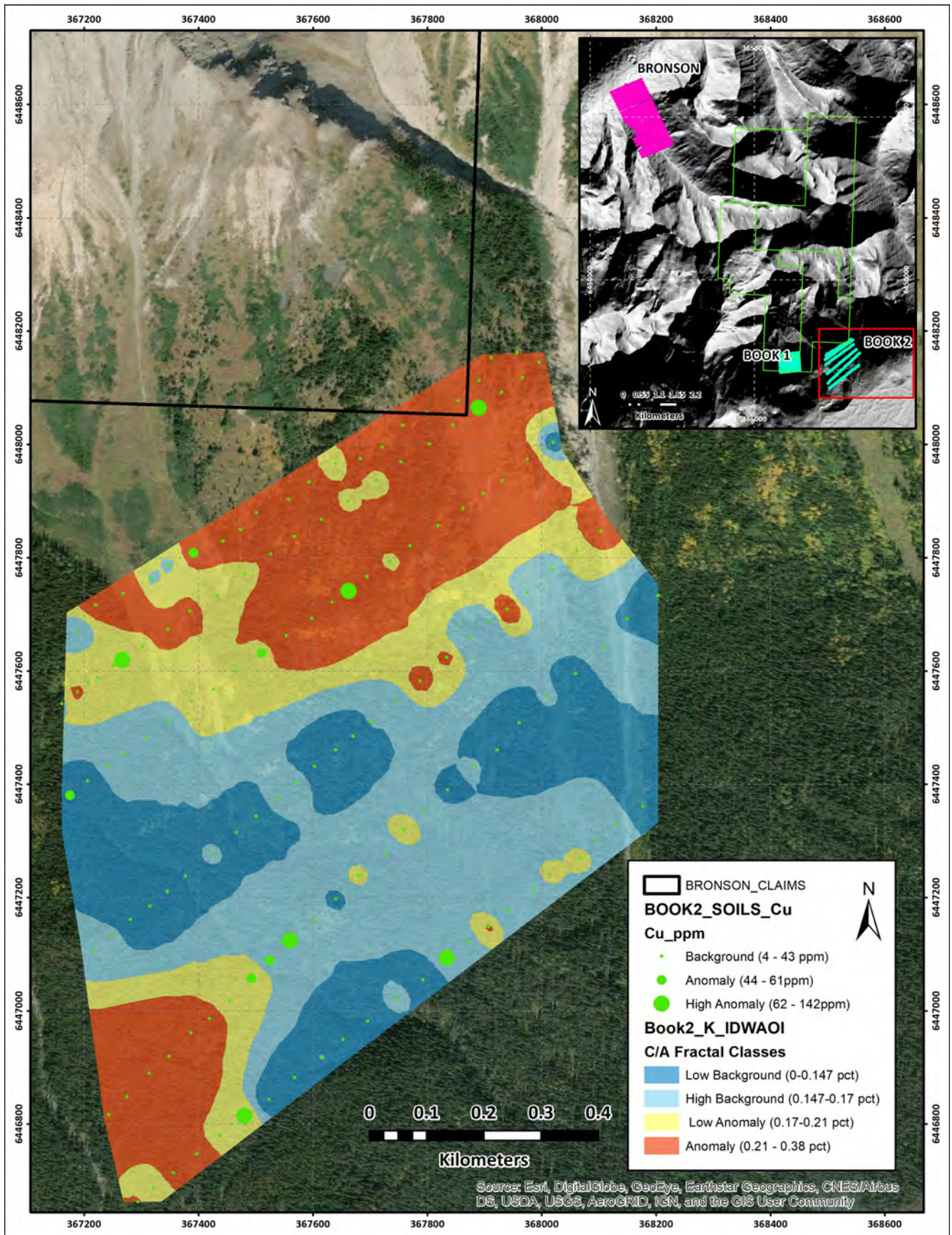


Figure 60: Graduated dot plots (K) superimposed on Cu IDW interpolation raster, Book 2 soil grid.

The **Bronson** soil grid shows moderate strength correlations between **Cu-B-Be-Ca-Co-Ni-S-Sc and Sr**. Scatterplot diagrams (**Fig. 61**) also indicate weaker positive correlations between Cu, Fe, Mn and Zn. Univariate dot plots and IDW interpolations plots are presented in **Figures 62-68** for Cu, Co and key pathfinders (**Ni-Ca-S-Mn-Zn**). Significant observations from the Bronson univariate soil geochemical data include:

- Small, spatially coincident zones of higher level Cu-Co anomalism enveloped by NNW trending zones of lower level Cu-Co anomalism (**Figs. 62-63**).
- Localized high of Ni anomalism associated with one zone of Cu-Co anomalism on the NE edge of the soil grid (**Fig. 64**).
- S and Mn anomalism that is spatially coincident with Cu-Co anomalism (**Figs. 65-66**).
- Broad zones of low-level Zn anomalism that appears independent of Cu-Co anomalism (**Fig. 67**).
- Discrete NNW trending zones of Ca anomalism characterized by downhill offset from Cu-Co anomalies (**Fig. 68**).

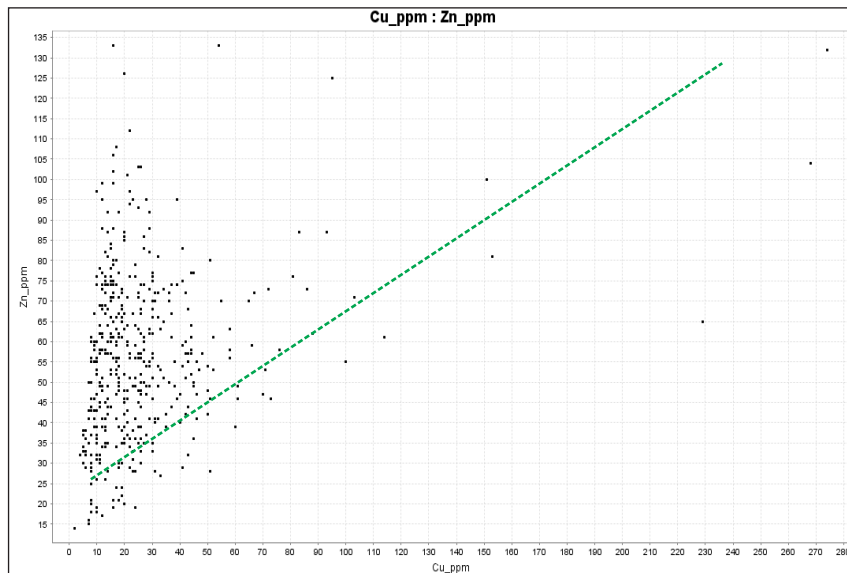
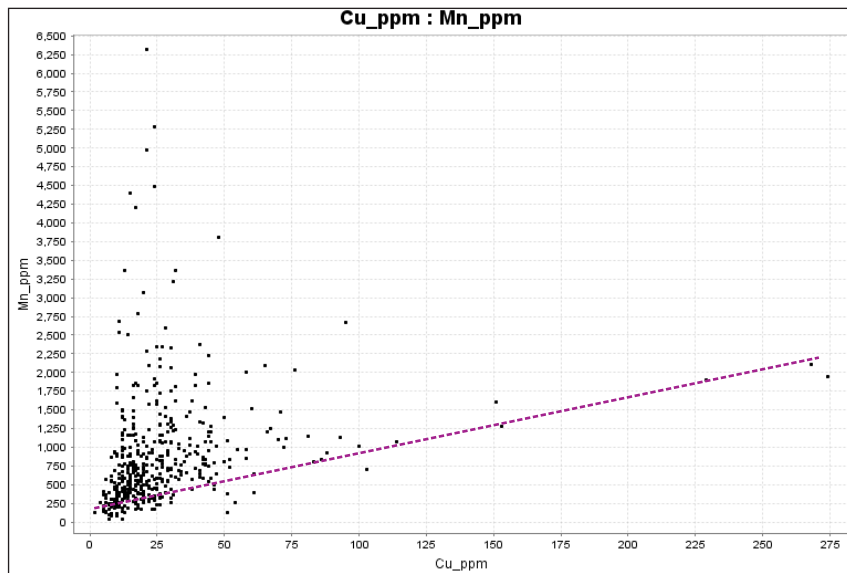
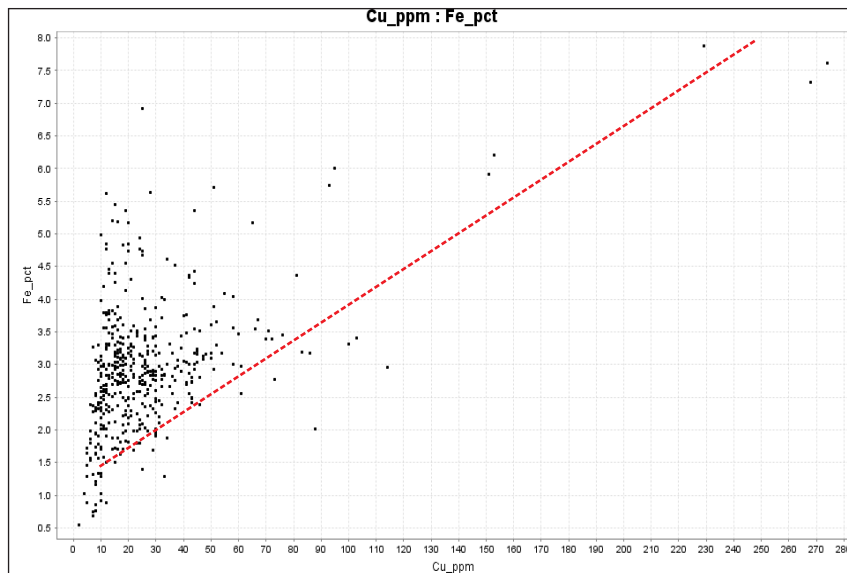


Figure 61: Scatterplots for Bronson soil grid showing weak correlations between Cu, Fe, Mn and Zn

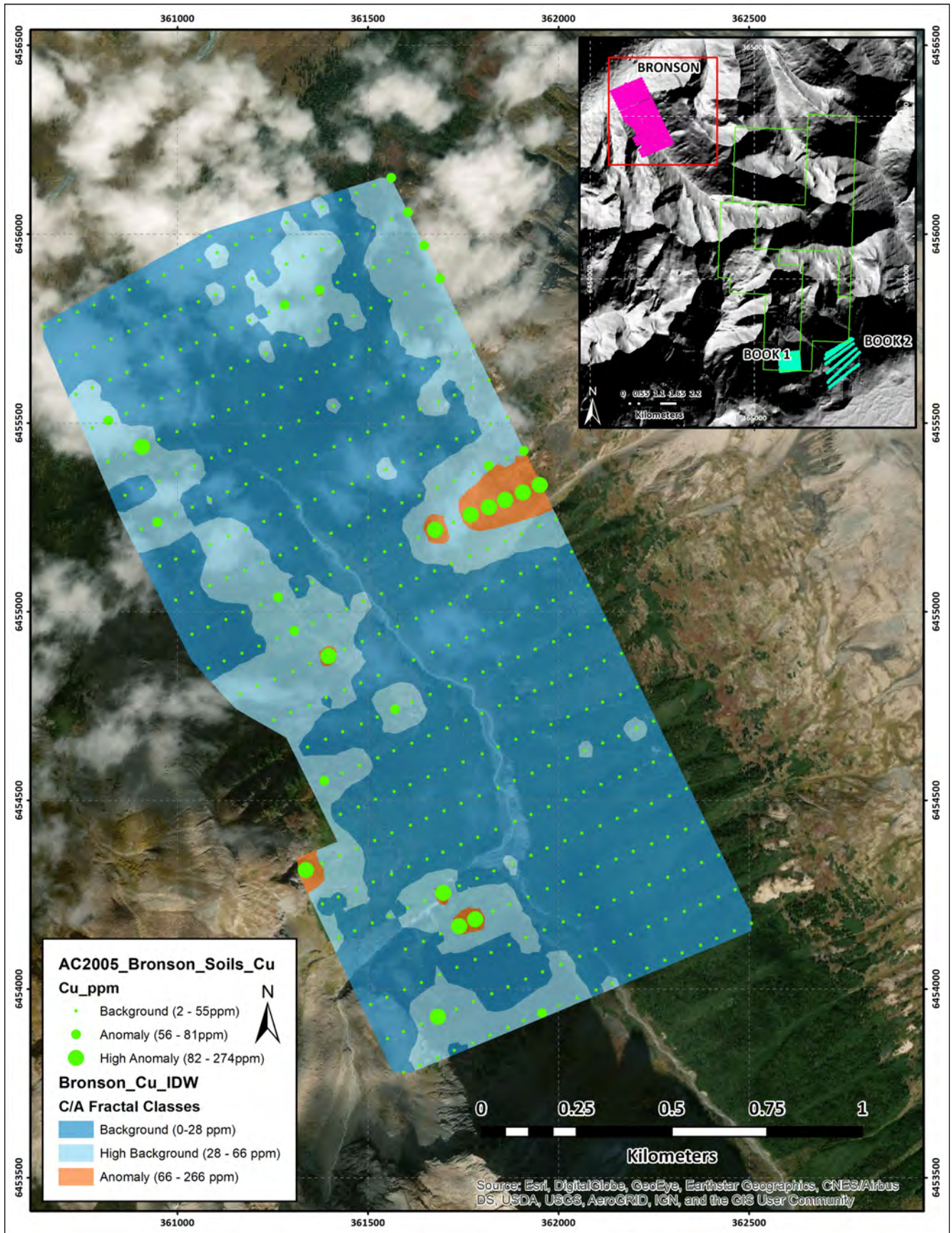


Figure 62: Graduated dot plots superimposed on IDW interpolation raster for Cu, Bronson soil grid

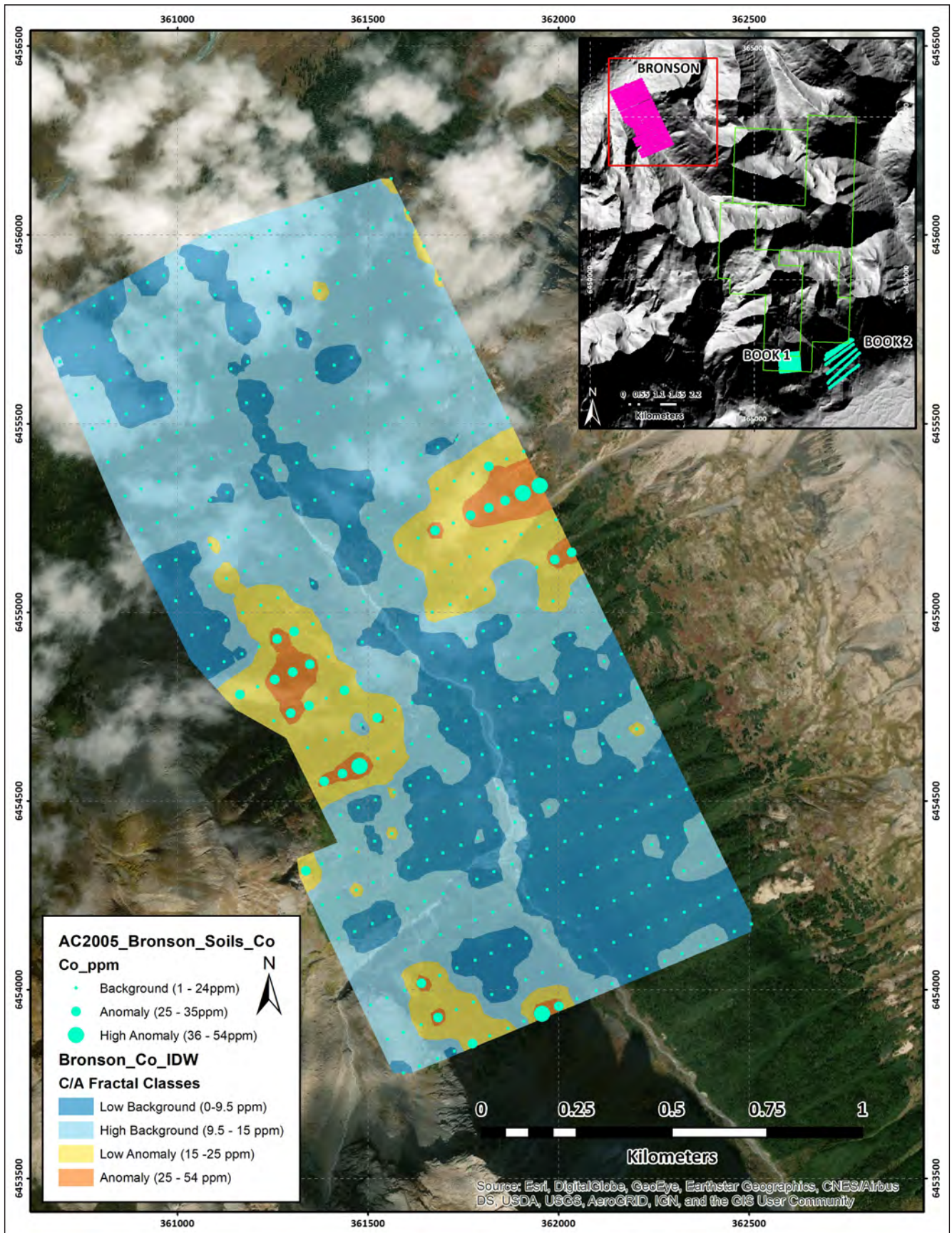


Figure 63: Graduated dot plots superimposed on IDW interpolation raster for Co, Bronson soil grid

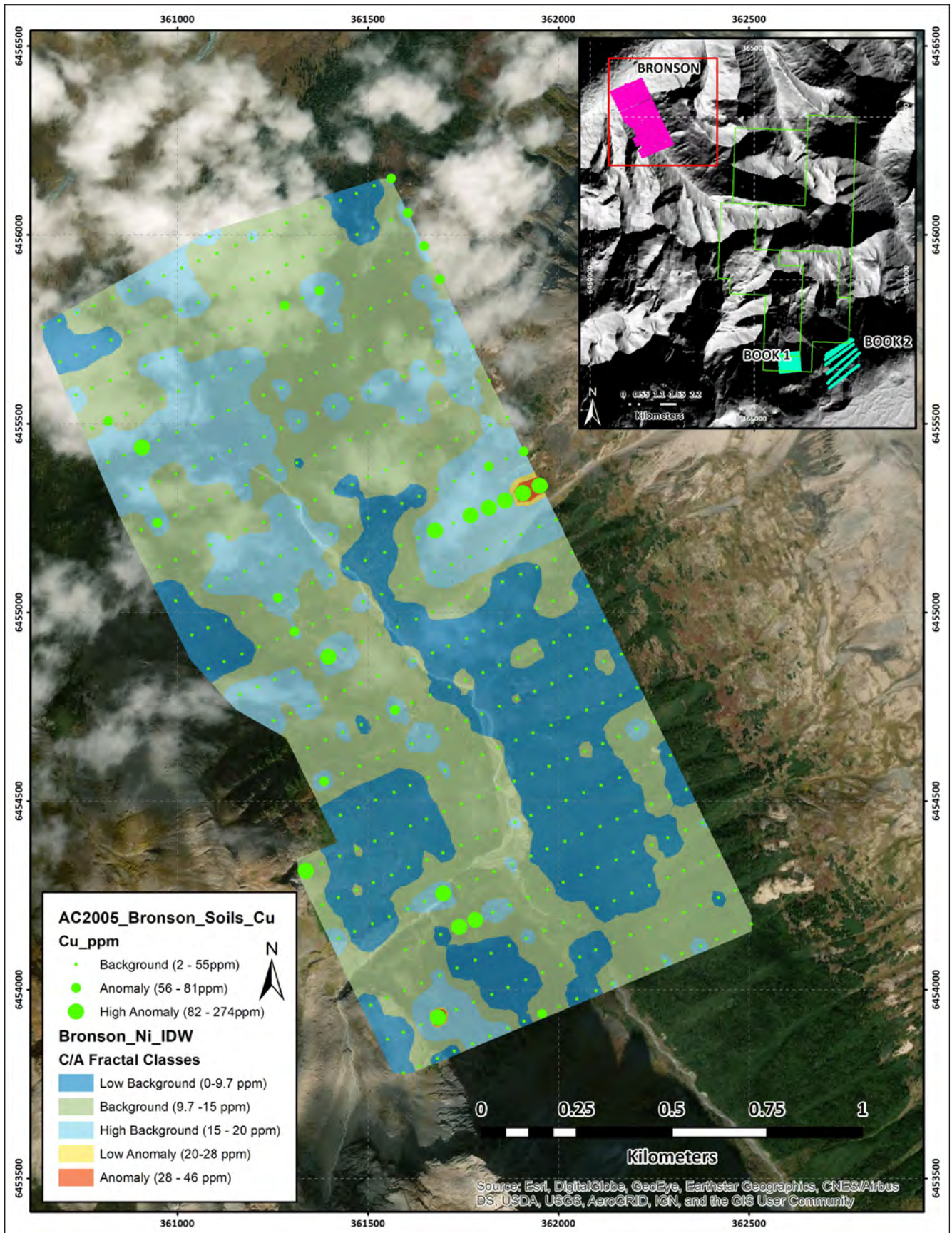


Figure 64: Graduated dot plots (Ni) superimposed on Cu IDW interpolation raster, Bronson soil grid.

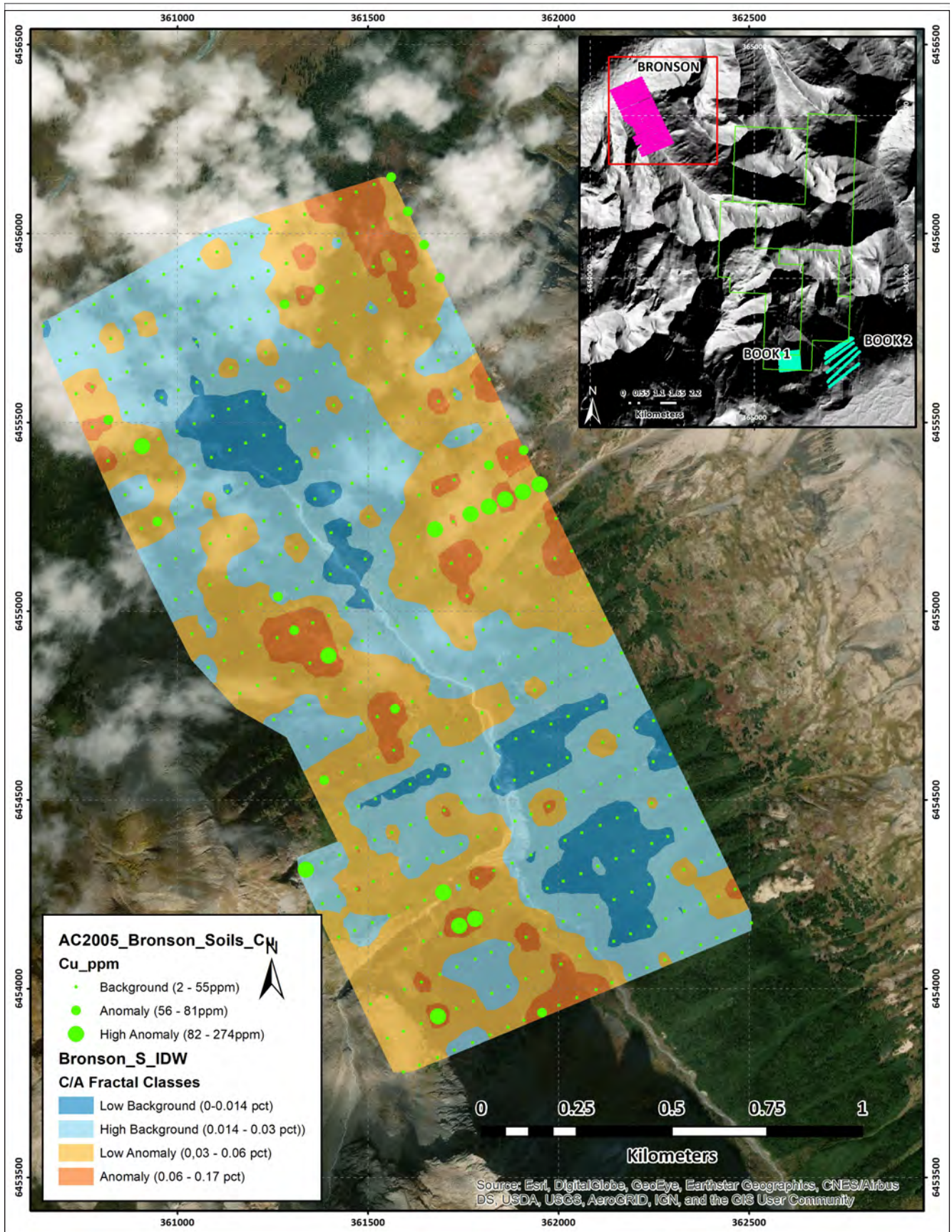


Figure 65: Graduated dot plots (S) superimposed on Cu IDW interpolation raster, Bronson soil grid.

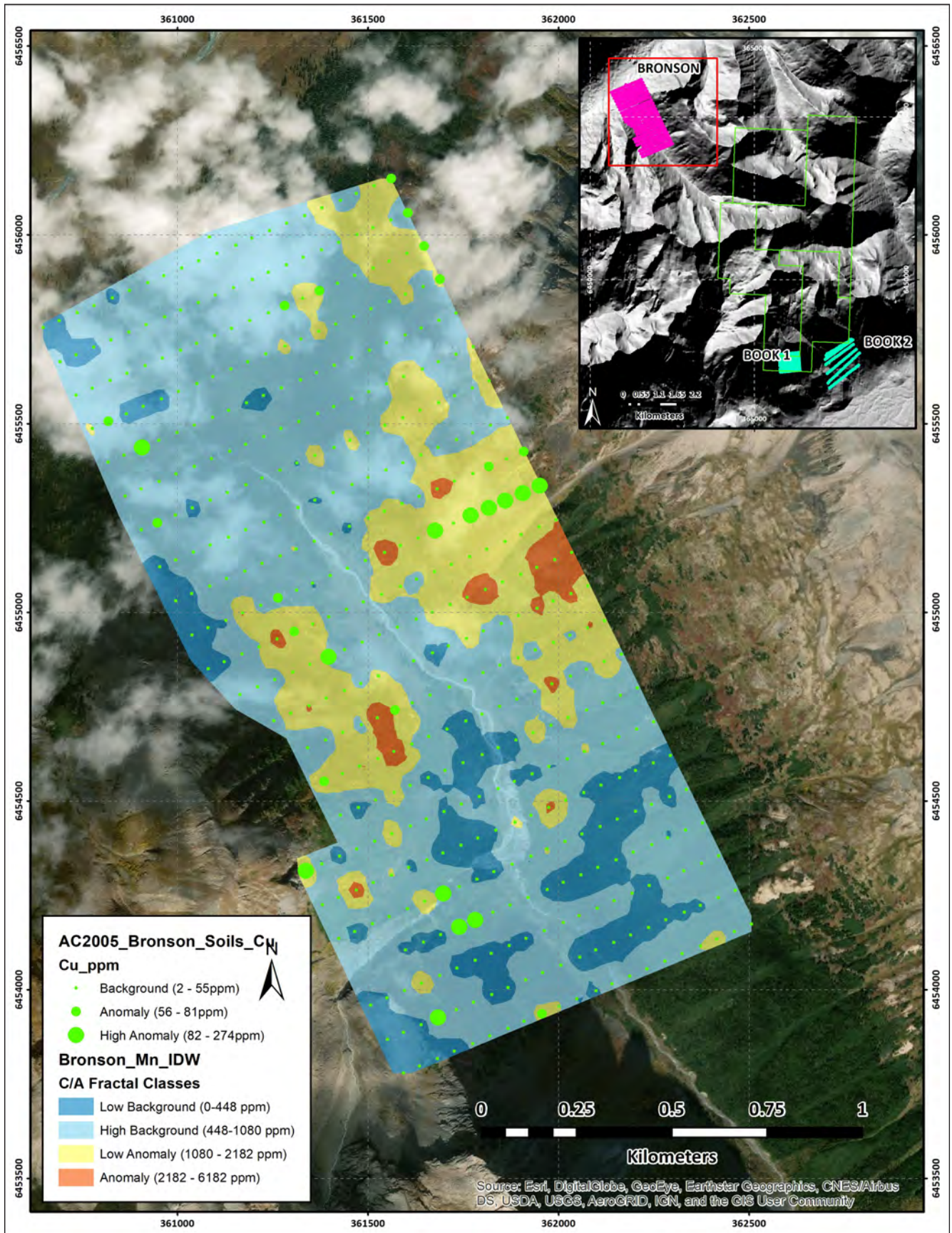


Figure 66: Graduated dot plots (Mn) superimposed on Cu IDW interpolation raster, Bronson soil grid.

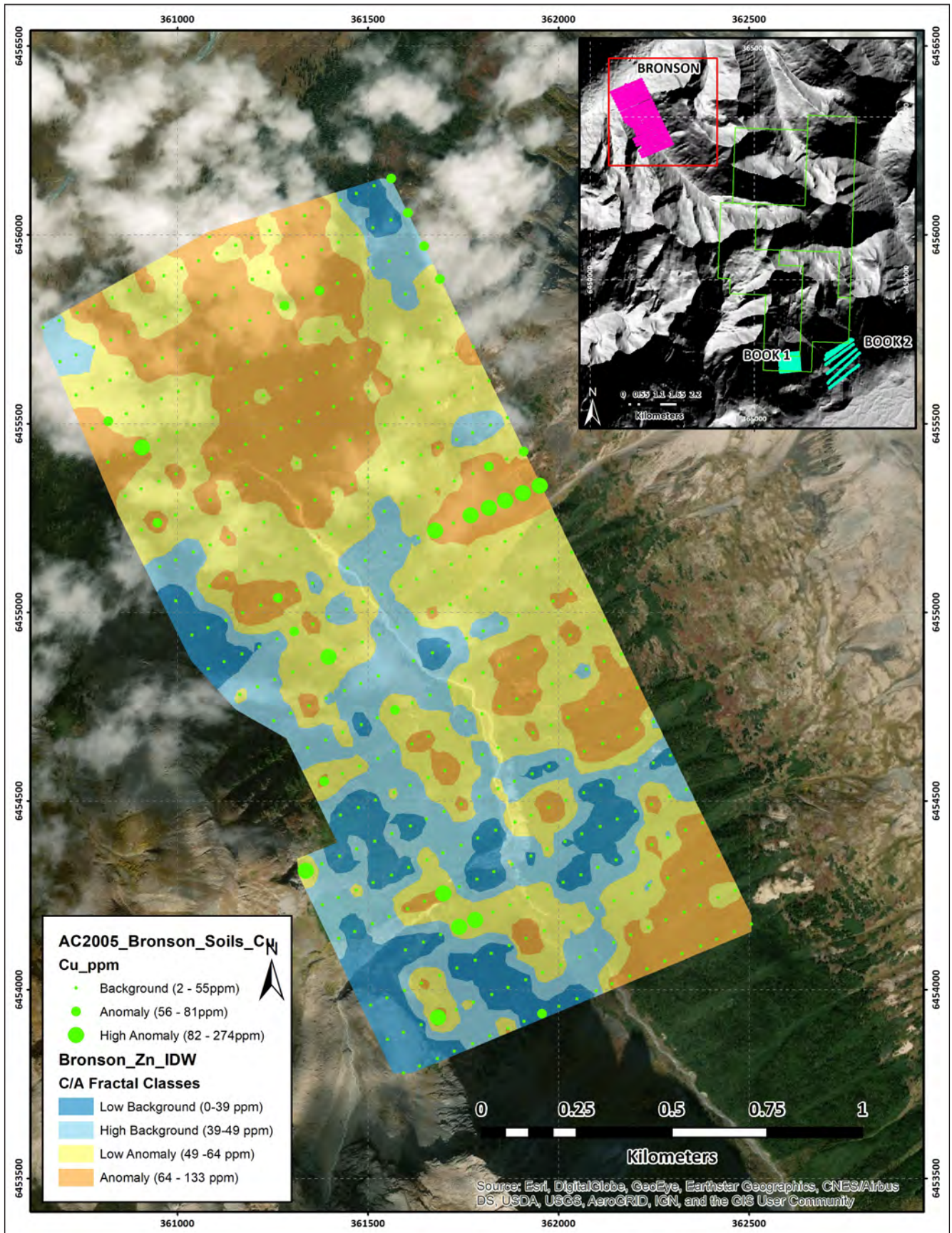


Figure 67: Graduated dot plots (Zn) superimposed on Cu IDW interpolation raster, Bronson soil grid.

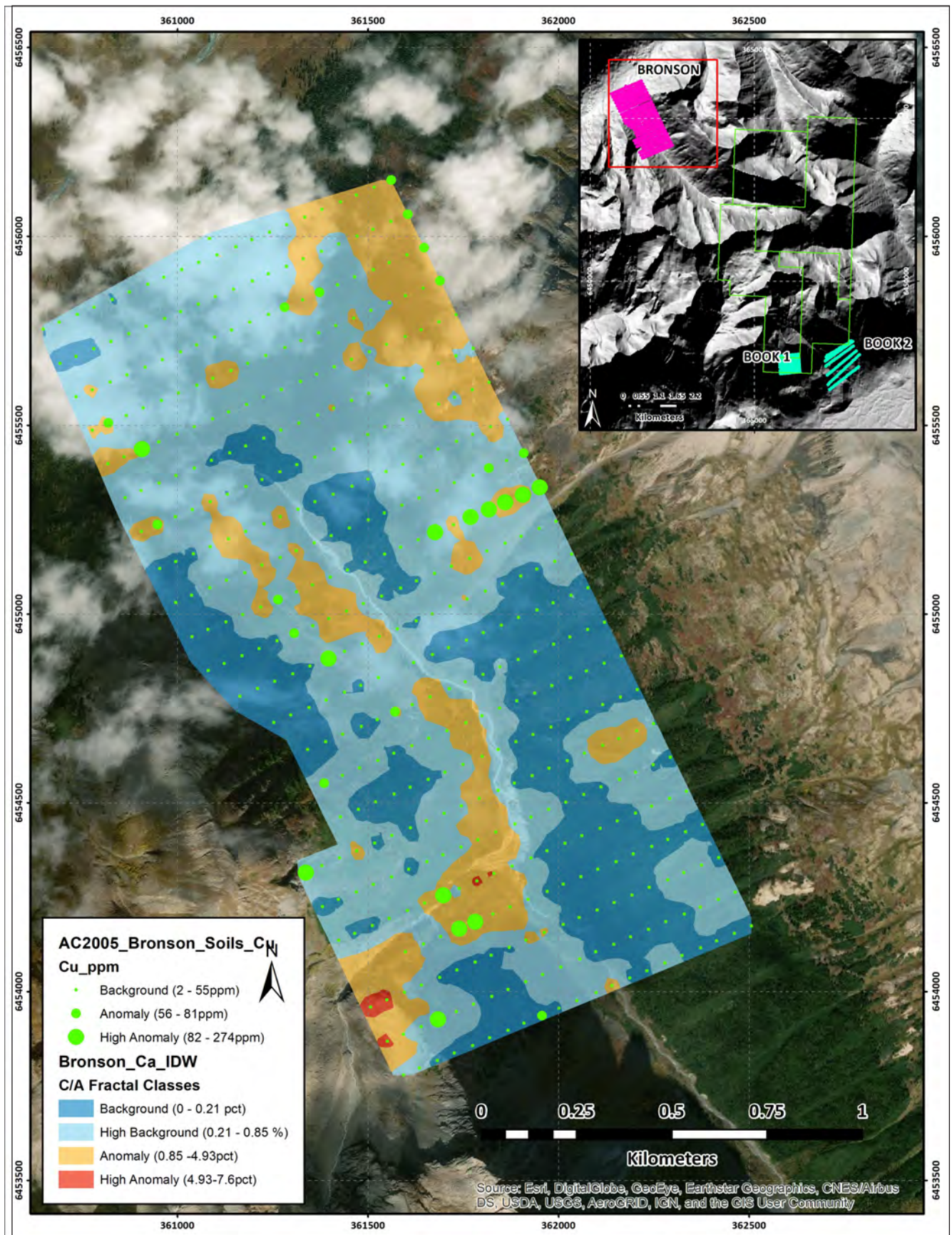


Figure 68: Graduated dot plots (Ca) superimposed on Cu IDW interpolation raster, Bronson soil grid.

Multivariate Results

Hierarchical cluster analysis was performed on the three Bronson soil grids data and the results are illustrated in **Figures 69**. The Book 1 soil grid yields 5 geochemical clusters.

Important observations include:

- (i) Cu is associated with Ca-Sr-P-S, forming a geochemical cluster separate from Co which is associated with Pb-Mn-Be
- (ii) Ag is associated with Sb-Mo-As
- (iii) The remaining clusters represent lithologically controlled geochemical variations

The Book 2 soil grid yields 6 geochemical clusters. Important observations include:

- (i) Cu is associated with P-S-Mn-Ca-Sr distinct from Co which is associated with Mg-Ni-Be-Sc
- (ii) As is associated with B-Na distinct from Ag which is associated with Sb.
- (iii) The remaining clusters represent lithologically controlled geochemical variations

The Bronson soil grid yields 5 geochemical clusters. Important observations include:

- (iv) Cu is associated with P-S-Mn-Be-Co-Ni.
- (v) As is associated with B-Sr-Mg-Sc.

- (vi) The remaining clusters represent lithologically controlled geochemical variations

The hierarchical cluster analysis indicates each soil grid has distinctly different multivariate geochemical associations. It is important to note the each grid occurs are slightly different elevations and vertical zonation within the mineralized system may be controlling the geochemical variability observed.

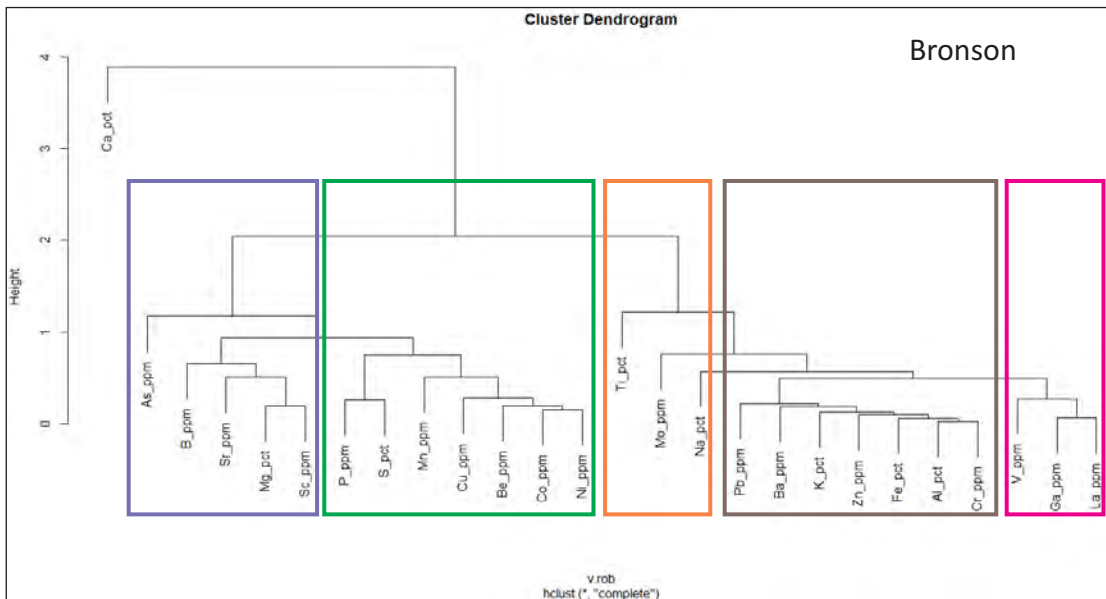
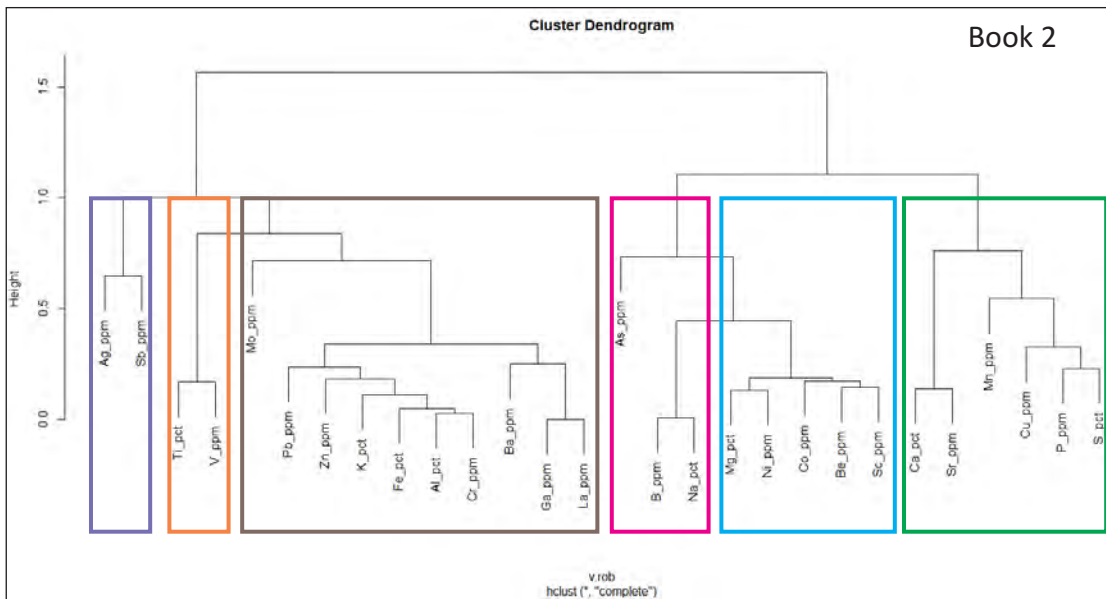
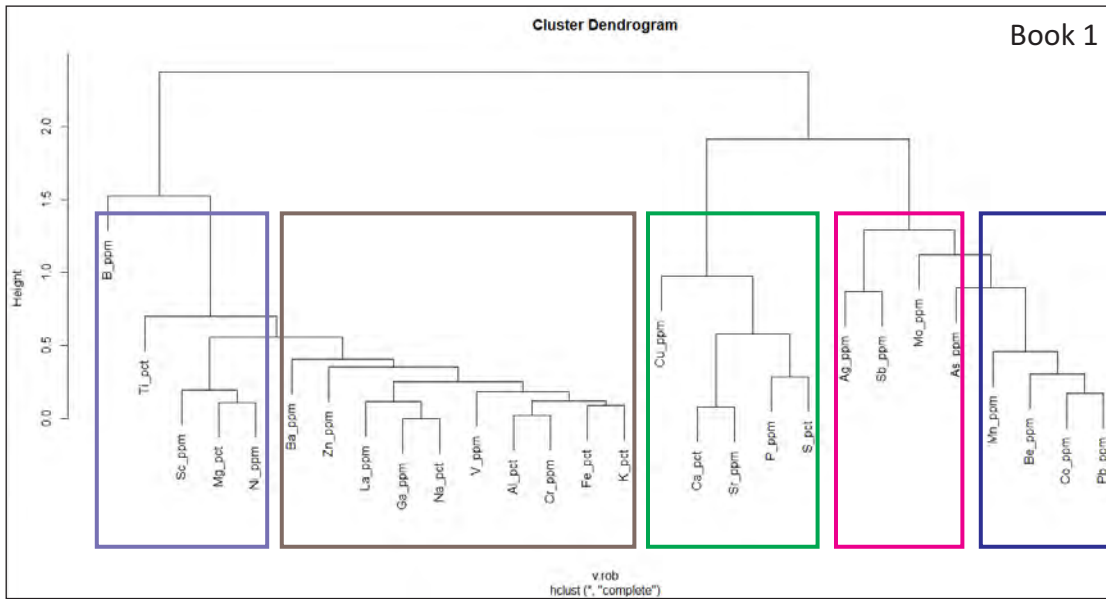


Figure 69: Hierarchical multivariate cluster analysis results for the Book 1, Book 2 and Bronson soil grids.

7.0 SUMMARY AND RECOMMENDATIONS

Mineralization encountered within the Bronson claims consists of copper-bearing quartz iron carbonate veining hosted in Proterozoic carbonates. A spatial correlation exists between this vein-hosted mineralization and the presence of Neoproterozoic diabase units. No data currently exists demonstrating a temporal relationship, however given the spatial coincidence of the two features and exploitation of similar structures, it is plausible they are genetically related.

High-resolution satellite imagery was used to map out the extent of diabase within Proterozoic hosts rocks occurring in an area of interest delineated from regional geophysical datasets. The analysis has delineated a large area of prospectivity in which Cu-Co mineralization may occur. The diabase mapping exercise also demonstrates that Jurassic-Cretaceous deformation is significant and overprints the Cu vein-hosted mineralization in the area.

Diabase dykes appear to have been emplaced in two main generations, which exploited pre-existing trans-tensional fault systems, several of which host Cu mineralization.

Integration of historical geological mapping results and new structural interpretations derived from high resolution colour satellite imagery highlights the presence of a trans-tensional fault system associated with Cu mineralization within the Bronson claims. Two main diabase suites are present including an older NNW-trending suite and a younger, overprinting NE trending suite. Cu mineralized veins are spatially related to both diabase populations.

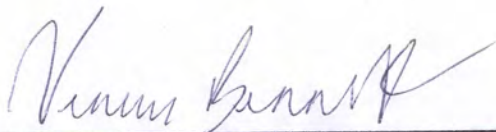
Univariate and multivariate geochemical analysis of historic rock, silt and soil data suggests that pathfinder elements associated with Cu mineralization are similar to pathfinders present in known IOCG deposits (Cu-S-As-Ag-Co-Fe-Mn and Ni). Sample catchment basin analysis has identified numerous catchment areas characterized by both univariate and multivariate anomalies within and adjacent to the Bronson claim block. Geochemical analysis of historic Bronson soil datasets has identified several areas of Cu-Co anomalism that warrants ground follow-up.

Key recommendations include:

1. Structural/stratigraphic mapping of the Bronson claims (1: 5000) scale, with a focus on
(i) understanding structural controls on the diabase suite 2 associated mineralization (ii)
understanding structural controls on NNW-trending vein-hosted Cu mineralization.
2. District-scale gravity survey
3. Drone-magnetic survey over the Bronson claims.

Respectfully submitted,

Geomantia Consulting



Venessa Bennett, Ph. D., P.Geo. Adv. Dip RS/GIS

8.0 REFERENCES

Agterberg, F.P., 1994. Fractals, multifractals, and change of support. In: Geostatistics for the next century. Springer, pp 223–234.

Aitchison, J., 1986, The Statistical Analysis of Compositional Data: Chapman and Hall.
Bonham-Carter, G.F., Rogers, P.J., Ellwood, D.J., 1987. Catchment basin analysis applied to surficial geochemical data, Cobequid Highlands, Nova Scotia. J. Geochem. Explor. 29, 259–278.

Campbell, K.V., 2016. Preparatory surveys, structural study and geological remote sensing investigation of the Toro Property. Unpublished report prepared for A.R. Raven., B.C. Mineral Resources Assessment Report; 71pp.

Carne, R.C., 2006. Assessment report describing geological mapping, prospecting, soil sampling, airborne magnetic surveys and diamond drilling at the Muskwa property; unpublished report prepared for Twenty-seven Capital Corp., B.C. Mineral Resources Assessment Report 28281; 376pp.

Carranza, E.J.M., 2016. Geochemical Mineral Exploration: Should We Use Enrichment Factors or Log-Ratios? Natural Resources Research (2016). DOI: 10.1007/s11053-016-9318-z

Cheng, Q., Agterberg, F.P., Ballantyne, S.B., 1994. The separation of geochemical anomalies from background by fractal methods. Journal of Geochemical Exploration 51, 109–130.

Cheng, Q., Xu, Y., Grunsky, E., 2000. Integrated spatial and spectrum method for geochemical anomaly separation. Nat. Resour. Res. 9, 43–52.

Cheng, Q., 2012. Singularity theory and methods for mapping geochemical anomalies caused by buried sources and for predicting undiscovered mineral deposits in covered areas. J. Geochem. Explor. 122, 55–70.

Coetzee, G., 2007. Progress report on the geological work done at the Sox, Magnum and Missy projects plus the regional geological interpretation of Trident project. Internal company report unpublished, p34pp.

Dmitrijeva, M., Ehrig, K.J., Ciobanu, C.L., Cook, N.J., Verdugo-Ihl, M.R., and Metcalfe, A.V., 2019. Defining IOCG signatures through compositional data analysis: a case study of litho-geochemical zoning from the Olympic Dam deposit, South Australia. Ore Geology Reviews. Volume 105, February 2019, Pages 86-101.

Filzmoser P, Hron K, Reimann C., 2009. Univariate statistical analysis of environmental (compositional) data: problems and possibilities. Sci Total Environ; 407: 6100–8.

Filzmoser, P., Hron, K., and Templ, M., 2018. Applied Compositional Data Analysis with Worked Examples in R. Springer International Publishing. 280pp.

Gabriel, K.R., 1971. The Biplot Graphic Display of Matrices with Application to Principal Component Analysis. *Biometrika*, 58, 453-467.

Groves, D.I., Bierlein, F.P., Meinert, L.D. and Hitzman, W.M, 2010. Iron Oxide Copper-Gold (IOCG) Deposits through Earth History: Implications for Origin, Lithospheric Setting, and Distinction from Other Epigenetic Iron Oxide Deposits: *Economic Geology*, 105, 641-654.

Grunsky, E., 2010. The interpretation of geochemical survey data. *Geochemistry-exploration Environment Analysis - GEOCHEM-EXPLOR ENVIRON ANAL.* 10. 27-74. 10.1144/1467-7873/09-210.

Grunsky, E.C., de Caritat, P, 2017. Advances in the Use of Geochemical Data for Mineral Exploration. *Geochemistry Paper 31* In "Proceedings of Exploration 17: Sixth Decennial International Conference on Mineral Exploration" edited by V. Tschirhart and M.D. Thomas, 2017, p. 441–456.

Hawkes, H.E., 1976. The downstream dilution of stream sediment anomalies. *J. Geochem. Explor.* 6, 345–358.

Hill, E. J., N. H. Oliver, L. Fisher, J. S. Cleverley, and M. J. Nugus, 2014. Using geochemical proxies to model nuggety gold deposits: An example from Sunrise Dam, Western Australia: *Journal of Geochemical Exploration*, 145, 12 –24.

Mark, G., Oliver, N.H.S. & Williams, P.J., 2006. Mineralogical and chemical evolution of the Ernest Henry Fe oxide–Cu–Au ore system, Cloncurry district, northwest Queensland, Australia. *Miner Deposita* 40, 769.

Porter, T.M., 2010 - Current Understanding of Iron Oxide Associated-Alkali Altered Mineralised Systems: Part I, An Overview; in Porter, T.M., (ed.), *Hydrothermal Iron Oxide Copper-Gold and Related Deposits: A Global Perspective*, v. 3 - Advances in the Understanding of IOCG Deposits; PGC Publishing, Adelaide, pp. 5-32

Preto, V.A. 1971 Lode Copper Deposits of the Racing River-Gataga River Area Geology, Exploration, and Mining in British Columbia British Columbia Department of Mines and Petroleum Resources, British Columbia pp. 75-104.

Reimann, C., Filzmoser, P., Fabian, K., Hron, K., Birke, M., Demetriades, A., Dinelli, E., and Ladenberger, A., 2017. The concept of compositional data analysis in practice--total major element concentrations in agricultural and grazing land soils of Europe. *Sci Total Environ.* 2012 Jun 1; 426:196-210. doi: 10.1016/j.scitotenv.2012.02.032. Epub 2012 Apr 12.

Rezza, C., Attila, P., Albanese, S., Lima, A., Minolfi, G., and De Vivo, B., 2018. Mo, Sn and W patterns in topsoils of the Campania Region, Italy. *Geochemistry Exploration Environment Analysis*. 18. 331-342. 10.1144/geea2017-061.

Ross, et al., G.M., Villeneuve, M.E., and Theriault, R J. 2001 Isotopic provenance of the lower Muskwa assemblage (Mesoproterozoic, Rocky Mountains, British Columbia): New clues to correlation and source areas: *Precambrian Research*, v. 11 1, p. 57-77.

Shahrestani, S., Mokhtari, A.R. & Alipour-Asll, M. Assessment of Estimated Bedrock and Stream Sediment Geochemical Backgrounds in Catchment Basin Analysis. *Nat Resour Res* 28, 1071–1087 (2019)

Taylor, G.C., and Stott, D.F., 1973; Tuchodi Lakes Map-Area, British Columbia, Geological Survey of Canada, Memoir 373.

Wang, C., Carranza, E. J. M., Zhang, S., Liu, J., Zhang, D., Sun, X., et al. (2013). Characterization of primary geochemical haloes for gold exploration at the Huanxiangwa gold deposit, China. *Journal of Geochemical Exploration*, 124, 40–58.

APPENDIX I

AUTHOR'S STATEMENT OF QUALIFICATIONS

STATEMENT OF QUALIFICATIONS

I, Venessa R.C. Bennett, geologist, with business and residential addresses in Whitehorse, Yukon Territory and, hereby certify that:

1. I graduated from the Macquarie University, Sydney, Australia in 1996 with a B.Sc. (Hons) in geology, in 2008 from Memorial University of Newfoundland with a Ph.D. majoring in geology and in 2015 from the Centre of Geographic Sciences, Nova Scotia with an advanced diploma in Geographic Information Systems and Remote Sensing.
2. I am a Professional Geoscientist registered with the Association of Professional Engineers and Geoscientists of the Province of Alberta (registration number - 192895).
3. From 1996 to present, I have been actively engaged as a geologist in mineral exploration, geoscience research and government geoscience both internationally and nationally.
4. I personally participated in and supervised the field work reported herein and have interpreted all data resulting from this work.

Venessa R.C. Bennett Ph.D., P.Geo., Adv. Dip GIS/RS

APPENDIX II

STATEMENTS OF COSTS

BRONSON PROPERTY

Statement of Costs
Bronson Project 2019 Season

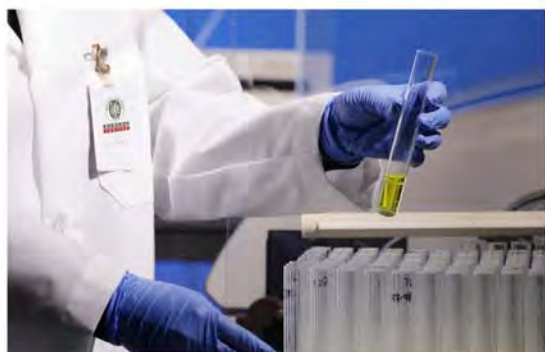
<u>Consultants</u>		<u>Units</u>	<u>Rate</u>	<u>Cost</u>
Aurora Geosciences	V. Bennett, P. Geo	2 days	900.00	1,800.00
Aurora Geosciences	field assistant	2 days	500.00	1,000.00
JMK Geological Services	J. Kowalchuk, P. Geo	1 day	600.00	600.00
<u>Helicopter</u>	Highland Helicopters - Fort Nelson	4 hours	1,986.00	7,944.00
<u>Accommodation/Meals</u>	Toad River Lodge/Jack's Place	6 man/day	210.00	1,260.00
<u>Analytical Services</u>	Bureau Veritas	3 samples	25.80	77.40
<u>Transportation</u>	4x4 pickup	3 days	60.00	180.00
<u>Mobe/Demobe</u>	allocated costs			500.00
<u>Winter Data Analysis Work</u>				
20/04/2019 - 25/04/2019	New Bronson Geological Map/ Structural Interpretation	5 days	900	4,500.00
09/12/2019 - 14/12/2019	New Geochemical synthesis and advanced geochemical analysis Geomantia Consulting	6 days	900	5,400.00
<u>Assessment Report</u>				
18/05/2019 - 23/05/2019	Geomantia Consulting	5 Days	900	4,500.00
			Total Costs	\$ 27,761.40

Note: All GST costs have been removed from statement
Exploration carried out on the Bronson project was done in conjunction with other programs in the area.

Two field days were spent attempting to carry out field work on Bronson Claims

APPENDIX III

ANALYTICAL CERTIFICATES



**BUREAU
VERITAS**

MINERALS

► AQ300, AQ200

Package Description	Geochemical aqua regia digestion
Sample Digestion	HNO ₃ -HCl acid digestion
Instrumentation Method	ICP-ES (AQ300, AQ200), ICP-MS (AQ200)
Legacy Code	1D, 1DX
Applicability	Sediment, Soil, Non-mineralized Rock and Drill Core

► METHOD DESCRIPTION

Prepared sample is digested with a modified Aqua Regia solution of equal parts concentrated HCl, HNO₃ and DI H₂O for one hour in a heating block or hot water bath. Sample is made up to volume with dilute HCl. Sample splits of 0.5g are analyzed optional 15g or 30g digestion available for AQ200.

Limitations:

Au solubility can be limited by refractory and graphitic samples.

ELEMENT	AQ300 DETECTION	AQ200 DETECTION	UPPERLIMIT
Ag	0.3 ppm	0.1 ppm	100 ppm
Al*	0.01 %	0.01 %	10 %
As	2 ppm	0.5 ppm	10000 ppm
Au	-	0.5 ppb	100 ppm
B*^	20 ppm	20 ppm	2000 ppm
Ba*	1 ppm	1 ppm	10000 ppm
Bi	3 ppm	0.1 ppm	2000 ppm
Ca*	0.01 %	0.01 %	40 %
Cd	0.5 ppm	0.1 ppm	2000 ppm
Co	1 ppm	0.1 ppm	2000 ppm
Cr*	1 ppm	1 ppm	10000 ppm
Cu	1 ppm	0.1 ppm	10000 ppm
Fe*	0.01 %	0.01 %	40 %
Ga*	-	1 ppm	1000 ppm
Hg	1 ppm	0.01 ppm	50 ppm
K*	0.01 %	0.01 %	10 %
La*	1 ppm	1 ppm	10000 ppm
Mg*	0.01 %	0.01 %	30 %

ELEMENT	AQ300 DETECTION	AQ200 DETECTION	UPPERLIMIT
Mn*	2 ppm	1 ppm	10000 ppm
Mo	1 ppm	0.1 ppm	2000 ppm
Na*	0.01 %	0.001 %	5 %
Ni	1 ppm	0.1 ppm	10000 ppm
P*	0.001 %	0.001 %	5 %
Pb	3 ppm	0.1 ppm	10000 ppm
S	0.05 %	0.05 %	10 %
Sb	3 ppm	0.1 ppm	2000 ppm
Sc	-	0.1 ppm	100 ppm
Se	-	0.5 ppm	100 ppm
Sr*	1 ppm	1 ppm	10000 ppm
Te	-	0.2 ppm	1000 ppm
Th*	2 ppm	0.1 ppm	2000 ppm
Ti*	0.01 %	0.001 %	5 %
Tl	5 ppm	0.1 ppm	1000 ppm
U*+	8 ppm	0.1 ppm	2000 ppm
V*	1 ppm	2 ppm	10000 ppm
W*	2 ppm	0.1 ppm	100 ppm
Zn	1 ppm	1 ppm	10000 ppm

* Solubility of some elements will be limited by mineral species present. ^Detection limit = 1 ppm for 15g / 30g analysis. + Available upon request





BUREAU VERITAS MINERAL LABORATORIES
Canada

www.bureauveritas.com/um

Bureau Veritas Commodities Canada Ltd.
9050 Shaughnessy St Vancouver British Columbia V6P 6E5 Canada
PHONE (604) 253-3158

Client: **Fabled Copper and Gold Corp.**
2300 - 1066 West Hastings St.
Vancouver British Columbia V6E 3X1 Canada

Submitted By: John Kowalchuk
Receiving Lab: Canada-Whitehorse
Received: October 01, 2019
Report Date: November 20, 2019
Page: 1 of 3

CERTIFICATE OF ANALYSIS

WHI19000616.1

CLIENT JOB INFORMATION

Project: Church Key
Shipment ID:
P.O. Number
Number of Samples: 56

SAMPLE DISPOSAL

RTRN-PLP Return After 90 days
RTRN-RJT Return After 60 days

Bureau Veritas does not accept responsibility for samples left at the laboratory after 90 days without prior written instructions for sample storage or return.

Invoice To: Fabled Copper and Gold Corp.
2300 - 1066 West Hastings St.
Vancouver British Columbia V6E 3X1
Canada

CC: Al Raven
Eugene Hodgson
John Harper
Venessa Bennett

SAMPLE PREPARATION AND ANALYTICAL PROCEDURES

Procedure Code	Number of Samples	Code Description	Test Wgt (g)	Report Status	Lab
PRP70-250	56	Crush, split and pulverize 250 g rock to 200 mesh			WHI
AQ370	56	1:1:1 Aqua Regia digestion ICP-ES analysis	1	Completed	VAN
SHP01	56	Per sample shipping charges for branch shipments			VAN
SLBHP	0	Sort, label and box pulps			WHI
GC820	3	Copper Assay by Classical Titration	0.5	Completed	VAN

ADDITIONAL COMMENTS



This report supersedes all previous preliminary and final reports with this file number dated prior to the date on this certificate. Signature indicates final approval; preliminary reports are unsigned and should be used for reference only. All results are considered the confidential property of the client. Bureau Veritas assumes the liabilities for actual cost of analysis only. Results apply to samples as submitted.

*** asterisk indicates that an analytical result could not be provided due to unusually high levels of interference from other elements.



Bureau Veritas Commodities Canada Ltd.

9050 Shaughnessy St Vancouver British Columbia V6P 6E5 Canada

PHONE (604) 253-3158

Client: **Fabled Copper and Gold Corp.**

2300 - 1066 West Hastings St.

Vancouver British Columbia V6E 3X1 Canada

Project: Church Key

Report Date: November 20, 2019

Page: 3 of 3

Part: 1 of 2

CERTIFICATE OF ANALYSIS

WHI19000616.1

Method	WGHT	AQ370	AQ370	AQ370	AQ370	AQ370	AQ370	AQ370	AQ370	AQ370	AQ370	AQ370	AQ370	AQ370	AQ370	AQ370	AQ370	AQ370	AQ370	AQ370	AQ370
Analyte	Wgt	Mo	Cu	Pb	Zn	Ag	Ni	Co	Mn	Fe	As	Sr	Cd	Sb	Bi	Ca	P	Cr	Mg	Al	
Unit	kg	%	%	%	%	ppm	%	%	%	%	%	%	%	%	%	%	%	%	%	%	
MDL	0.01	0.001	0.001	0.01	0.01	2	0.001	0.001	0.01	0.01	0.01	0.001	0.001	0.001	0.01	0.01	0.001	0.001	0.01	0.01	
Y646064	Rock	1.69	<0.001	0.711	<0.01	<0.01	<2	0.001	0.002	0.11	4.65	<0.01	0.005	<0.001	<0.001	<0.01	5.03	0.028	<0.001	2.31	0.47
Y646065	Rock	1.13	<0.001	1.747	<0.01	<0.01	<2	0.002	0.002	0.01	3.11	<0.01	0.002	<0.001	<0.001	<0.01	0.90	0.098	<0.001	0.51	0.34
Y646066	Rock	0.92	<0.001	7.039	<0.01	<0.01	<2	0.002	0.002	0.08	3.53	<0.01	0.011	<0.001	<0.001	<0.01	6.63	0.633	<0.001	2.46	0.21
Y646067	Rock	1.17	<0.001	6.116	<0.01	<0.01	<2	0.002	0.005	0.05	7.56	0.02	0.005	<0.001	<0.001	<0.01	2.94	0.043	<0.001	1.05	0.46
Y646068	Rock	0.99	<0.001	1.542	<0.01	<0.01	<2	0.002	0.003	0.04	1.88	<0.01	0.002	<0.001	<0.001	<0.01	1.74	0.026	<0.001	1.02	1.23
Y646069	Rock	1.02	<0.001	0.024	<0.01	<0.01	<2	0.004	0.002	0.04	4.55	<0.01	0.028	<0.001	<0.001	<0.01	2.17	0.110	0.004	0.91	2.11
Y646070	Rock	1.26	<0.001	0.007	<0.01	0.01	<2	0.003	0.003	0.12	9.93	<0.01	0.002	<0.001	<0.001	<0.01	1.93	0.201	0.005	3.96	3.79
Y646071	Rock	1.19	<0.001	0.005	<0.01	0.01	<2	0.002	0.002	0.16	6.88	<0.01	0.014	<0.001	<0.001	<0.01	11.11	0.084	0.002	2.82	3.15
Y646072	Rock	0.99	<0.001	>10	<0.01	<0.01	5	0.004	0.006	<0.01	21.80	0.11	0.001	<0.001	0.003	<0.01	0.02	0.022	<0.001	0.06	0.12
Y646073	Rock	0.92	<0.001	1.184	<0.01	<0.01	<2	0.002	0.002	0.02	5.25	<0.01	0.004	<0.001	<0.001	<0.01	1.34	0.042	<0.001	1.29	1.44
Y646074	Rock	0.73	<0.001	1.530	<0.01	0.02	<2	0.003	0.002	0.04	3.62	<0.01	0.008	<0.001	<0.001	<0.01	2.32	0.039	0.002	1.25	1.14
Y646075	Rock	0.97	<0.001	>10	<0.01	0.02	23	0.003	0.002	0.01	22.78	<0.01	<0.001	<0.001	<0.001	<0.01	0.49	0.105	<0.001	0.46	0.34
Y646076	Rock	1.52	<0.001	0.739	<0.01	<0.01	<2	0.002	<0.001	0.07	3.73	<0.01	0.006	<0.001	<0.001	<0.01	3.57	0.014	<0.001	1.45	1.39
Y646077	Rock	1.34	<0.001	6.069	<0.01	<0.01	<2	0.001	<0.001	0.03	2.13	<0.01	<0.001	<0.001	<0.001	<0.01	0.38	0.031	<0.001	0.47	0.76
Y646078	Rock	0.96	<0.001	0.008	<0.01	0.01	<2	0.003	0.004	0.08	7.89	<0.01	0.013	<0.001	<0.001	<0.01	4.04	0.081	0.003	4.83	4.23
Y646079	Rock	1.31	<0.001	0.009	<0.01	<0.01	<2	<0.001	<0.001	<0.01	0.58	<0.01	<0.001	<0.001	<0.001	<0.01	0.07	0.003	<0.001	0.02	0.10
Y646080	Rock	1.07	<0.001	0.132	<0.01	<0.01	<2	0.002	<0.001	0.08	1.79	<0.01	0.012	<0.001	<0.001	<0.01	5.09	0.041	0.001	3.14	1.30
Y646081	Rock	2.75	<0.001	0.014	<0.01	<0.01	<2	<0.001	<0.001	<0.01	0.61	<0.01	<0.001	<0.001	<0.001	<0.01	0.59	0.024	<0.001	0.30	0.16
Y646082	Rock	1.20	<0.001	<0.001	<0.01	<0.01	<2	<0.001	<0.001	0.16	0.95	<0.01	0.020	<0.001	<0.001	<0.01	17.94	0.009	<0.001	10.39	0.17
Y646083	Rock	1.41	<0.001	<0.001	<0.01	<0.01	<2	<0.001	<0.001	0.17	3.57	<0.01	0.017	<0.001	<0.001	<0.01	9.81	0.020	<0.001	4.00	0.11
Y646084	Rock	1.86	<0.001	2.636	<0.01	<0.01	2	0.009	0.008	<0.01	4.03	<0.01	<0.001	<0.001	<0.001	<0.01	0.20	0.001	<0.001	0.11	0.06
Y646085	Rock	1.41	<0.001	1.245	<0.01	<0.01	<2	0.004	0.004	0.04	1.31	<0.01	0.001	<0.001	<0.001	<0.01	2.81	<0.001	<0.001	1.40	0.04
Y646086	Rock	1.21	<0.001	5.436	<0.01	<0.01	4	0.001	<0.001	0.02	6.72	<0.01	0.002	<0.001	<0.001	<0.01	1.82	0.056	<0.001	0.83	0.08
Y646087	Rock	2.24	<0.001	0.025	<0.01	<0.01	<2	<0.001	<0.001	0.04	1.36	<0.01	0.002	<0.001	<0.001	<0.01	2.01	0.063	<0.001	0.90	0.12
Y646088	Rock	1.08	<0.001	0.007	<0.01	<0.01	<2	0.004	0.006	0.15	8.92	<0.01	0.004	<0.001	<0.001	<0.01	7.90	0.092	0.002	6.36	2.76
Y646089	Rock	2.33	<0.001	0.037	<0.01	<0.01	<2	<0.001	<0.001	0.12	4.05	<0.01	0.003	<0.001	<0.001	<0.01	6.23	0.014	<0.001	3.17	0.27



Bureau Veritas Commodities Canada Ltd.

9050 Shaughnessy St Vancouver British Columbia V6P 6E5 Canada

PHONE (604) 253-3158

Client: **Fabled Copper and Gold Corp.**

2300 - 1066 West Hastings St.

Vancouver British Columbia V6E 3X1 Canada

Project: Church Key

Report Date: November 20, 2019

Page: 3 of 3

Part: 2 of 2

CERTIFICATE OF ANALYSIS

WHI19000616.1

Method	Analyte	AQ370	AQ370	AQ370	AQ370	AQ370	GC820
		Na	K	W	Hg	S	Cu
Unit		%	%	%	%	%	%
MDL		0.01	0.01	0.001	0.001	0.05	1
Y646064	Rock	<0.01	0.11	<0.001	<0.001	1.90	
Y646065	Rock	<0.01	0.14	0.001	<0.001	1.99	
Y646066	Rock	<0.01	0.10	0.004	<0.001	2.16	
Y646067	Rock	<0.01	0.24	0.004	<0.001	6.16	
Y646068	Rock	<0.01	0.32	<0.001	<0.001	0.73	
Y646069	Rock	0.03	0.04	<0.001	<0.001	<0.05	
Y646070	Rock	0.04	0.22	<0.001	<0.001	0.70	
Y646071	Rock	0.01	0.02	<0.001	<0.001	<0.05	
Y646072	Rock	<0.01	0.06	0.013	<0.001	20.59	20.33
Y646073	Rock	<0.01	0.24	<0.001	<0.001	1.55	
Y646074	Rock	<0.01	0.12	<0.001	<0.001	1.15	
Y646075	Rock	<0.01	0.02	0.022	<0.001	14.71	22.69
Y646076	Rock	<0.01	0.14	<0.001	<0.001	0.47	
Y646077	Rock	<0.01	0.27	0.004	<0.001	0.71	
Y646078	Rock	0.01	0.04	<0.001	<0.001	0.18	
Y646079	Rock	<0.01	0.11	<0.001	<0.001	<0.05	
Y646080	Rock	<0.01	0.83	<0.001	<0.001	0.15	
Y646081	Rock	<0.01	0.13	<0.001	<0.001	<0.05	
Y646082	Rock	0.02	0.11	<0.001	<0.001	0.06	
Y646083	Rock	0.01	0.10	<0.001	<0.001	<0.05	
Y646084	Rock	0.01	0.05	0.002	<0.001	2.59	
Y646085	Rock	0.01	0.04	<0.001	<0.001	0.45	
Y646086	Rock	<0.01	0.06	0.003	<0.001	5.13	
Y646087	Rock	0.01	0.10	<0.001	<0.001	0.64	
Y646088	Rock	<0.01	0.08	<0.001	<0.001	2.00	
Y646089	Rock	<0.01	0.08	<0.001	<0.001	2.64	



Bureau Veritas Commodities Canada Ltd.
9050 Shaughnessy St Vancouver British Columbia V6P 6E5 Canada
PHONE (604) 253-3158

Client: Fabled Copper and Gold Corp.
2300 - 1066 West Hastings St.
Vancouver British Columbia V6E 3X1 Canada

Project: Church Key
Report Date: November 20, 2019

Page: 1 of 1

Part: 1 of 2

QUALITY CONTROL REPORT

WHI19000616.1

Method	WGHT	AQ370	AQ370	AQ370	AQ370	AQ370	AQ370	AQ370	AQ370	AQ370	AQ370	AQ370	AQ370	AQ370	AQ370	AQ370	AQ370	AQ370	AQ370	AQ370	AQ370
Analyte	Wgt	Mo	Cu	Pb	Zn	Ag	Ni	Co	Mn	Fe	As	Sr	Cd	Sb	Bi	Ca	P	Cr	Mg	Al	
Unit	kg	%	%	%	%	ppm	%	%	%	%	%	%	%	%	%	%	%	%	%	%	
MDL	0.01	0.001	0.001	0.01	0.01	2	0.001	0.001	0.01	0.01	0.01	0.001	0.001	0.001	0.01	0.01	0.001	0.001	0.01	0.01	
Pulp Duplicates																					
Y646059	Rock	2.14	<0.001	0.570	<0.01	<0.01	<2	0.001	0.002	0.07	1.73	<0.01	0.005	<0.001	<0.001	<0.01	4.39	0.028	<0.001	2.24	0.20
REP Y646059	QC		<0.001	0.560	<0.01	<0.01	<2	0.001	0.002	0.07	1.72	<0.01	0.005	<0.001	<0.001	<0.01	4.34	0.028	<0.001	2.23	0.20
Y646072	Rock	0.99	<0.001	>10	<0.01	<0.01	5	0.004	0.006	<0.01	21.80	0.11	0.001	<0.001	0.003	<0.01	0.02	0.022	<0.001	0.06	0.12
REP Y646072	QC																				
Y646084	Rock	1.86	<0.001	2.636	<0.01	<0.01	2	0.009	0.008	<0.01	4.03	<0.01	<0.001	<0.001	<0.001	<0.01	0.20	0.001	<0.001	0.11	0.06
REP Y646084	QC		<0.001	2.659	<0.01	<0.01	2	0.009	0.008	<0.01	4.04	<0.01	<0.001	<0.001	<0.001	<0.01	0.20	0.001	<0.001	0.11	0.06
Core Reject Duplicates																					
Y646062	Rock	0.75	<0.001	0.094	<0.01	<0.01	<2	0.002	<0.001	0.04	2.01	<0.01	0.004	<0.001	<0.001	<0.01	10.19	0.021	0.001	7.57	1.49
DUP Y646062	QC		<0.001	0.091	<0.01	<0.01	<2	0.002	<0.001	0.04	1.95	<0.01	0.004	<0.001	<0.001	<0.01	9.86	0.020	0.001	7.38	1.49
Reference Materials																					
STD CCU-1E	Standard																				
STD CCU-1E	Standard																				
STD CDN-ME-9A	Standard		<0.001	0.656	<0.01	<0.01	3	0.885	0.017	0.07	11.68	<0.01	0.006	<0.001	<0.001	<0.01	1.44	0.060	0.013	2.87	2.32
STD CDN-ME-14A	Standard		0.001	1.209	0.46	3.04	42	0.002	0.017	0.06	16.84	0.01	<0.001	0.009	0.002	<0.01	0.31	0.014	0.002	0.89	1.14
STD CDN-ME-9A	Standard		<0.001	0.640	<0.01	<0.01	4	0.870	0.016	0.07	11.34	<0.01	0.005	<0.001	<0.001	<0.01	1.27	0.058	0.013	2.79	2.07
STD CDN-ME-14A	Standard		0.002	1.280	0.50	3.13	45	0.002	0.018	0.06	17.86	0.01	<0.001	0.009	0.002	0.01	0.31	0.014	0.002	0.92	1.13
STD CDN-ME-9A Expected			0.00033	0.654	0.003	0.0096	3.3	0.912	0.0165	0.066	11.73	0.00125	0.006	0	0.00014	0.0002	1.37	0.0583	0.0134	2.84	2.21
STD CDN-ME-14A Expected			0.0015	1.24	0.488	2.97	42.3	0.0018	0.017	0.0589	17.29	0.0105	0.00036	0.0088	0.0024	0.0096	0.298	0.0127	0.0019	0.8787	1.14
STD CCU-1E Expected																					
BLK	Blank		<0.001	<0.001	<0.01	<0.01	<2	<0.001	<0.001	<0.01	<0.01	<0.01	<0.001	<0.001	<0.001	<0.01	<0.01	<0.001	<0.001	<0.01	<0.01
BLK	Blank		<0.001	<0.001	<0.01	<0.01	<2	<0.001	<0.001	<0.01	<0.01	<0.01	<0.001	<0.001	<0.001	<0.01	<0.01	<0.001	<0.001	<0.01	<0.01
Prep Wash																					
ROCK-WHI	Prep Blank		<0.001	<0.001	<0.01	<0.01	<2	<0.001	<0.001	0.06	1.85	<0.01	0.002	<0.001	<0.001	<0.01	0.69	0.041	<0.001	0.51	0.95
ROCK-WHI	Prep Blank		<0.001	<0.001	<0.01	<0.01	<2	<0.001	<0.001	0.06	1.91	<0.01	0.002	<0.001	<0.001	<0.01	0.71	0.039	<0.001	0.54	0.98



Bureau Veritas Commodities Canada Ltd.

9050 Shaughnessy St Vancouver British Columbia V6P 6E5 Canada

PHONE (604) 253-3158

Client: **Fabled Copper and Gold Corp.**

2300 - 1066 West Hastings St.

Vancouver British Columbia V6E 3X1 Canada

Project: Church Key

Report Date: November 20, 2019

Page: 1 of 1

Part: 2 of 2

QUALITY CONTROL REPORT

WHI19000616.1

Method	AQ370	AQ370	AQ370	AQ370	AQ370	GC820
Analyte	Na	K	W	Hg	S	Cu
Unit	%	%	%	%	%	%
MDL	0.01	0.01	0.001	0.001	0.05	1
Pulp Duplicates						
Y646059	Rock	0.01	0.07	<0.001	<0.001	0.31
REP Y646059	QC	0.01	0.07	<0.001	<0.001	0.31
Y646072	Rock	<0.01	0.06	0.013	<0.001	20.59 20.33
REP Y646072	QC					20.17
Y646084	Rock	0.01	0.05	0.002	<0.001	2.59
REP Y646084	QC	0.01	0.05	0.002	<0.001	2.57
Core Reject Duplicates						
Y646062	Rock	<0.01	0.23	<0.001	<0.001	0.06
DUP Y646062	QC	<0.01	0.23	<0.001	<0.001	0.06
Reference Materials						
STD CCU-1E	Standard					22.79
STD CCU-1E	Standard					22.64
STD CDN-ME-9A	Standard	0.32	0.18	<0.001	<0.001	3.33
STD CDN-ME-14A	Standard	0.03	0.35	<0.001	<0.001	16.17
STD CDN-ME-9A	Standard	0.28	0.17	<0.001	<0.001	3.26
STD CDN-ME-14A	Standard	0.02	0.35	<0.001	<0.001	17.11
STD CDN-ME-9A Expected		0.309	0.1813	0	0	3.34
STD CDN-ME-14A Expected		0.0264	0.359		0.0015	16.52
STD CCU-1E Expected						23.07
BLK	Blank	<0.01	<0.01	<0.001	<0.001	<0.05
BLK	Blank	<0.01	<0.01	<0.001	<0.001	<0.05
Prep Wash						
ROCK-WHI	Prep Blank	0.08	0.10	<0.001	<0.001	<0.05
ROCK-WHI	Prep Blank	0.09	0.11	<0.001	<0.001	<0.05